Developing groundwater and surface water interaction methods for complex hydrological systems

A thesis
submitted in fulfilment
of the requirements for the degree
of

Doctor of Philosophy

at

The University of Waikato

by

Ali Shokri

THE UNIVERSITY OF
WAIKATO
Te Whare Wānanga o Waikato

2016

Abstract

Methods and models associated with the interaction of surface-subsurface water flow have been widely employed in many environmental studies over the last decade. However, in spite of considerable effort, understanding the impact of both artificial and natural aspects of the connection between surface water and groundwater systems still remains a challenge for groundwater and surface water models.

In this doctoral study, two types of complex and integrated problems are identified as knowledge gaps in coupled surface and subsurface flow studies (i) interaction situations that arise from use of artificial drains in agricultural catchments, and (ii) complex flow situations that sometimes arise as a result of a combination of near surface aquifers which are both perched and leaky. The specific objectives of this research project were (1) to improve classical tile drain spacing design methods; and (2) via a case study, to assess the role of semi-impermeable layers influencing the interaction between surface water and a regional groundwater system.

To meet the first objective the *DrainFlow* code is developed. *DrainFlow* is a new, fully distributed, physically based and integrated surface-subsurface flow code that is designed for water movement in tile/mole drains, open drains, and saturated/unsaturated zones. *DrainFlow*, applied to examples of drainage studies, is found to be quite flexible in terms of changing all or part of the model dimensions as required by problem complexity, scale, and data availability. This flexibility gives *DrainFlow* the capacity to be modified to meet the specific requirements of varying scale and boundary conditions as often encountered in drainage projects.

In addition, the classical well-known Hooghoudt drain spacing equation is modified. It is shown via comparison with numerical models that the Hooghoudt equation can overestimate water table height and therefore yield drain spacings which may be too wide. The modified expression yields improved accuracy as measured against the numerical reference model.

To meet the second objective, the effect of a thin semi-impermeable and fractured layer between two relatively permeable volcanic formations is investigated in an industrial catchment system at Kawerau, New Zealand. It is concluded that subtle near-surface geological features may have a critical role on controlling the volume and pattern of the flow exchange between the surface, subsurface flow and regional groundwater systems.

This doctoral thesis overcomes some weaknesses of isolated surface and subsurface flow models and some constructive and practical approaches are developed to enhance the previous methods.

Key Words: coupled, interaction, surface subsurface flow, *DrainFlow*, drainage, tile drain, open drain, semi-impermeable, perched, leaky

Acknowledgements

First and foremost, I would like to express my special appreciation and thanks to my chief supervisor Associate Professor Earl Bardsley for the continuous support of my PhD study and for his patience, motivation, and knowledge. Your guidance helped me a lot in all the time of this research. I also greatly appreciate the support from my secondary supervisor Dr Adrian Pittari and his valuable input and discussions.

Throughout this study, I was supported financially by Norske Skog Tasman and Carter Holt Harvey Pulp and Paper. Thank you to Mr Nick Eynon Richards, Ms Desirae Kirby, and Mr Chris Bruns who gave me valuable input for, and suggestions regarding the Ph.D. case study.

My sincere thanks also goes to my colleagues in Lincoln Agritech, a very special thanks to Dr Roland Stenger, Dr Simon Woodward, Dr Juliet Clague, Mr Brian Moorhead, Mr Scott Wilson, Mr Hugh Canard, Mr Jens Rekker, who provided me an opportunity to join their team. Without their precious support it would not be possible to conduct this research.

I have always been greatly supported by a lot of people at the University of Waikato. Thank you to everybody who was there when I needed help. Special thanks to Mrs Sydney Wright, Mr Dean Sandwell, Ms Varvara Vetrova, Mr Mohammed Majeed, Mr Malcolm Taylor, for valuable input and support. I would specially like to thank my friends Dr Medihah Bardsley, Mrs Ravaani Ghaemmaghamy and Mr. Danial Chapman. You have been such amazing friends and helped me in every possible way.

Eternal gratitude goes to my mother, for her endless love and support and believing in me. I also would like to thank my friends and family for supporting me spiritually throughout this research and my life in general.

Last but not least, thank you to my wonderful beloved wife, Mrs Atousa Nazeri for providing me with love and unwavering support. This work could not be finished without your support, patience, and help.

Table of Contents

List of Tables

List of Figures:

1 Chapter 1

Introduction

1.1 Overview and background

The hydrologic cycle contains a wide range of linked surface and subsurface flow processes. In spite of natural connections between surface water and groundwater, historically these processes have been studied separately. However, for the last few decades the interaction between surface water and groundwater has received increased attention from water scientists. It has been reported frequently that the use of a particular surface or groundwater resource may have an unwanted impact on the other. For example, pumping water from an unconfined aquifer in the vicinity of surface water bodies like rivers, streams and lakes could change the infiltration rate between surface water and groundwater systems (Childress, 1991; Lindgren & Landon, 2000; McCarthy, McFarland, Wilkinson, & White, 1992; Sheets, Darner, & Whitteberry, 2002; Steele & Verstraeten, 1999; Zarriello, Ries, Management, Protection, & Survey, 2000). Similarly, sometimes surface water is recharged to groundwater for aquifer rehabilitation (Galloway, Alley, Barlow, Reilly, & Tucci, 2003). In both scenarios pumping water from/to aquifers or surface water bodies can change the direction, rate, and

location of water interchanges between rivers and groundwater (Galloway et al., 2003; Glennon, 2004; Stromberg, Tiller, & Richter, 1996).

In some cases, water is simply pumped from groundwater for cooling purposes and then discharged into a surface water body. In spite of minor water loss, this action may have a considerable impact on the aquifer and surface water interaction (Andrews & Anderson, 1978; Hutson, 2004).

Besides inland groundwater, coastal aquifers also have received a growing attention by coastal and marine scientists studying interaction between freshwater groundwater and saltwater components (Barlow, Wild, & Survey, 2002; Bokuniewicz, 1980; Linderfelt & Turner, 2001; Moore, 1996, 1999). Submarine groundwater discharge from coastal aquifers is important for marine life sensitive to salinity and nitrate levels (Johannes, 1980; Johannes & Hearn, 1985; Simmons, 1992; Taniguchi, Burnett, Cable, & Turner, 2002; Valiela et al., 1990). Pumping water from coastal aquifers can evidently change the surface/subsurface flow interaction even at locations far from a coastline (Simmons, 1992). In rivers, the aquifer and river exchange rates and the exact locations of groundwater discharge in rivers are vital for fish habitat (Garrett, Bennett, Frost, & Thurow, 1998; I. A. Malcolm, Soulsby, Youngson, & Petry, 2003; Iain A. Malcolm, Youngson, & Soulsby, 2003; Power, Brown, & Imhof, 1999).

Quantifying the connection between rivers and groundwater also has been studied frequently. So far, several field techniques and methods have been reported in the literature to quantify the exchange rate between surface and subsurface water flow. These techniques are classified here into ten classes as follows:

(1) *River discharge measurements*: differencing discharges at different locations of a stream channel can give the net seepage exchange rate between groundwater and streams over a given river reach (Donato, 1998; Harte, Division, & Survey, 1997; Herbert, Thomas, Survey, Rights, & Resources, 1992; Hill, Protection, Energy, & Survey, 1992; Kaleris, 1998);

(2) S*eepage measurement:* measuring seepage directly from a river bed can be achieved by isolating a relatively small area of channel bottom and measure the exchange water between the sub-channel aquifer and river water (Cable, Burnett, Chanton, Corbett, & Cable, 1997; Carr & Winter, 1980; Fellows & Brezonik, 1980; David Robert Lee, 1977; David R Lee & Cherry, 1979; Oxtobee & Novakowski, 2002);

(3) *Water level measurements:* the head gradient between surface water and groundwater can be used to calculate flow direction and flow rate. Usually hydraulic potentio-manometer probes can be used to measure the hydraulic head gradient between groundwater and surface water for small scale studies (Cambareri & Eichner, 1998; LaBaugh, Rosenberry, & Winter, 1995; T. M. Lee & Swancar, 1997; Puckett, Cowdery, McMahon, Tornes, & Stoner, 2002; Simonds & Sinclair, 2002; Wentz, Rose, & Webster, 1995; Zekster, 1995);

(4) *Thermal profiling:* temperature gradient between interacting groundwater and surface water bodies can be detected by aerial infrared photography and imagery techniques (Banks, Paylor, & Hughes, 1996; Campbell & Keith, 2000; Robinove, 1965). However, in a small scale projects temperature differences between surface water and groundwater can be detected by using in situ temperature measurements and towing a

tethered temperature probe to locate groundwater and surface water interaction zones and quantify the flux exchange between surface water and groundwater. However, this method is limited to use where a noticeable thermal gradient between groundwater and surface water temperatures observes (Baskin, 1998; Hare, Briggs, Rosenberry, Boutt, & Lane, 2015; Donald O Rosenberry, Striegl, & Hudson, 2000; Stonestrom, Constantz, & Survey, 2003);

(5) *Tracer application:* artificial and conservative environmental tracers can be used in surface water or groundwater to provide a direct quantitative measurement for groundwater/surface water interaction (Aley & Fletcher, 1976; J. W. Harvey, Wagner, & Bencala, 1996; Hatch, Fisher, Revenaugh, Constantz, & Ruehl, 2006; W. K. Jones, 1984; Kalbus, Reinstorf, & Schirmer, 2006; Kilpatrick & Cobb, 1985; Mull, Liebermann, Smoot, & Woosley, 1988; Smart & Laidlaw, 1977)+[From Sara Comments];

(6) *Isotope methods and dating:* measuring the ratios of stable oxygen isotopes (^{18}O and ^{16}O) and hydrogen isotopes (protium, deuterium and tritium) in water have been used to determine the portion of groundwater discharge into surface water bodies for a few decades (David, Carl, Carol, & Joel, 1994; Kendall & McDonnell, 2012; LaBaugh et al., 1997; Sacks, District, & Survey, 2002). In addition, measurements of radon and radium isotopes have been used to distinguish the portion of groundwater in surface water bodies (Burnett & Dulaiova, 2003; Corbett, Burnett, Cable, & Clark, 1998; Moore, 2000). More specifically conservation environmental tracers such as $^{2}H^{18}O$ use for groundwater sources, isotopes such as ^{222}Rn use to infer the presence of groundwater and in some instances the

quantity of groundwater, and isotopes such as $^{3}H^{14}C$ frequently use for aging water to determine the portion of groundwater discharge to surface water.

(7) *Specific-conductance profiling*: specific-conductance profiling occurs in both the horizontal and vertical domain in much the same way that temperature profiling does, therefore specific-conductance probes can be used to detect the specific conductance gradient between surface water and groundwater to find the interaction areas. Similar to thermal profiling, this method is useful if there is a significant geochemical difference between surface water and groundwater observes(F. E. Harvey, Lee, Rudolph, & Frape, 1997);

(8) *Electrical resistivity profiling*: electrical resistivity probes can be used to detect salinity differences between groundwater and surface water to determine the groundwater discharge, especially in submarine groundwater aquifers (Belaval, Lane Jr, Lesmes, & Kineke, 2003; Day-Lewis, White, Johnson, Lane, & Belaval, 2006; Loke & Lane Jr, 2004; Manheim, Krantz, & Bratton, 2004);

(9) *Biological Indicators:* plant and animal responses to groundwater flow in surface water can be used as an indicator of direction and magnitude of groundwater discharge to surface water bodies (Baird & Wilby, 2005; Danielopol, et al., & Danielopol, 1997; Lodge, Krabbenhoft, & Striegl, 1989);

(10) *Hydrograph separation*: hydrograph separation techniques can be used in principle to determine the portion of groundwater in an event

hydrograph. In hydrograph separation techniques it is assumed steady base-flow in the river has a groundwater origin, in contrast to quick-flow that has a near-surface or surface flow origin (Arnold & Allen, 1999; Chapman, 1999; Eckhardt, 2005, 2008; Rutledge, 1998).

Besides measurement techniques, several numerical and analytical models like rainfall-runoff models have been developed to improve understanding of connection between surface flow and subsurface flow. These models were originally designed to relate rainfall, land surface recharge and groundwater discharge to temporal variability of flow in a river. However, rainfall-runoff models also can be applied to quantify the interaction between surface and subsurface flow in a catchment scale. For example, the analytical curve number (CN) method can be applied to quantify interaction between surface water and groundwater by approximating the CN value (Ponce & Hawkins, 1996; Rallison, 1980). Curve number values are defined empirically from hydrological soil group, land use, hydrological surface condition, and soil moisture condition.

In addition a number of distributed and semi-distributed rainfall-runoff numerical models like SWAT (Gassman, Reyes, Green, & Arnold, 2007) and TOPNET (Clark et al., 2008) have been developed. In this type of model a catchment may be partitioned into a number of sub-catchments and each sub-catchment may be divided into different hydrologic respond units (HRUs). These HRUs are some spatially consistent combination of land cover, soil and management type. A daily bucket-type water balance model runs separately for each HRUs to calculate the amount of water, nutrient, sediment and pesticide loading into the river network. In the

second phase, the routing phase, flow is routed through the river network using a variable storage coefficient method (Williams, 1969) or the Muskingum routing methods. The models generally are calibrated to match river flow at the outlet of a catchment or sub-catchment. Often the groundwater component for each HRU can be estimated during the calibration process. The main disadvantage of this type of models is that the groundwater component should be added as an external assumption to the model.

The current trend in hydrological model development is to combine distributed surface water models with distributed subsurface flow models in order to have better estimation of the temporal and spatial variability of the interaction between surface and subsurface flow (D.O. Rosenberry & Lebaugh, 2014). These types of numerical models are known as “Fully distributed coupled surface/subsurface flow models”.

The first blueprint of developing a fully distributed coupled surface/subsurface flow models goes back to 1969 with the work by Freeze and Harlan (R. Allan Freeze & Harlan, 1969). However, truly fully distributed coupled surface/subsurface flow models have only appeared in the literature recently (Bixio et al., 2002; J. P. Jones, Sudicky, Brookfield, & Park, 2006; Kollet & Maxwell, 2006, 2008a; Panday & Huyakorn, 2004; Qu & Duffy, 2007; VanderKwaak & Loague, 2001). Moreover, a range of interaction surface/subsurface flow codes have been developed, for example, ParFlow (Kollet & Maxwell, 2006, 2008a; Maxwell & Miller, 2005) PAWS (Shen & Phanikumar, 2010), CATHY(M. Camporese, Paniconi, Putti, & Orlandini, 2010), HydroGeoSphere (HGS) (Aquanty Inc., 2013;

Brunner & Simmons, 2012), InHM (Kumar, Duffy, & Salvage, 2009; Qu & Duffy, 2007), tRIBS + VEGGIE (Ivanov, Bras, & Vivoni, 2008; Ivanov et al., 2010; Kim, Ivanov, & Katopodes, 2013), and OpenGeoSys (OGS)(J.-O. Delfs, Blumensaat, Wang, Krebs, & Kolditz, 2012; J. O. Delfs, Kalbus, Park, & Kolditz, 2009; J. O. Delfs, Park, & Kolditz, 2009). Coupled surface/subsurface flow models cover a range of scales from hill-slope and farm-scale to catchment and regional studies. Applications of these models incorporate a range of environmental processes including irrigation and drainage (Banti, Zissis, & Anastasiadou-Partheniou, 2011; Dong, Xu, Zhang, Bai, & Li, 2013; Morrison, 2014; Rozemeijer et al., 2010; Schoups et al., 2005; Ali Shokri, 2011; Zerihun, Furman, Warrick, & Sanchez, 2005a, 2005b), solute transport and particle-tracking (Sudicky, Jones, Park, Brookfield, & Colautti, 2008; Weill, Mazzia, Putti, & Paniconi, 2011), sediment transport (S. Li & Duffy, 2011; Ran, Heppner, VanderKwaak, & Loague, 2007), flood control (Liang, Falconer, & Lin, 2007), residence time and hydrograph separation (Bayani Cardenas, 2008; Kollet & Maxwell, 2008b; Liggett, Werner, Smerdon, Partington, & Simmons, 2014; Meyerhoff & Maxwell, 2011; Partington et al., 2013; Partington et al., 2011), land surface recharge (Guay, Nastev, Paniconi, & Sulis, 2013; Lemieux, Sudicky, Peltier, & Tarasov, 2008; Smerdon, Mendoza, & Devito, 2008), and runoff generation (Matteo Camporese, Paniconi, Putti, & Salandin, 2009; J.-O. Delfs, Wang, Kalbacher, Singh, & Kolditz, 2013; Ebel et al., 2007; Gauthier, Camporese, Rivard, Paniconi, & Larocque, 2009; Heppner, Loague, & VanderKwaak, 2007; J. P. Jones, Sudicky, & McLaren, 2008; Q. Li et al., 2008; Maxwell & Kollet, 2008; Meyerhoff &

Maxwell, 2011; Mirus, Loague, VanderKwaak, Kampf, & Burges, 2009; Qu & Duffy, 2007; Sulis, Paniconi, & Camporese, 2011).

In spite of considerable research in this field, the development of hydrological and hydrogeological models for understanding the effect of artificial and natural aspects on the linkage between surface and subsurface water components still remains a challenge for hydrology and hydrogeological models.

Two types of complex and integrated environmental problems that often cause difficulties in developing groundwater and surface water models are investigated for this doctoral study; (I) the first problem is the hydrological and hydrogeological integrated conditions that occur because of artificial drains, such as tile, mole and open drains, in agricultural catchments; and (II) the second problem is a complex condition that sometimes happens as a result of perched and leaky formations and fractures in the integration between surface water and the regional groundwater system.

(I) Artificial drained catchments

To date, many empirical and analytical expressions (Barua & Tiwari, 1996a, 1996b; Childs, 1969; Çimen, 2008; Collis-George & Youngs, 1958; Dagan, 1964 ; Ernst, 1962; Hammad, 1962; Hooghoudt, 1940; Kirkham, 1958, 1966; List, 1964; Lovell & Youngs, 1984; Miles & Kitmitto, 1989; Mishra & Singh, 2007, 2008; Moody, 1966; Sakkas & Antonopoulos, 1981; Van der Molen & Wesseling, 1991; E. Youngs, 2012, 2013; E. G. Youngs, 1965, 1975) and numerical solutions (Castanheira & Santos, 2009; Chavez, Fuentes, Zavala, & Brambila, 2011a; Chavez, Fuentes, Zavala, &

Zatarain, 2011b; Gureghian & Youngs, 1975; Jiang, Wan, Yeh, Wang, & Xu, 2010; Kalcic, Frankenberger, & Chaubey, 2015; Khan & Rushton, 1996a, 1996b, 1996c; Koch, Bauwe, & Lennartz, 2013; Liu, Chen, Yao, & Chen, 2015; Moriasi et al., 2013; Pandey, Bhattacharya, Singh, & Gupta, 1992; Rocha, Roebeling, & Rial-Rivas, 2015; A. Shokri & Bardsley, 2014; Smedema, Poelman, & De Haan, 1985; Henryk Zaradny, 2001; H. Zaradny & Feddes, 1979; Manuel Zavala, Fuentes, & Saucedo, 2007) have been developed to identify a true relationship between tile drain discharge, soil hydrodynamic properties, tile drain depth and drain spacing. However, developing a comprehensive model for artificial drainage on a catchment scale still remains a challenge for existing hydrological and hydrogeological models. With a strong connection between subsurface drainage and surface water, the hydrological and hydrogeological models are faced with enormous difficulties to simulate water flow in such a complex condition (R. W. Skaggs, 1980).

Moreover, while drain spacing can be estimated perfectly well by numerical models, analytical and empirical solutions of tile drain spacing, such as the well-known Hooghoudt expression (1940), still has the attraction of its ease of application.

The derivation of the Hooghoudt expression is based on the one-dimensional Boussinesq equation by using Dupuit – Forchheimer (DF) assumptions for flow to two parallel drains. The derivation assumes that the effect of radial flow from the centre of the drain to $D/\sqrt{2}$ $\mathrm{D}/\sqrt{2}$ is significant, where *D* is the thickness of the soil layer below the drains.

To allow for the effect of radial flow near the drains and to reduce the DF approximation error, Hooghoudt (1940) replaced *D* in his equation with an "equivalent depth" *d,* which is an imaginary depth under the drains that is always smaller than *D*. Moody(1966) and Sakkas and Antonopoulos (1981) present simple estimating expressions for *d* , while Van Schilfgaarde (1963) describes a graphical estimation approach. Beers (1979) gives a dimensionless nomogram to avoid the trial-and-error solution of the Hooghoudt equation. Mishra and Singh (2007) derive a new equivalent depth table for the Hooghoudt equation by changing the assumption of the effect of the radial flow from $\mathrm{D}/\sqrt{2}$ to a combination of $2D/\pi$ and the area of groundwater flow above the drain in the radial zone.

Despite considerable work to improve the Hooghoudt equation, a comparison between the Hooghoudt expression and numerical models indicates that the Hooghoudt equation overestimates water table height and therefore gives drain spacings which may be too wide. It will be shown here that this is because the Hooghoudt drain spacing equation in fact has a concealed dependency on Van Genuchten soil-water retention curve parameters, which can bias the water table estimates unless adjustments are made explicitly.

(II) Perched and leaky aquifer

The second type of integrated environment, which is investigated in this doctoral study, is a complex condition that often occurs for fractured perched aquifers. Despite the fact that perched groundwater tables have long been classified as aquifers (Fetter & Fetter, 2001; R.A. Freeze & Cherry, 1979), the importance of leaky and perched aquifers on the

connection between surface, subsurface flow and regional groundwater is not addressed adequately in the literature.

Previous studies indicate perched aquifers can effectively redirect the land surface recharge along a horizontal impermeable layer to springs, streams, wetlands, and lakes (Amit, Lyakhovsky, Katz, Starinsky, & Burg, 2002; Driese, McKay, & Penfield, 2001; O'Driscoll & Parizek, 2003; Rabbo, 2000; Von der Heyden & New, 2003), consequently decreasing the volume of vertical recharge to the regional groundwater aquifers (Bagtzoglou, Timothy L. Tolley, Stothoff, & Turner, 2000). Furthermore, continuity and permeability of the perched layer play an important role in the connection between surface-subsurface flow and the regional groundwater system. Where perched layers are fully continuous and impermeable, surface and subsurface flow would be completely isolated from the regional groundwater system (Golden et al., 2014; Pirkle & Brooks, 1959). However, a semi-impermeable perched layer with an internal discontinuity, fractures, and faults may have unpredictable effects on the hydrologic environment.

Despite the important role of leaky and perched aquifers on the connection between surface and subsurface flow components, relatively little is known about how a leaky and perched aquifer controls flux exchange in the total hydrological system. In fact, the importance of perched aquifers in regional groundwater conceptual models tends to be neglected (Cable Rains, Fogg, Harter, Dahlgren, & Williamson, 2006), due to either lack of information or the scale of the studies concerned.

1.2 Research objectives

The objectives of this project are:

1. to improve classical tile drain spacing design methods;
2. via a case study, to assess the role of semi-impermeable layers influencing the interaction between surface water and a regional groundwater system.

1.3 Thesis structure

The thesis comprises five chapters, of which three (chapters 2-4) have been written in the style of stand-alone journal articles for the purpose of publication. Consequently, there is some duplication in the introductory comments and methods between the chapters. Briefly, the first chapter provides a general literature review and introduction. Chapters 2, 3 and 4 each contain a stand-alone introduction, background literature review, materials and methods, results and discussion sections. Chapter 5 concludes this doctoral thesis with a general discussion, summary and recommendations for future work. Chapter 3 and 4 are related to the first PhD research objective and chapter 5 is related to obective2.

Chapter 2 develops, tests and applies the *DrainFlow* code. The *DrainFlow* includes several modules: overland flow, open drain, surface water network, and tile/mole drain modules for surface water flow, and a saturated-unsaturated module for subsurface flow.

To develop the code, first the surface and subsurface flow modules are formulated separately, then each module is connected to the other parts.

The *DrainFlow* code has been presented in some conferences and workshops (Ali Shokri, 2011, April 2015, December 2011, Nov 2014, Sep 2015; Ali Shokri & Bardsley, 2015). In addition, at the time of writing, chapter 2 had been submitted to a high rank international journal for review. However, the editorial format of the chapter 2 might be differed from the journal publication because of the journal requirements.

Chapter 3 compares the Hooghoudt equation with the results of some numerical models for a steady state condition including one tile. As a result a modified Hooghoudt equation is presented that has the advantage of giving more accurate results than the original expression and should find applications to practical drainage design. The literature review and methodology are described and the results are reported and discussed.

This chapter was presented in two conferences (Ali Shokri, December 2012, November 2013) and has been published in *Journal of Irrigation and Drainage Engineering* (A. Shokri & Bardsley, 2014), however the editorial format of chapter 3 differs from the journal publication because of the journal requirements.

Chapter 4 identifies and assesses a thin semi-impermeable and fractured layer between two relatively permeable volcanic formations (Rotoiti Pyroclastics and Matahina Ignimbrite) that is causing a leaky and perched aquifer in the Rotoiti Pyroclastics. A high resolution finite element groundwater model of the shallow aquifer is developed to simulate groundwater flow in the shallow and leaky groundwater system. The effect of the perched and leaky layer in connection between surface water and regional groundwater system is discussed.

This chapter is going to submit to a high rank international journal, however the editorial format of chapter 4 may differ from the journal publication because of the journal requirements.

Chapter 5 concludes this thesis with a general discussion, summary and recommendations for future work.

2 Chapter 2

Development, test and application of DrainFlow: a fully distributed integrated surface-subsurface flow model for drainage study

1.1 Abstract

Hydrological and hydrogeological investigation of drained land can be considered as a complex and integrated procedure. The scale of drainage studies may vary from a high-resolution small scale project through to a comprehensive catchment or regional scale investigation. This wide range of scales and integrated system behaviour poses a significant challenge for the development of a suitable drainage model. To meet these requirements, a fully distributed coupled surface-subsurface flow model named henceforth DrainFlow is developed and described here. DrainFlow includes both the Saint Venant equations for surface flow components (overland flow, open drain, tile drain) and the Richards equation for saturated/unsaturated zones.

To overcome the non-linearity problem created from switching between wet and dry boundaries, a smooth switching technique is introduced to

buffer the model at tile drains and interface surface-subsurface flow boundaries. This gives a continuous transition between Dirichlet and Neumann boundary conditions. *DrainFlow* applied to some drainage study standard examples is found to be quite flexible in terms of changing all or part of the model dimensions as required by problem complexity, problem scale, and data availability. This flexibility gives *DrainFlow* the capacity to be modified to meet the specific requirements of varying scale and boundary conditions, as often encountered in drainage studies. Compared to traditional drainage models, *DrainFlow* has the advantage of estimating the land surface recharge directly from the partial differential form of Richards equation rather than through analytical or empirical infiltration approaches like the Green and Ampt equation.

Keywords: drainage, physically based, interaction, linked, surface-subsurface, flow, integrated, coupled, groundwater, surface flow, subsurface flow, irrigation

2.1 Introduction

During a rain recharge event water infiltrates from the ground surface through the soil profile to the saturated zone, raising the water table. Water in the saturated zone then moves to tile drains. If the rainfall rate exceeds the infiltration capacity, because of either a change in rainfall or infiltration rate, ponding may occur at the ground surface as water accumulates at ground surface micro-topography. After filling surface depressions, further rainwater moves as surface overland flow or along small micro-channels. After rainfall cessation, infiltration will continue until the remnant surface water either drains away or evaporates.

Developing a comprehensive model for an artificially drained land area remains a challenge for hydrological and groundwater models. The reason is that modelling is made difficult because the subsurface drainage process as described above strongly connects to surface flow (R. W. Skaggs, 1980). Furthermore, the modelled spatial scale may vary from high-resolution small scale investigations through to comprehensive catchment or regional-scale studies.

Many empirical and analytical expressions (Barua & Tiwari, 1996a, 1996b; Childs, 1969; Çimen, 2008; Collis-George & Youngs, 1958; Dagan, 1964 ; Ernst, 1962; Hammad, 1962; Hooghoudt, 1940; Kirkham, 1958, 1966; List, 1964; Lovell & Youngs, 1984; Miles & Kitmitto, 1989; Mishra & Singh, 2007, 2008; Moody, 1966; Sakkas & Antonopoulos, 1981; Van der Molen & Wesseling, 1991; E. Youngs, 2012, 2013; E. G. Youngs, 1965, 1975) and numerical solutions (Castanheira & Santos, 2009; Chavez et al., 2011a; Chavez et al., 2011b; Gureghian & Youngs, 1975; Jiang et al., 2010; Khan & Rushton, 1996a, 1996b, 1996c; Pandey et al., 1992; A. Shokri & Bardsley, 2014; Smedema et al., 1985; Henryk Zaradny, 2001; H. Zaradny & Feddes, 1979; Manuel Zavala et al., 2007) have been developed to identify the relation between tile drain discharge and soil hydrodynamic properties, tile drain depth, and drain spacing. In addition, a number of special-purpose computer codes have been developed for estimating optimal drain spacing, including *DRAINMOD* (R.W. Skaggs, 1980), *DRENAFEM* (Castanheira & Santos, 2009) and *MHYDAS-DRAIN* (Tiemeyer, Moussa, Lennartz, & Voltz, 2007). However, both analytical and numerical drainage models rarely incorporate both the surface and subsurface flow with connection between overland flow and groundwater

movement. In fact, neither subsurface nor surface flow models alone are capable to reflect the complete surface-subsurface flow behaviour in an artificially drained catchment.

Coupled surface-subsurface flow has been extensively investigated over the last decade in many hydrological and hydrogeological studies. The literature describes a range of environmental process applications including irrigation and drainage (Banti et al., 2011; Dong et al., 2013; Morrison, 2014; Rozemeijer et al., 2010; Schoups et al., 2005; Ali Shokri, 2011; Zerihun et al., 2005a, 2005b), solute transport and particle-tracking (Sudicky et al., 2008; Weill et al., 2011), sediment transport (S. Li & Duffy, 2011; Ran et al., 2007), flood control (Liang et al., 2007), residence time and hydrograph separation (Bayani Cardenas, 2008; Kollet & Maxwell, 2008b; Liggett et al., 2014; Meyerhoff & Maxwell, 2011; Partington et al., 2013; Partington et al., 2011), land surface recharge (Guay et al., 2013; Lemieux et al., 2008; Smerdon et al., 2008), and runoff generation (Matteo Camporese et al., 2009; J.-O. Delfs et al., 2013; Ebel et al., 2007; Gauthier et al., 2009; Heppner et al., 2007; J. P. Jones et al., 2008; Q. Li et al., 2008; Maxwell & Kollet, 2008; Meyerhoff & Maxwell, 2011; Mirus et al., 2009; Qu & Duffy, 2007; Sulis et al., 2011).

In addition, some interaction surface and subsurface flow models have been developed. This includes, for example, *ParFlow* (Kollet & Maxwell, 2006, 2008a; Maxwell & Miller, 2005) *PAWS* (Shen & Phanikumar, 2010), *CATHY* (M. Camporese et al., 2010), *HydroGeoSphere* (HGS) (Aquanty Inc., 2013; Brunner & Simmons, 2012), *InHM* (Kumar et al., 2009; Qu & Duffy, 2007), *tRIBS + VEGGIE* (Ivanov et al., 2008; Ivanov et al., 2010;

Kim et al., 2013), and *OpenGeoSys (OGS)* (J.-O. Delfs et al., 2012; J. O. Delfs, Kalbus, et al., 2009; J. O. Delfs, Park, et al., 2009). In spite of the considerable effort in this field, none of the available codes are specialized to allow for the scale variation that is often encountered in drainage studies. This wide range of scales poses a significant challenge for the development of a suitable general drainage model.

As a contribution to the subject area, a fully distributed new coupled surface-subsurface model named hereafter as *DrainFlow* is presented here. *DrainFlow* includes several modules for surface flow: overland flow, open drain, tile/mole drains and surface water networks. Subsurface flow is incorporated via a saturated/unsaturated module. To develop the complete model, surface and subsurface flow modules are formulated separately and then each component connected to all the others. All modules interact to yield soil moisture water level in the subsurface domain, overland flow, and outflow in tile and open drains.

To overcome the non-linearity problem created from switching between dry and wet boundaries, a new technique is included in *DrainFlow* as a guard against this nonlinearity issue. The new technique provides smooth switching between wet and dry boundary conditions to buffer the model at tile drains and interface surface-subsurface flow boundaries.

The most useful feature of *DrainFlow* is that it has the capability to alter its dimensioning of surface and subsurface flow domains, depending on the complexity of the problem, scale, and the availability of data. Even though higher dimensions define a wider range of problems, in many cases useful solutions can be obtained via lower-dimension surface and subsurface

flow models. Also, in contrast to traditional analytical and numerical drainage models, *DrainFlow* has the advantage of estimating land surface recharge directly from the partial differential Richards equation (Richards, 1931) rather than using analytical and empirical methods like Green and Ampt .

With reference to the structure of this chapter, sections 2.2 to 2.4 introduce the surface and subsurface flow modules, relevant equations, and the methodology applied to couple the equations and modules. *DrainFlow* was tested against five well-known integrated surface-subsurface flow problems and results are discussed in the section 2.5. In addition two applications of *DrainFlow* in some examples are described in Section 6.

2.2 Model development

2.3 Overview

In a tile drained catchment, the hydrological components such as tile/mole drains, open drains, rivers network, groundwater table, and soil moisture are hydrologically connected. To give best approximation to an environmental system, all model elements should reflect these distinctive but interacting hydrological elements. That is, the modules need to interact to properly mimic reality.

From this conception, application of DrainFlow requires initial separate formulation of the surface and subsurface flow modules, and then each module connects to the related components. Consequently, DrainFlow incorporates a wide range of modules including overland flow, tile/mole

drain, open drain, river network, and subsurface flow. The general form of the DrainFlow conceptual model and components is shown in Fig 2.1.

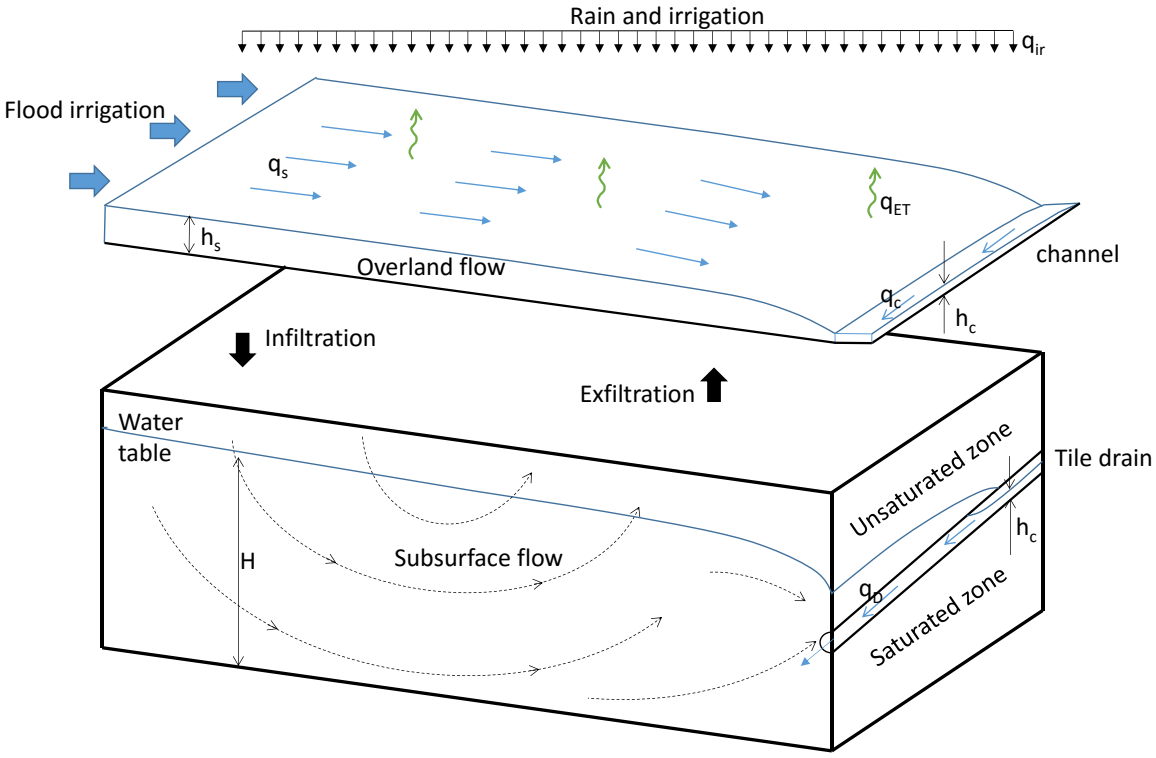

Fig 2.1 Schematic overview of the DrainFlow structure and components, q_s is the overland flow, h_s is the water depth, q_{ET} is the time series of evapotranspiration per unit area, h_{sc} is the water depth in channel, q_{sc} is the flow in chanel, H is the total groundwater head, qsd is the flow in tile drain, and $h_{sD}$is the water depth in tile drain

2.3.1 DrainFlow Overland flow module (OL)

Overland flow is defined by the governing equation which includes a mass conservation law and two momentum equations known as the Saint-Venant (shallow water) equations:

$$\begin{cases} \frac{\partial H_s}{\partial t} + \frac{\partial (h_s u)}{\partial x} + \frac{\partial (h_s v)}{\partial y} = q_e \\ \frac{\partial (h_s u)}{\partial t} + \frac{\partial (h_s u^2)}{\partial x} + \frac{\partial (h_s uv)}{\partial y} + g h_s \left(\frac{\partial H_s}{\partial x} + S_{fx} \right) = 0 \\ \frac{\partial (h_s v)}{\partial t} + \frac{\partial (h_s v^2)}{\partial y} + \frac{\partial (uv)}{\partial x} + g h_s \left(\frac{\partial H_s}{\partial y} + S_{fy} \right) = 0 \end{cases} \quad (2.1)$$

where h_s is the water depth, $H_s = h_s + Z_s$ and Z_s is ground surface elevation, u and v are the depth-averaged flow velocity in the x and y directions, S_{fx} and S_{fy} are friction slopes in x and y directions, g is the gravitational acceleration, qe represents source–sink terms per unit area:

$$q_e = q_{ir} - q_{ET} - q_{21} \quad (2.2)$$

where q_{ir} is the time series of rainfall and/or irrigation per unit area, q_{ET} is the time series of evapotranspiration per unit area, q_{21} is the exchange flux between the subsurface flow and overland flow per unit area.

It is important to note that a number of approximations are made for derivation of the Saint Venant equations: constant fluid density, hydrostatic pressure distribution, zero surface shear stress with air, neglecting other source–sink terms in flow field, neglecting the momentum flux due to eddy viscosity, and neglecting external momentum-impulse. In addition, water depth h_s is required to be much smaller than wave length or the characteristic length of the water body. The Saint Venant equations are therefore only valid for situations of shallow water and gentle slopes (Weiyan, 1992).

Despite the simplifications involved, solving the Saint Venant equations in their comprehensive form remains a challenge. To overcome this difficulty the first three terms of momentum equations are assumed to be negligible. This is known as the “diffusive-wave” or “zero-inertia” assumption. If the friction slope is approximated by the Manning formula then *u* and *v* velocities can be expressed as (Smerdon et al., 2008):

$$u = -\frac{1}{n_x}\left(\frac{h_s}{1+S_{0x}^2}\right)^{\frac{2}{3}}\frac{1}{\sqrt{\left|\frac{\partial H_s}{\partial x}\right|}}\frac{\partial H_s}{\partial x} \quad ; \quad v = -\frac{1}{n_y}\left(\frac{h_s}{1+S_{0y}^2}\right)^{\frac{2}{3}}\frac{1}{\sqrt{\left|\frac{\partial H_s}{\partial y}\right|}}\frac{\partial H_s}{\partial y} \tag{2.3}$$

where S_{0x} and S_{0y} are ground surface slope, and n_x and n_y are the Manning roughness coefficients in the x and y directions, respectively. The mass balance equation can now be rewritten by substituting Eq 2.3 into the first formula of Eq 2.1 as:

$$\frac{\partial H_s}{\partial t} - \frac{\partial}{\partial x}\left(\frac{hs^{5/3}}{n_x\left(1+S_{0x}^2\right)^{2/3}}\frac{1}{\sqrt{\left|\frac{\partial H_s}{\partial x}\right|}}\frac{\partial H_s}{\partial x}\right) - \frac{\partial}{\partial y}\left(\frac{hs^{5/3}}{n_y\left(1+S_{0y}^2\right)^{2/3}}\frac{1}{\sqrt{\left|\frac{\partial H_s}{\partial y}\right|}}\frac{\partial H_s}{\partial y}\right) = q_e \tag{2.4}$$

Eq 2.4 can be further simplified by replacing $\sqrt{|\partial H_s/\partial x|}$ and $\sqrt{|\partial H_s/\partial y|}$ by $\sqrt{|S_{0x}|}$ and $\sqrt{|S_{0y}|}$ respectively, known as linearized or semi diffusive wave approach, yielding:

$$\frac{\partial H_s}{\partial t} - \frac{\partial}{\partial x}\left(\frac{hs^{5/3}}{n_x\left(1+S_{0x}^2\right)^{2/3}}\frac{1}{\sqrt{|S_{0x}|}}\frac{\partial H_s}{\partial x}\right) - \left(\frac{hs^{5/3}}{n_y\left(1+S_{0y}^2\right)^{2/3}}\frac{1}{\sqrt{|S_{0y}|}}\frac{\partial H_s}{\partial y}\right) = qe \tag{2.5}$$

DrainFlow incorporates two types of boundary condition for the overland flow module, critical depth (Eq 2.6) and the zero depth gradient condition (Eq 2.7) (Panday & Huyakorn, 2004).

$$\frac{\partial H}{\partial x} = \sqrt{g h_s^3} \tag{2.6}$$

$$\frac{\partial H}{\partial n} = \frac{hs^{5/3}}{n_n\left(1+S_{0n}^2\right)^{2/3}} \frac{1}{\sqrt{|S_{0n}|}} \quad (2.7)$$

where n_n and S_{0n} are the Manning roughness coefficient and slope in the direction perpendicular to the boundary respectively.

2.3.2 Tile drains (TD)

The unsteady and non-uniform flow in tile drains is a form of spatially-varied flow (Lemieux et al., 2008), and in *DrainFlow* the free-surface flow in the tile drains is represented by a one-dimensional open circular channel:

$$\begin{cases} \frac{\partial A}{\partial t} + \frac{\partial (AV_D)}{\partial s} = q_{eD} \\ \frac{\partial (AV_D)}{\partial t} + \frac{\partial (AV_D^2)}{\partial s} + gA(\frac{\partial H_{sD}}{\partial s} + s_{fD}) = 0 \end{cases} \quad (2.8)$$

where s is the flow direction in the tile drain, V_D is the velocity magnitude in s direction, A is the cross section area perpendicular to s direction, q_{eD} represents the tile drain source–sink terms, S_{fD} is the friction slope in the s direction.

H_{sD} is the total head:

$$H_{sD} = h_{sD} + Z_D \quad (2.9)$$

where h_{sD} is water depth in tile drain, and Z_D is the elevation of the tile drain base. Beside the other assumptions listed for Eq 2.1, the density and viscosity of the drained water from the tile drain is assumed as for fresh water.

Using the diffusive wave approach and the Manning formula for friction slope, drain velocity (V_D) is expressed as:

$$V_D = -\frac{1}{n_D}\left(\frac{R}{1+S_{0D}^2}\right)^{\frac{2}{3}} \frac{1}{\sqrt{\left|\frac{\partial H_{sD}}{\partial s}\right|}} \frac{\partial H_{sD}}{\partial s} \tag{2.10}$$

where n_D is the pipe drain Manning roughness coefficient, S_{0D} is the pipe drainage slope in flow direction, and R is hydraulic radius (Smerdon et al., 2008).

The geometrical elements of tile drains are defined as:

$$\begin{cases} A = (\theta - sin\theta)\frac{r_0^2}{2} \\ R = \frac{A}{P} = \frac{(\theta - sin\theta)}{\theta}\frac{r_0}{2} \\ T = \frac{2r_0 \sin\theta}{2} \\ \theta = 2\cos^{-1}\left(1 - \frac{2y}{d}\right) \end{cases} \tag{2.11}$$

where P is the wetted perimeter, T is top width of the free surface and θ is the tile drain cross section central angle in radians (J.-O. Delfs et al., 2013). Geometrical elements of a cross section of a tile drain are shown in Fig 2.2.

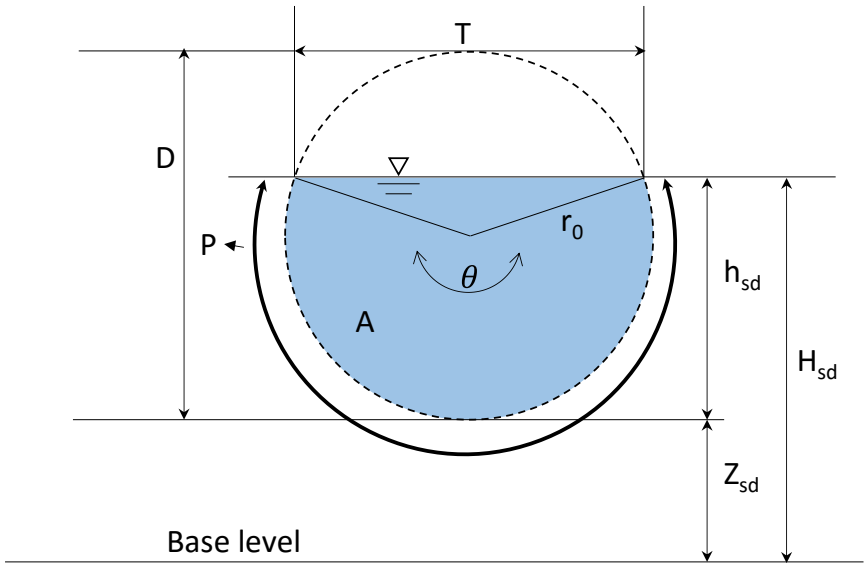

Fig 2.2 Geometrical cross section elements of a tile drain

Combining Eq 2.10 and the Saint-Venant equation, the governing equation of fluid flow in a tile drain is:

$$T\frac{\partial H_{sD}}{\partial t}-\frac{\partial}{\partial s}\left(\frac{AR^{\frac{2}{3}}}{n_d\left(1+S_{0D}^2\right)^{\frac{2}{3}}}\frac{1}{\sqrt{\left|\frac{\partial H_{sD}}{\partial s}\right|}}\frac{\partial H_{sD}}{\partial s}\right)=q_{eD} \quad (2.12)$$

When the tile drain is completely full, any extra water flow from the further upstream tiles may cause the inside pressure of the tile drain to be more than the outside pressure. As a result, the seepage direction would change and the tile drain would then serve as a source of water for groundwater. *DrainFlow* always checks the computed pressure of tile drains to detect the discharge/recharge sources in the model.

2.3.3 Open drains, channels and river networks (ODCR)

The overland flow module is able to predict the surface flow and depth in the open drains, channels and rivers. However, a high density model mesh is required in the open drain locations. To accelerate the *DrainFlow* simulation procedure, it is assumed that flow in the open drains is one dimensional, therefore to simulate flow in open drains the 2-dimensional Saint Venant equations is simplified as:

$$\frac{\partial H_{sc}}{\partial t}-\frac{\partial}{\partial c}\left(\frac{hsc^{\frac{5}{3}}}{n_c\left(1+S_{0c}^2\right)^{\frac{2}{3}}}\frac{1}{\sqrt{|S_{0c}|}}\frac{\partial H_{sc}}{\partial c}\right)=q_{ec} \quad (2.13)$$

where c is the flow direction in open drain, h_{sc} is the water depth in channel, n_c and S_{0c} are the channel Manning roughness coefficient and slope in the c direction, q_{ec} is the sink/source term, and H_{sc} is the channel total head:

$$H_{sc}=h_{sc}+Z_c \quad (2.14)$$

where Z_c is the channel base elevation.

2.3.4 Subsurface flow module (SSM)

In the *DrainFlow* code, saturated and unsaturated flow in a porous medium utilises Richards equation as the governing equation:

$$\nabla.(K_r K_s \nabla H) = S_s S_w \frac{\partial h_p}{\partial t} + \varphi \frac{\partial S_w}{\partial t} + qe_s \qquad (2.15)$$

where K_s is the saturated hydraulic conductivity tensor, S_s is the specific storage coefficient, S_w is the water saturation, $h_p = H-Z$ is the pressure head , H is the total head, Z is the elevation above an arbitrary datum, φ is the porosity, K_r is the relative permeability, and qe_s represent subsurface flow source-sink terms per unit area.

In order to solve the Richards equation the relationships between S_w-h_p and K_r-S_w are required. In the *DrainFlow* code an analytical expression between the S_w-h_p and K_r-S_w terms is implemented following Van-Genuchten (1980):

$$S_e = \begin{cases} (1+|\alpha h_p|^{n_{VG}})^{-m_{VG}} & \text{if } h_p < 0 \\ 1 & \text{if } h_p \geq 0 \end{cases} \qquad (2.16)$$

$$K_r = S_e^{l_{VG}} (1-(1-S_e^{1/m_{VG}})^{m_{VG}})^2 \qquad (2.17)$$

where S_e is the effective saturation, l_{VG} is a pore connectivity parameter (usually assume to be 0.5), α and $n_{VG}>1$ are the two Van Genuchten fitting curve parameters and $m_{VG}=1-1/n_{VG}$.

2.4 Coupling methods

For coupling the overland and subsurface flow modules, the overland flow module is a boundary condition for the subsurface flow domain. Similarly, open drains are a boundary condition for the overland flow domain. The tile drains, however, are considered as an internal boundary condition for the subsurface flow module, which allows the infiltration rate to be calculated directly from the Richards equation for the tile drain module. Fig2. 3 shows all potential connections between the modules in *DrainFlow.*

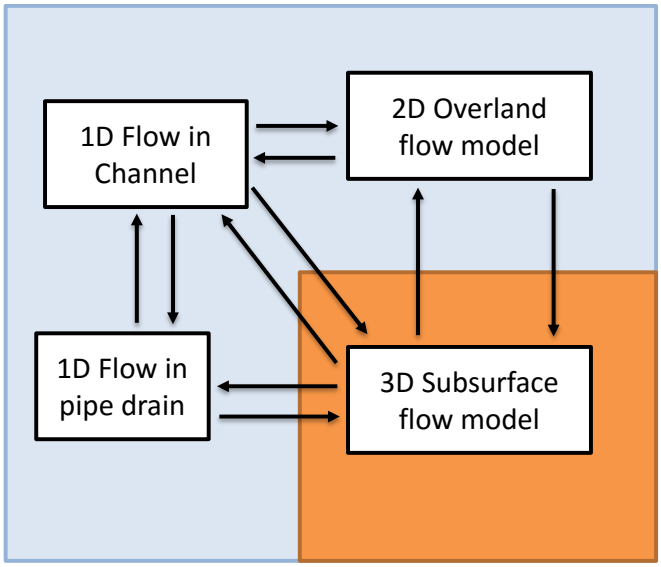

Fig. 2.3 *DrainFlow* modules and potential connections

2.4.1 Subsurface and overland flow connection

At the start of each time step, surface flow depth (h_s), infiltration rate (I) and effective rainfall rate (q_{IR}) for all surface-subsurface flow interface boundaries are calculated, respectively, by the overland flow module, Eqs 2.18 and 2.19.

$$I = K_s K_r \nabla H \tag{2.18}$$

$$q_{IR} = q_{ir} - q_{ET} \tag{2.19}$$

The calculated values are then used as decision making parameters to select either Neumann or Dirichlet boundary conditions for the interface boundaries between overland flow and subsurface flow domain.

The current infiltration rate of the model is compared with effective rainfall. If the infiltration rate is larger than the effective rainfall ($I>q_{IR}$) or runoff does not show up on the overland flow ($h_s \leq 0$), then all the effective rainfall infiltrates to the subsurface model. Consequently, in the overland flow module the exchange flux between subsurface flow and overland flow (q_{21}) is set as the effective rainfall, while in the subsurface flow module the interface boundary condition is set as a Neumann boundary condition with q_{IR} specified flux.

DrainFlow keeps these conditions until either the infiltration rate becomes smaller than effective rain ($I \leq q_{IR}$) or runoff flows off as overland flow ($h_s > 0$). Then, the excess rainfall to the infiltration flows as runoff on the overland flow domain. In this situation, the interface boundaries in the subsurface flow module switches from the specified flux (Neumann) to a constant head (Dirichlet) boundary condition. The constant head boundary would be provided by the overland flow module (H_s) in each time step. Consequently, in the overland flow module the exchange flux between subsurface flow and overland flow (q_{21}) is set as the infiltration rate (I).

To provide an automatic switching mechanism between Neumann and Dirichlet boundary conditions a mixed boundary condition is introduced to the *DrainFlow* code:

$$\begin{cases} K_r K_s \nabla H = N_0 + R_b (H_s - H) \\ R_b = K'_s / M \end{cases} \qquad (2.20)$$

where H_s is the surface water total head, H is the groundwater total head, R_b is the conductance of the interface boundary material, K's and M are respectively the hydraulic conductivity and the thickness of a thin layer next to the interface boundary. Eq 2.20 represents a Neumann boundary condition when $R_b(H_s-H)=0$, and a Dirichlet boundary condition when R_b is a large number and N_0 =0 (Chui & Freyberg, 2007).

By using a Heaviside function ($Hv(x)$),

$$Hv_{(x)} = \begin{cases} 0, & x < 0 \\ 1, & x \geq 0 \end{cases} \quad (2.21)$$

where x is the Heaviside function variable, the infiltration rate exchange between the overland flow and groundwater can be defined by:

$$I_{OL\leftrightarrow SSM} = [Hv(-h_p)\, Hv(-h_s)]\, q_{IR} + [Hv(-h_p) + Hv(-h_s)]\, R_b(H_s - H) \quad (2.22)$$

where $I_{OL\leftrightarrow SSM}$ is infiltration exchange between the overland flow and subsurface flow.

2.4.2 Tile drain and subsurface module connections

A seepage-face boundary condition is implemented for tile drains in the subsurface flow module. Once water flows in a tile drain or the pressure head at the drain boundary calculated by the subsurface model becomes greater than zero, the seepage-face boundary switches from a zero-flux to a constant head boundary condition.

By using a Heaviside function the infiltration rate exchange between tile drain and groundwater can be expressed as:

$$I_{DM\leftrightarrow SSM} = (Hv_{(hp)} + Hv_{(hsd)})RD_b(H_{sd} - H) \quad (2.23)$$

where $I_{DM\leftrightarrow SSM}$ is the infiltration rate exchange between tile drain and subsurface flow and RD_b is the entrance seepage conductance due to minor head loss at tile drains entrance.

H_{SD} is the total head in the tile drain:

$$H_{sD} = Z_{out} + S_{0D} \times l_{sD} + h_{sD} \quad (2.24)$$

where Z_{out} is the tile drain outlet elevation, S_{0D} is the pipe drainage slope in flow direction, and l_{sD} is distance from the tile drain outlet .

2.4.3 Open drain connections to overland flow and subsurface flow module

To connect the overland flow and the open drain modules, at the start of each time step, the exchange flux rate between overland flow and open drain (q_{oc}) is calculated by the overland flow module. Then q_{oc} adds to the sink/source terms of open drain equation (Eq 2.13).

In addition, to connect the subsurface flow and open drain modules, the exchange infiltration rate between open drain and subsurface flow ($I_{OD\leftrightarrow SSM}$) is calculated as:

$$I_{OD\leftrightarrow SSM} = [Hv(-hp)\ Hv(-hsc)]\, bc \times q_{IR} + [Hv(-hp) + Hv(-hsc)]\, R_{bc}(H_c - H) \quad (2.25)$$

where bc is the open drain width, Rb_C is the conductance of open drain materials.

$I_{OD\leftrightarrow SSM}$ also adds to the sink/source terms of the channel equation.

Therefore, by adding q_{oc} and $I_{OD\leftrightarrow SSM}$ to the sink/source terms of the channel equation, q_{ec} is expressed as:

$$q_{ec} = q_{oc} + I_{OD\leftrightarrow SSM} + q_{ir} - q_{ET} \quad (2.26)$$

where q_{oc} is the surface runoff as calculated directly by the overland flow module, and $I_{O\leftrightarrow SSM}$ is the exchange infiltration rate between open drain and subsurface flow.

2.4.4 Tile drain and open drain (ODCR) connections

Tile drains outflows often collect at an open drain known as the main drain. Flow in the main drains is simulated by the open drain module. To link the tile drains to a main drain (open drain), the computed tile drain outflow at the locations of each tile drains outlet are considered as an internal boundary condition for the main drain. Moreover, several tile drains as internal boundaries could be added to the main drain.

Alternatively, in some circumstances the main drain also could have effective impact on tile drains operation. For example, when water level in the main drain increases to an elevation higher than tile drain outlet level, then the main drain acts as a barrier for the tile drain flow and water push back into the tile drains.

For simulating this impact in the *DrainFlow* code, once the total head in the main drain increases to an elevation higher than the tile drain outlet level, the exceeded head over the tile drain outlet level automatically adds to the elevation of the tile drain base.

$$Z_{Do} = Z_{Db} + H_{mT} \quad (2.27)$$

where Z_{Do} is the calculated tile drain base elevation at the outlet, Z_{Db} is the actual elevation of the tile drain at the outlet and H_{mT} is the exceed head

over the tile drain base at the out let. The amount of H_{mT} is calculated by the main drain module for each time step.

2.5 Smoothed Heaviside function

Switching between Neumann and Dirichlet boundary condition can cause nonlinearity problems. In *DrainFlow* code to avoid these issues the Heaviside function *Hv(x)* is replaced by smoothed Heaviside functions. Many smoothed Heaviside functions are recommended in the literature, one utilised here being the logistic function:

$$Logistic(x, err) = (1 + exp(-\frac{x}{err}))^{-1} \quad (2.28)$$

where *err* is the specified smoothing factor.

Another example is the *flc2hs(x, err)* function of COMSOL (COMSOL, May 2012) which is a smoothed Heaviside function with continuous second derivative without overshoot. The values of the *flc2hs(x, err)* is defined as *0* for *x<-err*, *1* for *x>err* and a sixth-degree polynomial fitting curve for the gap between *-err and err (-err<x<err)*.

Fig 2.4 shows an approximation of logistic and *flc2hs(x, err)* smoothed Heaviside functions using a range of smoothing factors (*err*). Decision about the optimum *err* values is a trade-off between model accuracy and convergence time. Depending on the model condition, *err* values should be decided separately for each simulation.

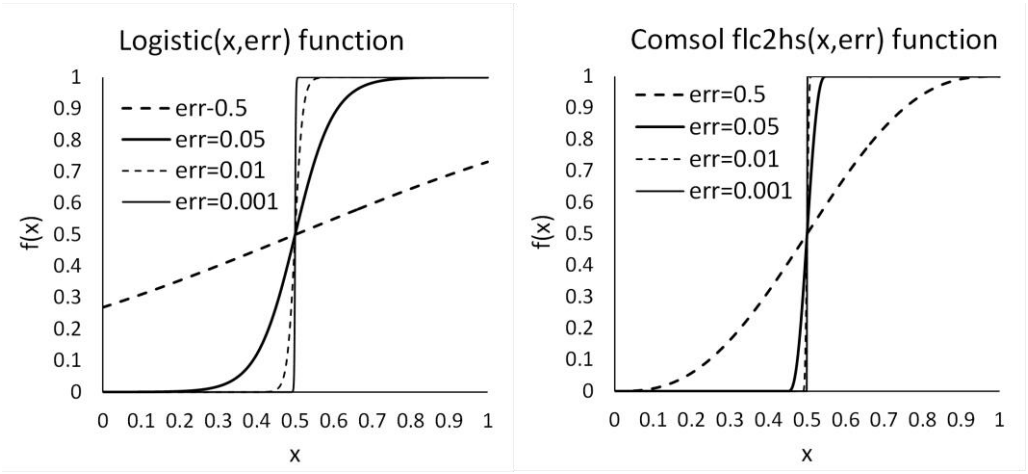

Fig 2.4 A comparison between smoothed Heaviside functions with different smoothed parameters: Logistic and Comsol flc2hs functions. These smoothed functions are used as replacements for the Heaviside function in *DrainFlow*.

2.6 Benchmark tests

To check the model capability on integrated surface-subsurface flow problems, this section gives some comparisons between *DrainFlow* and seven known coupled surface-subsurface flow codes: *CATHY* (M. Camporese et al., 2010), *HydroGeoSphere (HGS)* (Aquanty Inc., 2013; Brunner & Simmons, 2012), *OpenGeoSys (OGS)* (J.-O. Delfs et al., 2012; J. O. Delfs, Kalbus, et al., 2009; J. O. Delfs, Park, et al., 2009), *ParFlow* (Kollet & Maxwell, 2006; Maxwell & Miller, 2005), *PAWS* (Shen & Phanikumar, 2010), *PIHM* (Kumar et al., 2009; Qu & Duffy, 2007), and *tRIBS + VEGGIE* (Ivanov et al., 2008; Ivanov et al., 2010; Kim et al., 2013).

All codes apply the Richards equation for subsurface flow, coupled with some form of the Saint - Venant equations for estimation of surface flow discharge. However, they use a different formulation of partial differential

governing equations, interface boundary conditions and numerical methods.

The comparisons utilise five frequently published integrated surface-subsurface flow problems: infiltration excess (IE), saturation excess (SE), slab (Sb), return flow (RF) and V-catchment benchmarks (VC). These problems, organized in order of increasing complexity, are given by Maxwell et al. (Maxwell et al., 2014). The benchmarks have minimal complexity in domain geometry, topography, hydraulic hydrological properties and atmospheric forcing.

The benchmarks contain a simple tilted V-catchment or hill-slope for surface flow domain and a sloped layer of soil as subsurface flow domain. All simulations open with a rainfall event and follow by an evapotranspiration period with no further rainfall. The benchmarks all use the same values for Van-Genuchten parameters (α and n_{VG}), residual and saturated water content (S_{res} and S_{sat}), porosity (φ) and specific storage (S_s). However, different values are implemented for saturated hydraulic conductivity (K_s), initial water table (*Iwt*), ground surface slope (S_x) in each problem. A conceptual model with a list of utilised parameters for infiltration excess, saturation excess, slab and return flow benchmarks is illustrated in Fig 2.5.

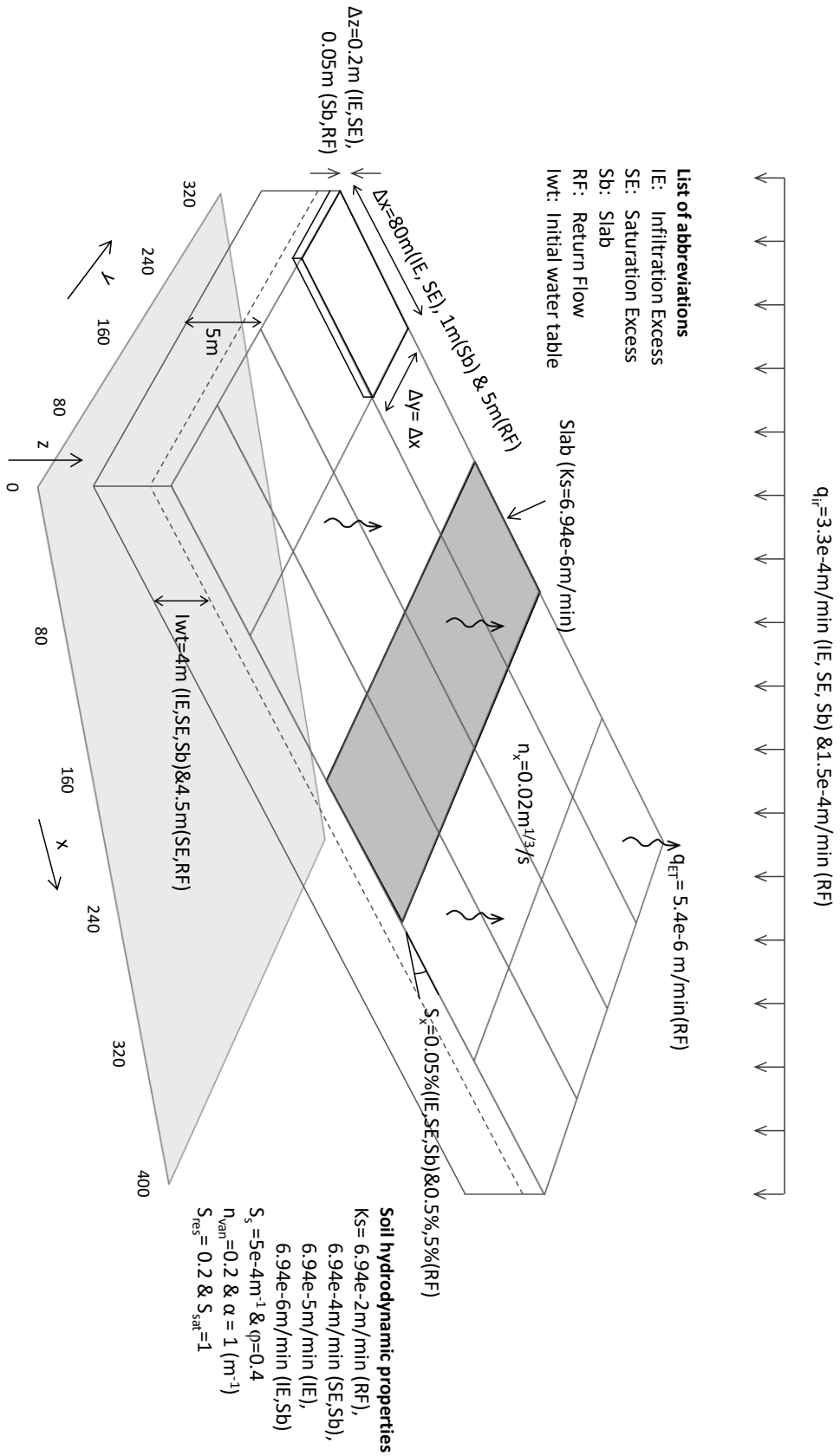

Fig 2.5 Conceptual model and list of parameters used in infiltration excess (IE), saturation excess (SE), slab (Sb) and return flow (RF) benchmarks.

2.6.1 Infiltration excess runoff scenarios

For the first test the *DrainFlow* code simulates infiltration excess overland flow, also known as Hortonian runoff. This exercise includes two scenarios: (i) saturated hydraulic conductivity at 6.94×10^{-6}m/min and (ii) saturated hydraulic conductivity at 6.94×10^{-5}m/min. The hydraulic conductivities for both scenarios were selected to be lower than the rainfall rate, generating a Hortonian runoff condition.

Both simulations start with a constant rainfall rate of 3.3×10^{-4} m/min for 200 min and followed by a 100 min of drainage period. Evapotranspiration was neglected for both scenarios. Therefore, the rainfall is equal to effective rainfall for this example.

Predicted discharge at the outlet by *DrainFlow* and the other integrated hydrologic models (called hereafter as “IHMs”) given by Maxwell et al (Maxwell et al., 2014) are shown in Fig 2.6.a. The simulated hydrographs show that in both scenarios runoff occur shortly after the beginning of rainfall. Apart from an earlier arrival at the steady state condition in the first scenario, *DrainFlow* has a reasonably good agreement with the other IHMs.

In addition, a sensitivity analysis was carried out to investigate the effect of the *M* parameter on the discharge peak in the second scenario. *DrainFlow* was run for a wide range of *M* from 0.1, 0.01 to 1e-7 m and the discharge peaks calculated as 7.18, 7.17 and 7.12 m^3/min respectively. Even with a large change in the *M* magnitude, *DrainFlow* does not show sensitivity in

predicting the discharge peak. However, simulation time is increased by implementing smaller values for *M*.

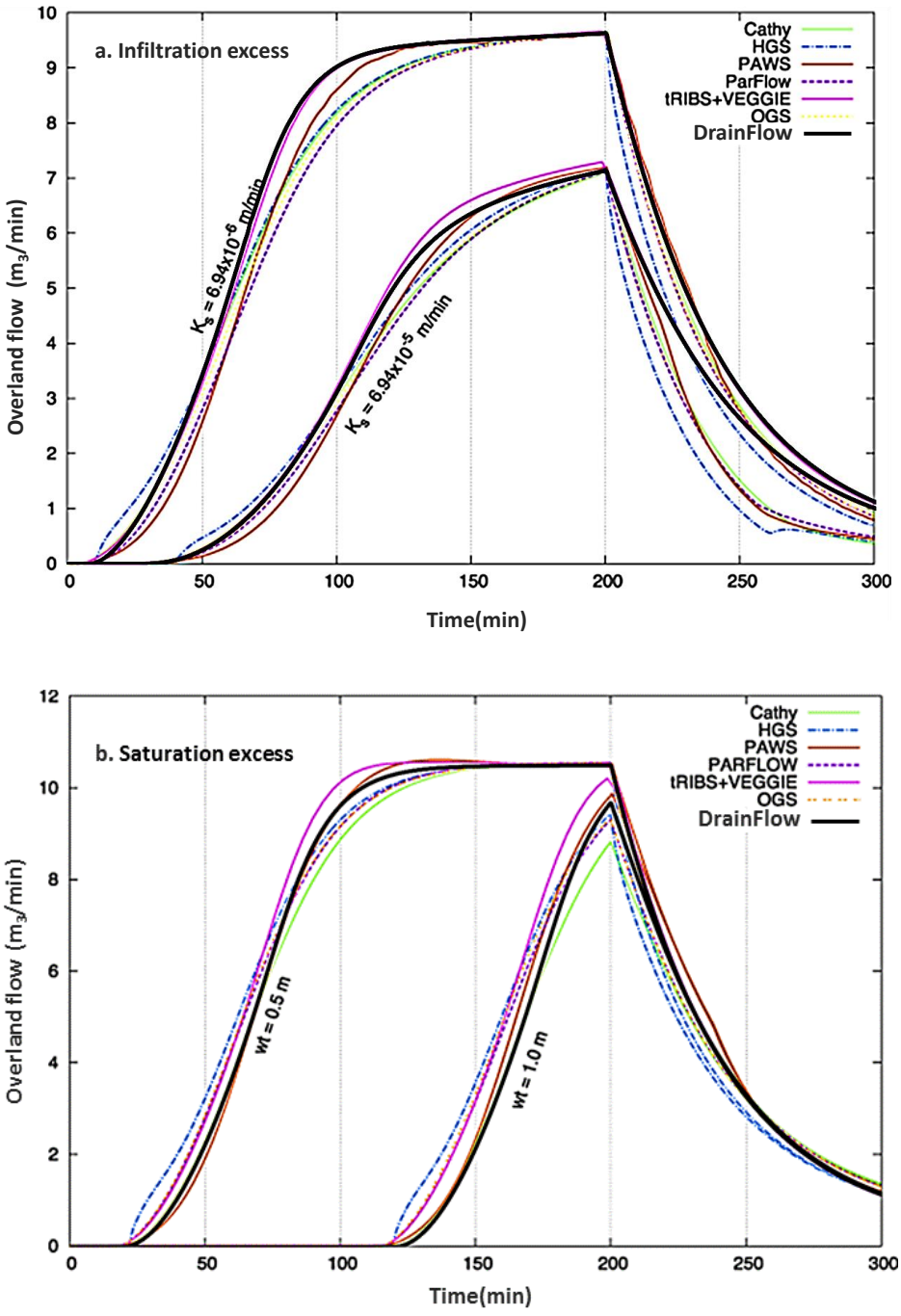

Fig 2.6 Comparisons between *DrainFlow* and the other IHMs (given by Maxwell et al. (Maxwell et al., 2014)) for predicting overland-flow hydrographs at the hill-slope toe; (a). infiltration excess runoff; (b). saturation excess runoff benchmarks

2.6.2 Saturation excess runoff scenarios

The saturation excess runoff benchmark is very similar to the infiltration excess cases but the hydraulic conductivity is larger than the rainfall rate ($q_{IR}/K_s = 0.467$). This benchmark also includes two scenarios: the initial water table located at 1 and 0.5 m below the ground surface level. The overland flow hydrographs at the hillslope outlet calculated by *DrainFlow* and the other models are shown in Fig 2.6.b.

At the start of both scenarios the entire amount of rainfall leads to raising the groundwater table. This process continues until the groundwater table reaches the ground surface. From this point (also known as ponding time) a portion of rainfall flows off as runoff. The model estimated the ponding times to occur at around 22 and 121 minutes for the first and second scenarios respectively. A comparison between the hydrographs of the various models in Fig 2.6.b indicates the *DrainFlow* hydrographs and ponding time predictions are similar to the other IHMs.

2.6.3 Slab case

The slab benchmark case was introduced by Kollet and Maxwell (Kollet & Maxwell, 2006) to challenge coupled surface-subsurface flow codes when the soil is not homogeneous. The slab benchmark domain is very similar to saturation excess runoff scenario, but a thin slab with low hydraulic conductivity is located at the top centre of the subsurface flow domain. The dimension of the slab is 100 m in length, 5 cm in thickness, and 320 m in width. The slab saturated hydraulic conductivity is 6.94×10^{-6} m/min, which is 100 times less than the rest of subsurface flow domain.

DrainFlow model runs for the slab benchmark and the calculated hydrograph at the outlet of the hill-slope are compared with the other surface-subsurface model in Fig 2.7.

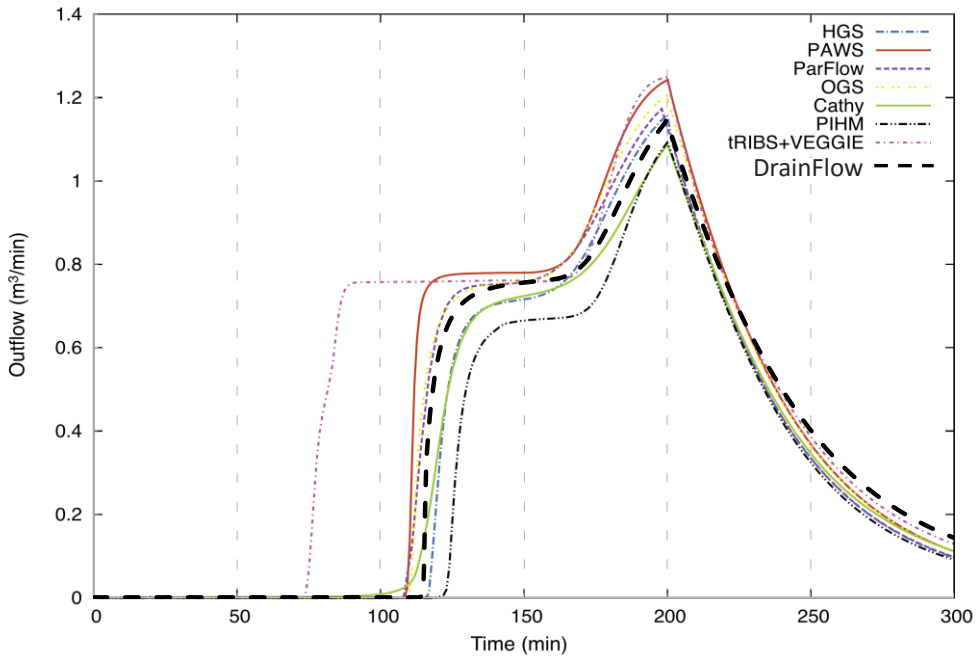

Fig 2.7 Comparison between *DrainFlow* and the other IHMs overland-flow hydrographs (Maxwell et al. (Maxwell et al., 2014)) at the hill-slope outlet

As a response to the soil heterogeneity specified in the benchmark, *DrainFlow* predicts step-like hydrographs at the hill slope outlet. The first jump in the hydrograph results from the runoff generated by the slab component. Fig 2.7 shows the *DrainFlow* overland flow hydrograph increases rapidly to 0.75 m^3/min at about 115 minutes and discharge almost remains stable for a short period of time. However, the hydrograph peaks again at 1.14 m^3/min at around 160 minutes due to late runoff generated by the part upper than the slab. Fig 2.7 shows the maximum discharge calculated by *DrainFlow* is very similar to the results of *Parflow* and *OGS* for the slab benchmark.

2.6.4 Return flow

The hill-slope in the return flow benchmark is much steeper than the other benchmarks. The *DrainFlow* code simulated two scenarios, with S_x set at 0.5% and 5% respectively. The model was run for continuous rainfall at 1.5×10^{-4} m/min for 200 minutes followed by an evapotranspiration period of 200 minutes with an evapotranspiration rate of 5.4×10^{-6} m/minute.

Fig 2.8 illustrates the intersection point between the water table and ground surface versus time, derived from *DrainFlow* and the other models given by Maxwell et al. (Maxwell et al., 2014).

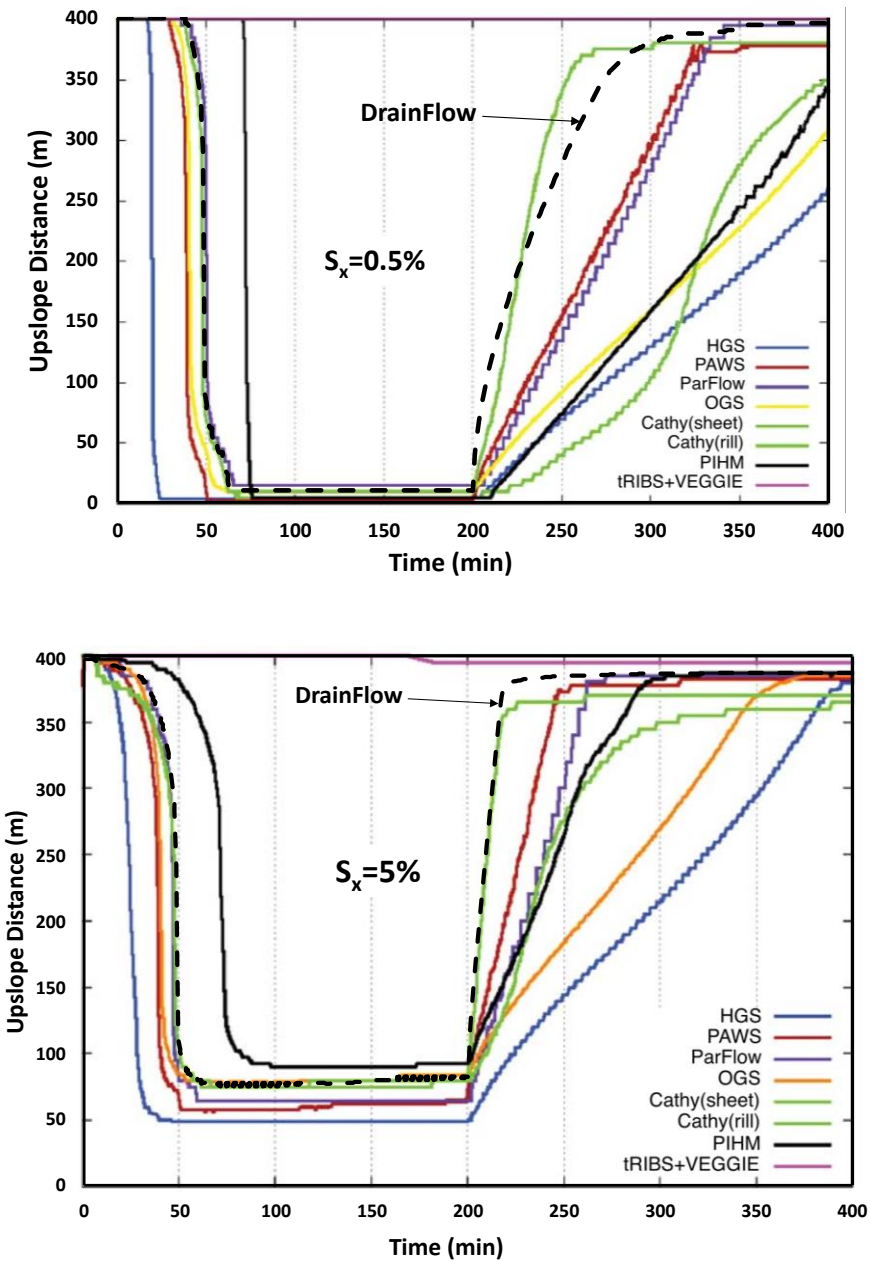

Fig 2.8 The intersection point between the water table and ground surface as a function of time for Sx=0.5 and 5% slope, as obtained from *DrainFlow* and other models.

Although there are some similarities, the coupled surface-subsurface flow models show a range of predictions. Results of *DrainFlow* for the period of rainfall are very similar to the *ParFlow* and *Cathy* codes and for the evaporation period are similar to the *Cathy* code prediction in both scenarios.

2.6.5 V-Catchment

The V-catchment benchmark comprises two 1000 x 800m tilt planes, joined by a 1000 x 20m channel in the middle (Fig 2.9). The ground surface slopes are 2% and 5%, respectively, parallel and perpendicular to the channel direction. The benchmark starts with a 90min uniform rainfall at the 1.8 10^{-4}m/min rate and follows by 90min recession period. Despite the fact that the V-catchment benchmark does not contain a subsurface flow domain, this test could challenge the methodology used to connect the 2D overland flow and 1D open drain modules. Fig 2.9 compares the channel hydrograph at the outlet predicted by *DrainFlow* with the other interaction surface-subsurface flow models of Maxwell et al. (Maxwell et al., 2014).

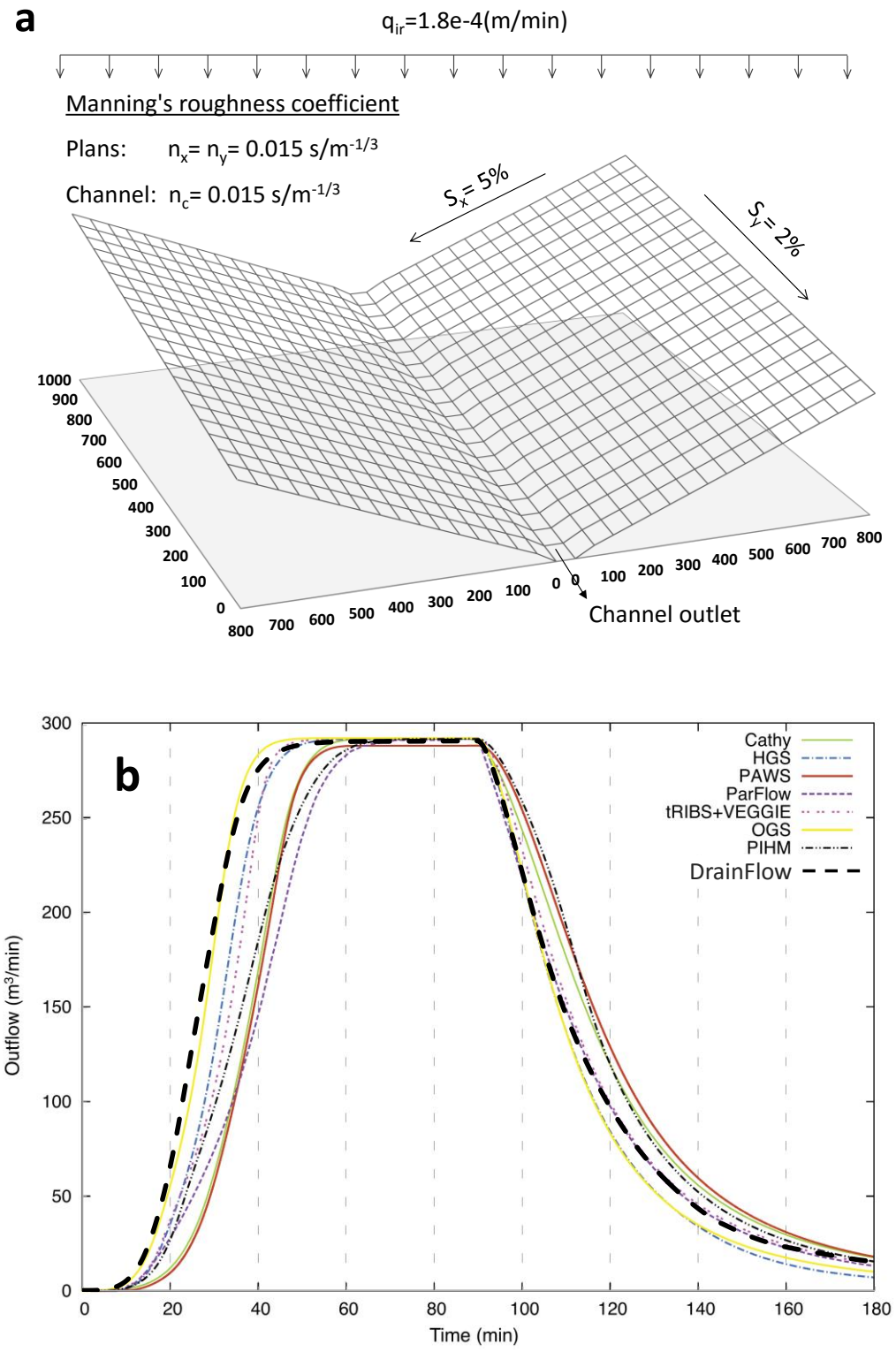

Fig 2.9 V-catchment benchmark: (a). conceptual model, (b). channel outflow hydrographs at the channel outlet predicted by *DrainFlow* and the other IHMs by Maxwell et al. (Maxwell et al., 2014)

The *DrainFlow* hydrograph is similar to the *OGS* code prediction in the rising limb and is close to the *Parflow* model in the falling limb. The

maximum discharge calculated by *DrainFlow* is 291.71 m^3/min and it is accrued at around 83 minutes.

2.7 Application of *DrainFlow* for tile drainage examples

DrainFlow was run for two hypothetical tile drainage examples. The first example includes a high-resolution and small-scale study containing a combination of different modules. The second example is designed to challenge the code in upscaling issues. For the second example the *DrainFlow* models an area 10 times larger than example 1 and contains up to 80 tile drains and two open drains.

2.7.1 Example 1

For the first example *DrainFlow* is set up for one tile drain which includes a 2D overland-flow, a 3D saturated-unsaturated flow, an open drain, and a tile drain module. The tile drain length is 100 m with a 10 cm radius, located at depth 2m below the ground surface. The subsurface flow domain comprised a homogenous and isotropic soil with a gentle 1-dimensional slope a right angles to the tile drain direction. The length, width and height of the soil layer are 100, 100 and 5m respectively. Fig2.10 shows the conceptual model and utilised parameter values.

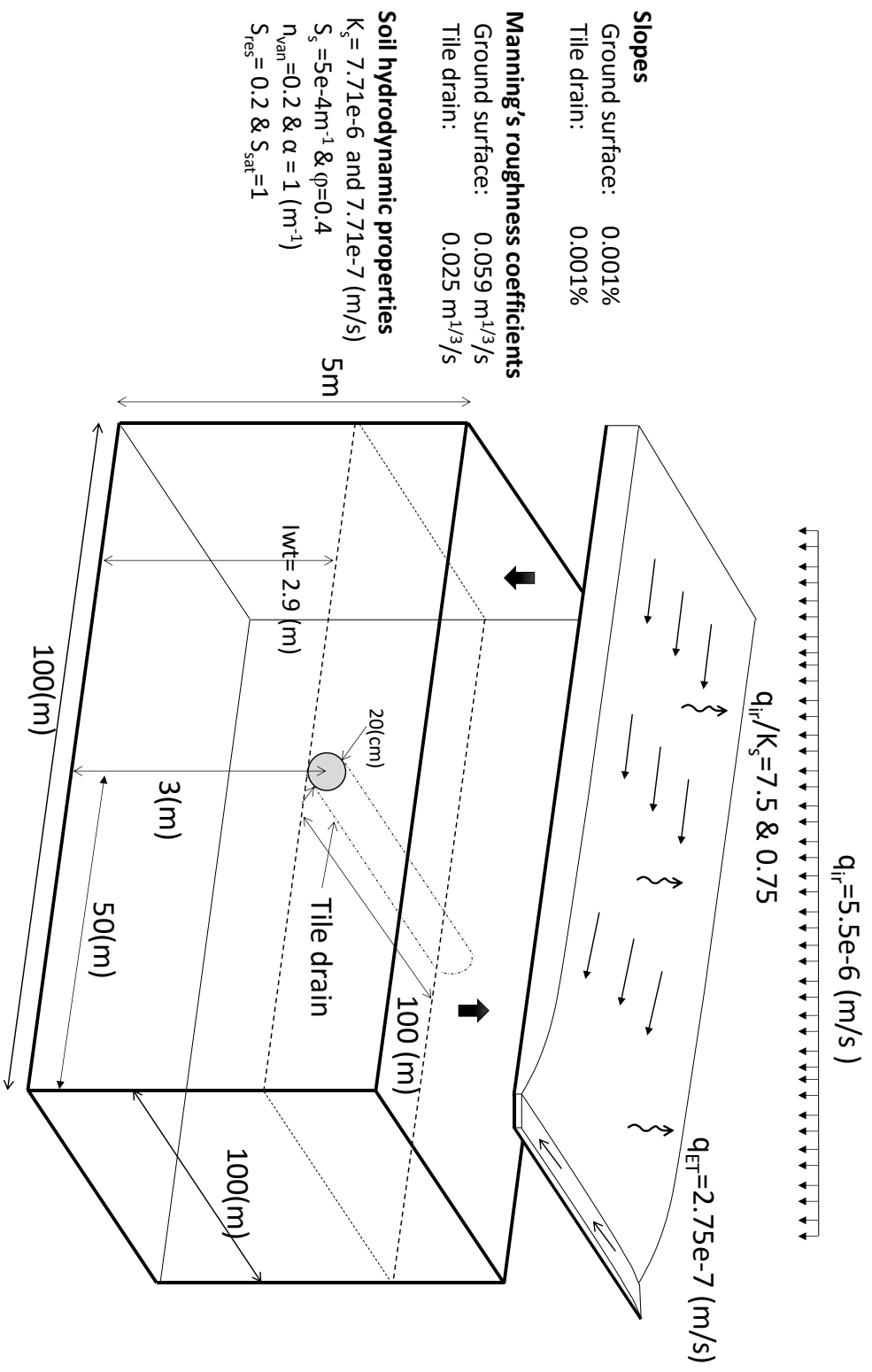

Fig 2.10 Example 1: untilised conceptual model of overland-flow, subsurface flow, tile drain, open drain module, and parameter values.

The model was run for two scenarios to simulate complete infiltration and saturation excess runoff conditions. The hydraulic conductivity values

were set as smaller and larger than the effective rainfall rate for the infiltration and saturation excess runoff scenarios respectively.

The rainfall was fixed at a uniform rate of 5.5×10^{-6} m/s for a two-day period, followed by 8 days of evapotranspiration at a constant 2.75×10^{-7} m/s. Hydraulic conductivity values were set at 7.71×10^{-7} and 7.71×10^{-6} m/s for the infiltration and saturation excess conditions, respectively. The initial water table was located at the base of the tile drain at 2.1m depth below the ground surface.

The simulated hydrographs at the outlets of the open drain and the tile drain are shown in Fig 2.11 for the infiltration and saturation excess scenarios.

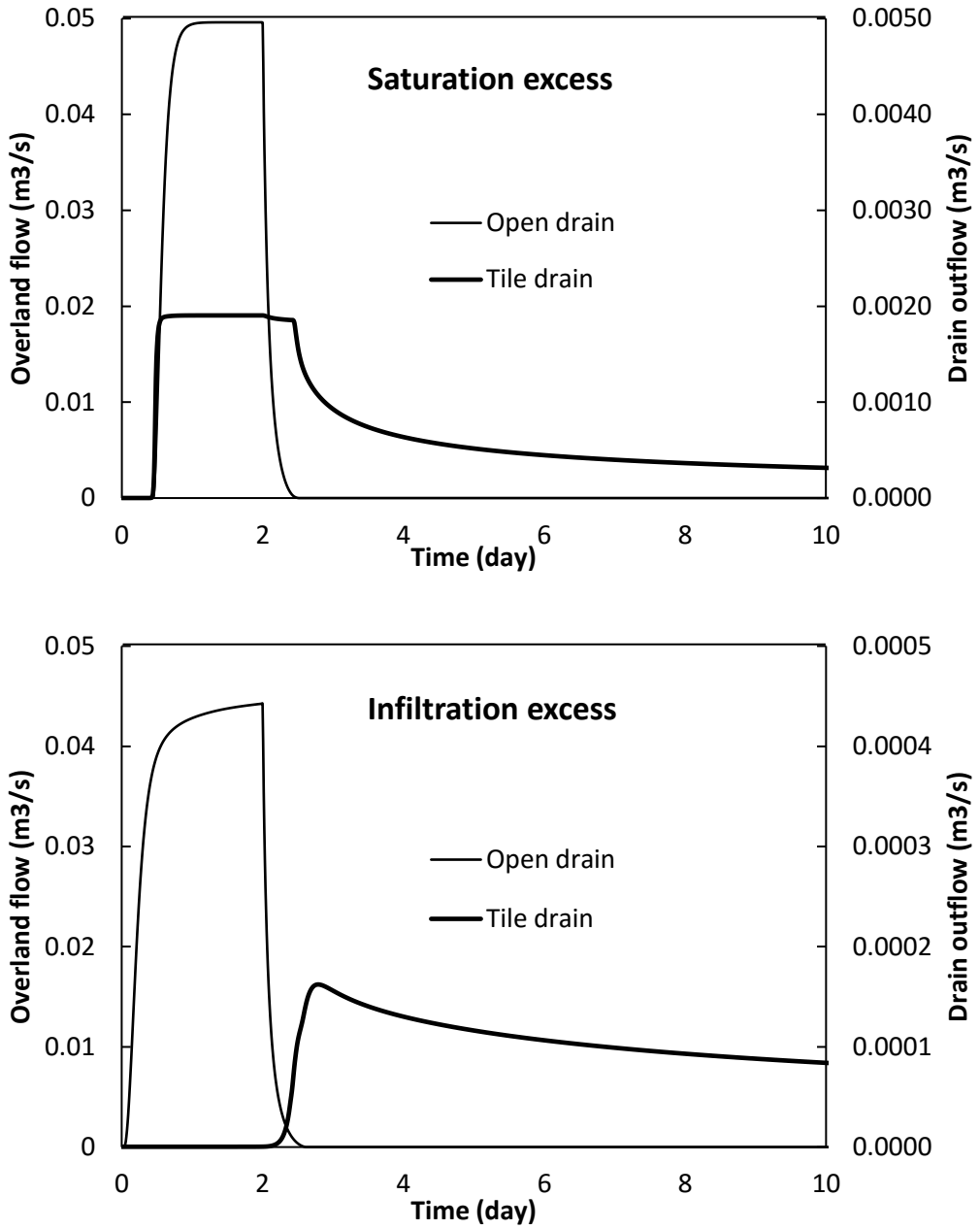

Fig 2.11 *DrainFlow* overland flow and tile drain hydrographs for saturated and infiltration excess scenarios for example 1

In the saturation excess scenario (infiltration rate > rainfall rate), all rainfall entirely infiltrates and raises the groundwater table for the first 11 hours of simulation. At this point (ponding time), the soil profile becomes fully saturated and thereafter a portion of rainfall flows toward the open drain via overland flow. From the ponding time the hydrograph has a rapid jump

to 0.049 m^3/s in less than *2* hours and then remains stable for the rest of rainfall period.

However, in the infiltration excess scenario (infiltration rate < rainfall rate) just a portion of rainfall infiltrates to the soil and the excess moves by overland flow to the open drain. This creates a hydrograph jump to $0.044m^3/s$ just after rainfall initiation and the outflow during the simulation time never reaches a steady state condition.

The tile drain hydrograph in the saturation excess scenario starts rising and reaches its peak almost at the same time as the overland flow, at around 11 hours. The tile drain hydrograph remains stable at about $0.002m^3/s$ to the end of the rainfall period. On the other hand, in the infiltration excess scenario, there is a 2.1 day delay between the beginning of the rainfall and the hydrograph peak in the tile drain. Similar to the open drain hydrograph, the tile drain hydrograph never reaches a steady state condition.

Effect of n and Sx on tile drain hydrograph

Compared to traditional drainage models, the *DrainFlow* code has the advantage of calculating the land surface recharge as a part of the model solution. Therefore, any change in the ground surface parameters (such as slopes, land use, evaporation and Manning roughness coefficient) has a direct effect on the land surface recharge. This then influences subsurface flow and tile drain outflows.

To illustrate these advantages, the saturation excess scenario model was run for a range of ground surface slopes and Manning roughness

coefficients: S_x = 10^{-4}, 10^{-5} and 10^{-6} and n_x = n_y = 0.1, 0.06 and 0.02. The simulated tile drain hydrographs for each model run are shown in Fig 2.12.

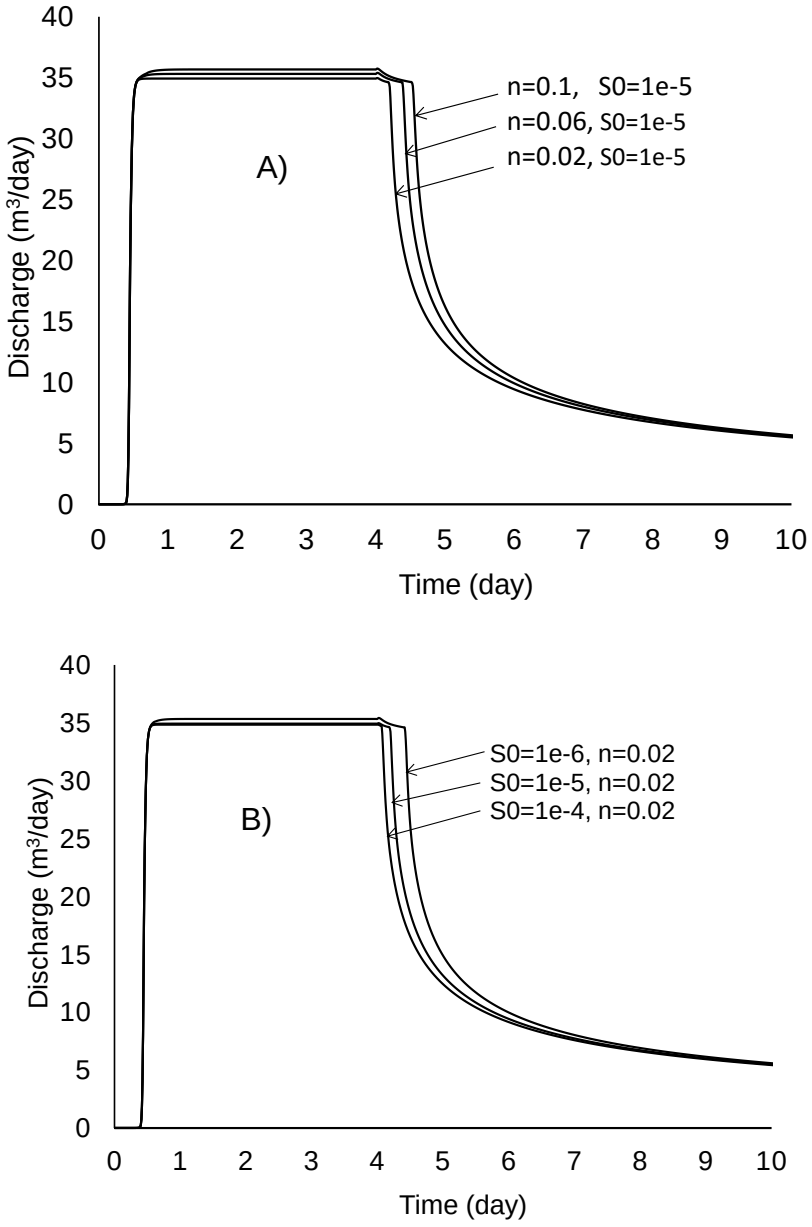

Fig 2.12 Tile drain hydrographs arising from (A). different ground surface Manning roughness coefficients and (B). ground surface slopes

The tile drain hydrographs show increasing the Manning roughness coefficient coupled with decreasing the ground surface slope would increase the total volume of water drained by the tile drain. Increasing Manning roughness coefficient from 0.02 to 0.06 and 0.1 $m^{1/3}/s$ resulted in

2.6% and 5.6% increases in the cumulative tile drain outflow respectively. However, reducing the ground surface slope from 0.0001 to 0.001 and 0.01%, respectively, resulted in 3.8% and 5.5% increments in cumulative tile drain outflow.

2.7.2 Example 2 (Upscaling):

For the second hypothetical tile drainage example the area of modelling is 10 times enlarged compared to Example 1. Also, the number of tile drains increase from one tile drain in first example to 10, 20, 40 and 80 tile drains. Moreover, another open drain module is added to collect the tile drain outflows as a main drain. However, the soil types, rainfall rate, evapotranspiration rate, tile drain types, and tile drains depth remains as for Example 1. Fig 2.13 shows a conceptual model for the case of 10 tile drains, together with utilised parameters.

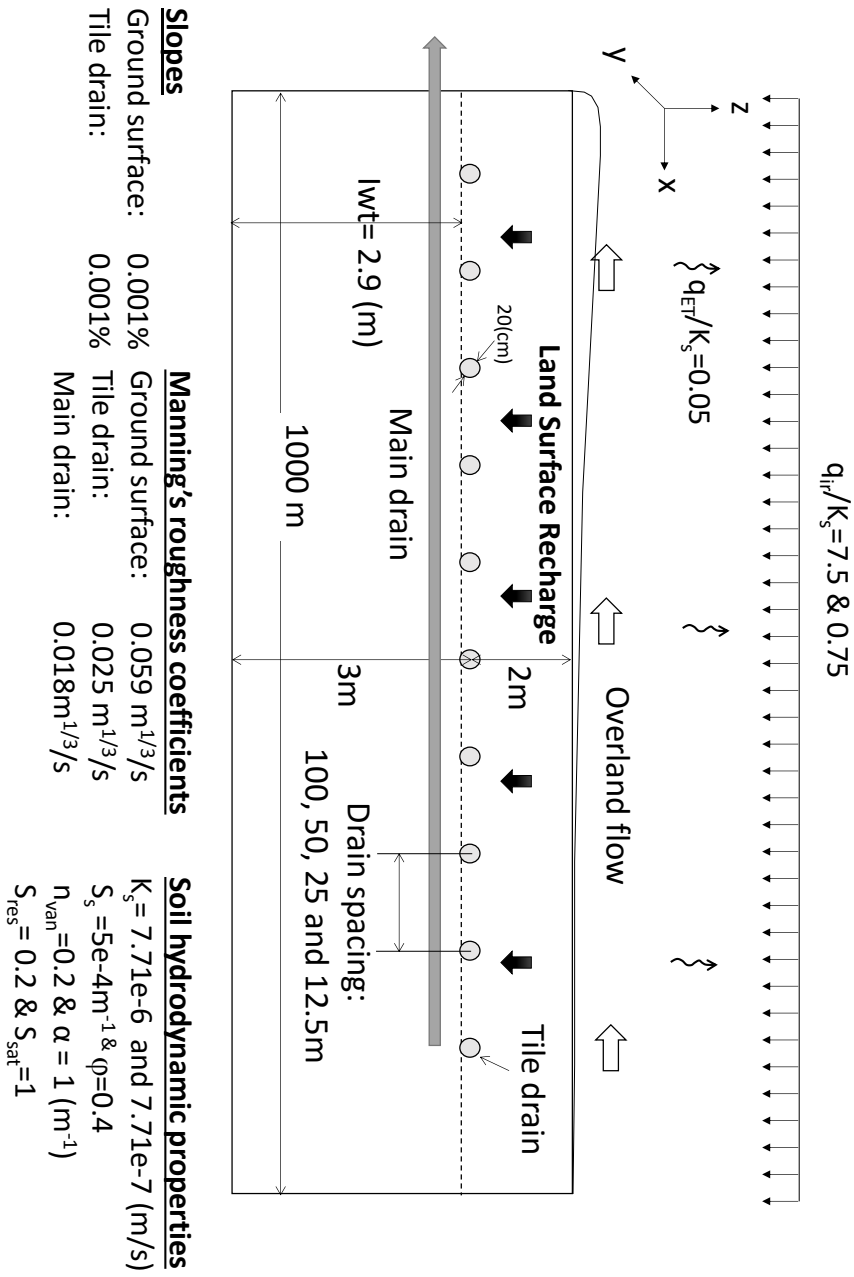

Fig 2.13 Example 2: conceptual model of overland-flow, subsurface flow, tile drains, main drain, and utilised parameters

It would be expected to take much longer to solve for Example 2 than Example 1, due to more finite elements cells (particularly in the subsurface flow domain), and more tile drain modules. However, making some simplification assumptions were made that significantly facilitates the simulation process.

The first simplification involves reducing the subsurface and overland flow dimensions. The surface and subsurface flow in the *y* direction, which is parallel to the tile drains direction, is assumed to be negligible. Therefore, the dimensions of overland flow module drops from 2 to 1 dimension. Similarly, the subsurface model dimension is dropped from 3 to 2-dimensions. This greatly reduces the number of utilised finite element cells in the model. For instance, in the 80 tile drains case the total number of finite element cells is reduced from 149,380 to 4,780 elements.

The second simplification assumption was to decrease the numbers of tile drain modules in the model by applying one tile drain module for the similar neighbour tile drains. This simplification could be made based on the similarities of parameters of the neighbour tile drains such as tile drain slopes, Manning roughness coefficients, and soil types.

These simplifications significantly decrease the computational solving time. For example, in the model consisting 80 tile drains, the computational solving time decreased from more than 10 days to less than 10 minutes by a standard desktop computer.

10 tile drains

The model of Example 2 containing 10 tile drains runs for a simulation period of 2 days rainfall followed by 8 days evapotranspiration for the saturated and infiltration excess runoff scenarios. *DrainFlow*-derived main drain and overland flow hydrographs at the outlets by *DrainFlow* are shown in Fig 2.14.

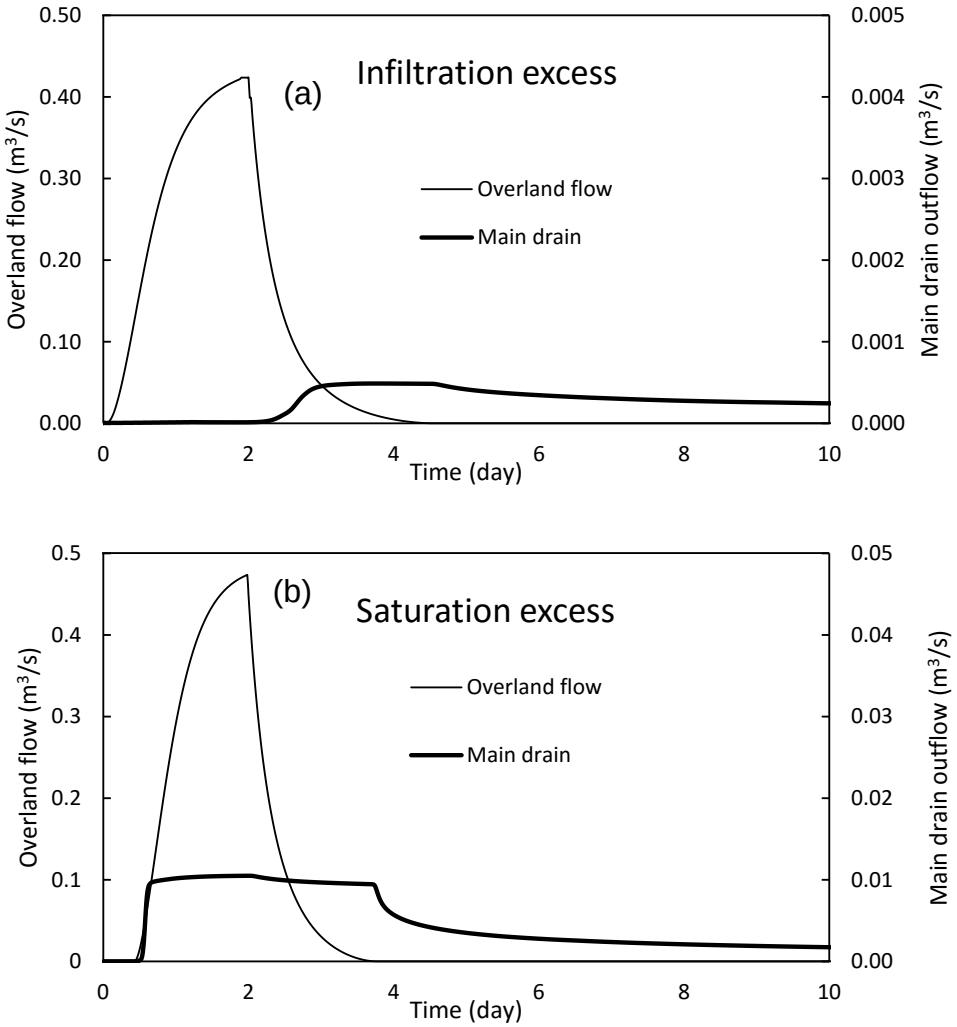

Fig 2.14 Overland flow and main-drain hydrographs: (a) infiltration and (b) saturated excess scenarios for the 10 tile drains domain

In the saturated excess runoff scenario, the overland flow and the main-drain hydrograph respond to the rain event approximately in the same time with about a half day delay from the beginning of the rainfall. However, in the infiltration excess runoff scenario, the overland flow hydrograph shows a very fast response to the rainfall in less than one hour. However, there is about 2 days delay between the beginning of rain and flow in the main drain. A comparison between overland flow hydrographs in Fig 2.14.a and 14.b indicates that the lower soil hydraulic conductivity in the infiltration

excess scenario causes a higher percentage of rainfall drained by the surface drainage system in infiltration excess scenario than in the saturation excess scenario.

20, 40 and 80 tile drains

DrainFlow was evaluated for 20, 40 and 80 tile drains. That is, for 50, 25 and 12.5 m tile drain spacing. The models were run to generate a saturation excess runoff condition, so hydraulic conductivity was set to be larger than the rainfall rate. Fig 2.15 shows the main drain and overland flow hydrographs for 10, 20, 40 and 80 tile drains, as computed *DrainFlow*.

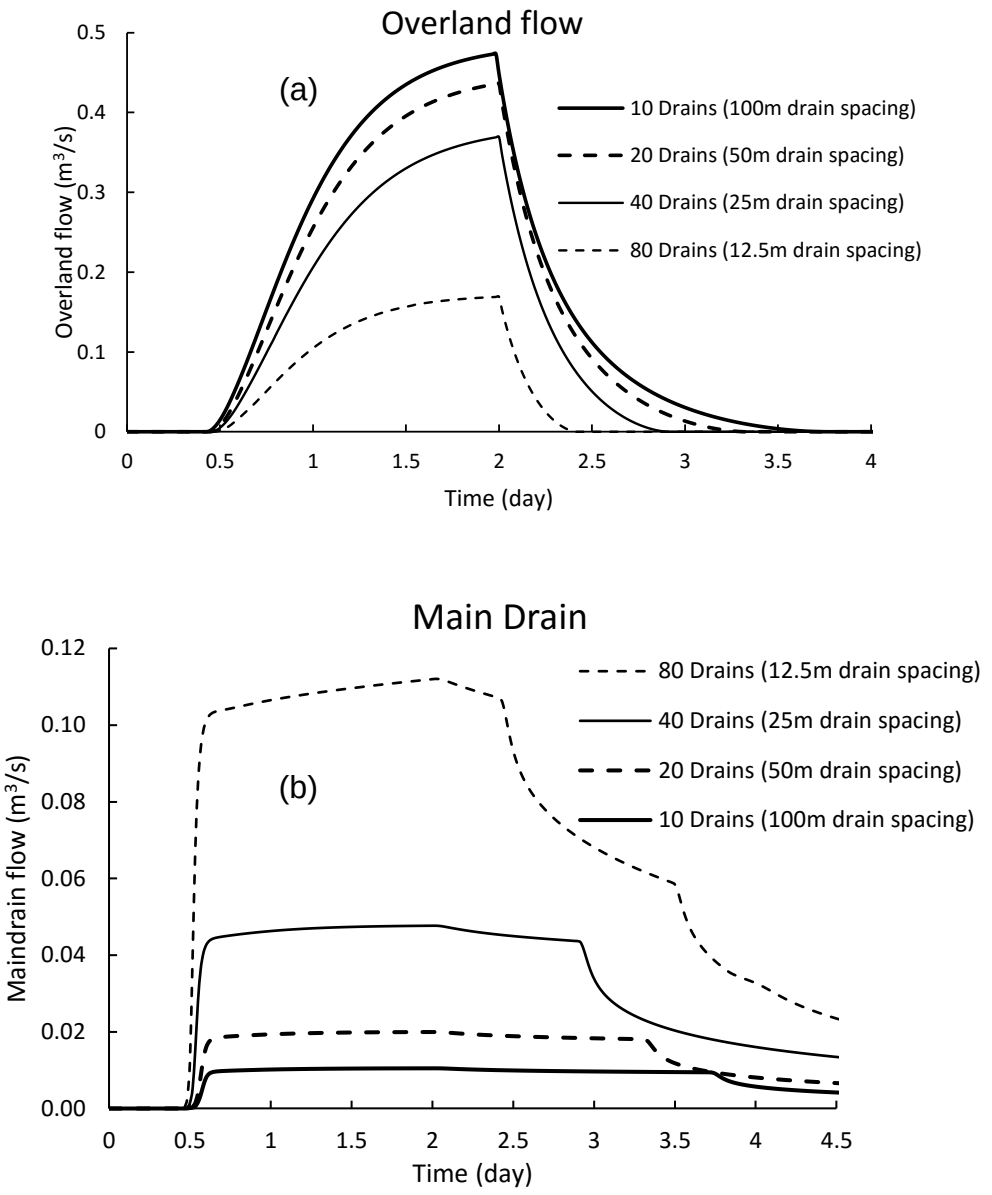

Fig 2.15 Comparisons between (a) overland flow and (b) tile drain hydrographs for saturation excess runoff condition

Comparing the overland flow and the main drain hydrographs shows that increasing the number of tile drains could reduce runoff discharge but amplifies the main drain outflow.

Fig 2.15 shows that when the tile drain spacing is 100, 50, 25 and 12.5m then the peak runoff discharges are 0.47, 0.41, 0.36 and 0.15 m^3/s and the corresponding maximum main drain outflows are 0.112, 0.048, 0.021 and 0.009 m^3/s respectively. Furthermore, the water balance shows around

12% of the total rainfall volume is drained by tile drains when the tile drain spacing is 100 m, but this percentage increases to about 30% when tile drain spacing is 12.5 m. Therefore it could be concluded that decreasing the tile drain spacing has effective impact on dropping the peak and cumulative runoff and increases the peak and total water drained water by the main drain.

2.8 Conclusion

DrainFlow is a fully distributed integrated surface and subsurface flow model, designed for drainage studies. Development, tests and applications of *DrainFlow* have been discussed. In contrast to the previous drainage models, *DrainFlow* has the advantage of calculating land surface recharge directly from the partial differential form of the Richards equation rather than implementing empirical methods.

To develop the model, a range of modules are separately formulated. Each module is then connected to the related modules. Consequently, all modules work together simultaneously by using outcomes of the other modules to yield the final result. A new technique is included in *DrainFlow* as a guard against the nonlinearity issue, which often occurs in coupled surface -subsurface flow models because of switching between dry and wet boundary conditions. This method provides for smooth switching between dry and wet boundary conditions.

To compare the *DrainFlow* code with the other coupled surface and subsurface flow models, some comparisons are made for five well-known integrated surface and subsurface benchmarks. As a result of these

comparisons, it is concluded that the *DrainFlow* code is in reasonably good agreement with the other coupled surface and subsurface flow codes.

In addition, two new hypothetical tile drainage examples were introduced and the *DrainFlow* code was run for these examples. The first example is designed to challenge the *DrainFlow* code in high-resolution and small-scale tile drainage studies. It was shown that *DrainFlow* code can compute effects of ground surface Manning roughness coefficients and slopes on the tile drain hydrographs, which was not predictable by traditional tile drainage models.

The second example was designed to challenge *DrainFlow* with model upscaling issue. As a result of two additional simplification assumptions the computational solving time declined dramatically from 10 days to less than 10 minutes in a model comprising 80 tile drains.

Finally, on the basis of various tests and applications it is concluded that in addition to comprehensiveness, *DrainFlow* is quite flexible. Based on required conceptual model complexity, scale and data availability, *DrainFlow* can be easily modified dimensionally or methodologically to a less or more complex model.

3 Chapter 3

An enhancement of the Hooghoudt drain-spacing equation

3.1 Abstract

The Hooghoudt equation is widely used as a simple means of specifying drain spacing when designing networks of parallel drains in drainage systems, based on estimating the maximum water table height between two drains. It is shown via comparison with a numerical model that the Hooghoudt equation can overestimate water table height and therefore yield drain spacings which may be too wide. This is because the Hooghoudt drain spacing equation in fact has a concealed dependency on Van Genuchten soil-water retention curve parameters, which can bias the water table estimates unless adjustments are made explicitly. A modification of the Hooghoudt equation is presented which incorporates two new dimensionless coefficients to make allowance for this dependency. The modified expression yields improved accuracy as measured against the numerical reference model.

Keywords: Drain-spacing, Richards equation, Hooghoudt equation, finite element model, van Genuchten, soil water water retention curve, drainage

3.2 Introduction

Artificial field drainage as a means to remove excess water in the root zone is now about 200 years old (Lambert K. Smedema, 2004) but estimating optimal drain spacing remains a challenging part of any drainage scheme design. If spacing is too wide then the water table between adjacent drains may rise to the root zone during heavy rain events or irrigation. On the other hand, needless construction costs are incurred if the drains are unnecessarily close. To find the optimal spacing, the between-drain water table height must be estimated by way of a suitable governing groundwater equation.

Laplace, Boussinesq, and Richards (1931) equations are widely mentioned in the literature as the partial differential governing equations for fluid flow in porous media and analytical solutions have been obtained for a range of special drainage cases.

For example, Hooghoudt (1940) derived an expression based on the one-dimensional Boussinesq equation by using Dupuit – Forchheimer (DF) assumptions for flow to two parallel drains. The derivation assumes that the effect of radial flow from the centre of the drain to $D/\sqrt{2}$ is significant, where D [L] is the thickness of the soil layer below the drains. To allow for the effect of radial flow near the drains and to reduce the DF approximation error, Hooghoudt (1940) replaced D in his equation with an "equivalent depth" d, which is an imaginary depth under the drains which is always smaller than D. Moody (1966) and Sakkas and Antonopoulos (1981) present simple estimating expressions for d , while Van Schilfgaarde (1963) describes a graphical estimation approach. Beers

(1979) gives a dimensionless nomogram to avoid trial- and- error solution of the Hooghoudt equation. Mishra and Singh (2007) derive a new equivalent depth table for the Hooghoudt equation by changing the assumption of the effect of the radial flow from $D/\sqrt{2}$ to a combination of $2D/\pi$ and the area of groundwater flow above the drain in the radial zone.

In related analytical approaches, Kirkham (1958) solves the 2D steady state Laplace equation in a conceptual confined flow domain for a constant drain discharge and ignores all flow above drain level. Van Der Molen and Wesseling (1991), Dagan (1964), Hammad (1962), and Ernst (1962) respectively use different approaches to derive some simpler solutions for the Kirkham equation. In addition Youngs (1965), (1975), Collis-George and Youngs (1958), and List (1964) present some inequalities and equations for upper and lower bounds of water table height between two parallel drains. Child (1969) fitted an empirical equation to data obtained from a sand tank physical model experiment devised by Collis-George and Youngs (1958). Miles and Kitmitto (1989) and Barua and Tiwari , 1996b) derive analytical drain spacing formula suitable for homogenous and layered anisotropic soils. Lovell and Youngs (1984) and Kirkham (1966) give comprehensive reviews of various analytical drainage equations.

As an alternative to analytical methods to obtain drain spacing, the governing equations of water movement in soil can be solved using numerical techniques with fewer assumptions. Gureghian and Youngs (1975) describe a finite element technique to solve the Laplace equation for drainage situations and apply it for both homogeneous and

heterogeneous soils. Zaradny and Feddes (1979) use the finite element Galerkin method to solve the 2D-Laplace equation applied to the vicinity of a tile drain. Smedema et al. (1985)use a finite element solution of the Laplace equation for homogeneous-anisotropic soil drainage and then compare the resulting drain spacing estimates with those from the Hooghoudt equation. They conclude that the Hooghoudt equation can be used with reasonable confidence for drain-spacing in both homogeneous and anisotropic soils.

Khan (Khan & Rushton, 1996a, 1996b, 1996c) applied a finite difference numerical approach to solve the 2D steady state Laplace equation for drainage applications and noted that drains must be represented as an internal boundary separated from the water table. Zaradny (2001) uses finite element methods to predict groundwater flow in a drainage zone and shows that in this context groundwater flow theory for confined aquifers can also be utilized for unconfined aquifers. Zavala et al. (2007) use a numerical solution of the Boussinesq equation, incorporating boundary conditions by use of two types of drainage flux equation as a function of water table elevation. Their study concluded that both types of boundary condition can give reasonable results consistent with laboratory experiments.

Castanheira and Santos (2009) develop a 2D Galerkin finite element steady state Richards equation model for finding optimal drain spacing and then compared their results with the Kirkham and Hooghoudt analytical solutions. Shokri (2011) describes a numerical surface/subsurface model which couples a 3D Richards equation and the

2D shallow water equations, enabling design of drainage schemes which may also serve to supply irrigation water.

Fuentes et al. (2009) give two expressions for relations between the storage coefficient and the soil-water retention curves of van Genuchten (1980) and Fujita–Parlange (Carlos Fuentes, Haverkamp, & Parlange, 1992), during water table drawdown between two drains. These expressions have been subsequently shown by Pandey et al. (1992) to be consistent with experimental data. Chavez et al. (Chavez et al., 2011a; Chavez et al., 2011b) used a finite difference method to solve a combination of the Boussinesq equation and the Van Genuchten soil-water retention curve to estimate drainable porosity, in order to study the hydrodynamics of groundwater flow near tile drains. Jiang et al. (2010) use finite elements to solve a 2D Laplace equation for both random hydraulic conductivity variation and hydraulic conductivity decreasing exponentially with depth, obtaining both the spatial hydraulic head distribution and drain discharge. Zavala et al. (2012) compared the result of the finite element 1D Boussinesq and 2D Richards equation in an agriculture subsurface drainage situation. This showed the limitations of the Boussinesq equation such as the DF assumptions for between-drain water table estimation. Recently Youngs (2012) and (2013) developed an analytical equation incorporating the capillary fringe to simulate steady state flow to tile drains in a hypothetical infinitely deep soil. In addition, a number of special-purpose computer codes are available for drain-spacing estimation, including DRAINMOD (1980), DRENAFEM (2009) and MHYDAS-DRAIN (2007).

Despite this considerable activity in the field, to date there is no available analytical solution of Richards equation for drain spacing estimation. Most of the current analytical and numerical drainage models are based on solutions of the partial differential Laplace and Boussinesq equations. The present thesis applies a dimensionless finite element solution of the partial differential Richards equation to obtain an enhancement of the analytical Hooghoudt equation. It will be shown that the coefficients of the original Hooghoudt equation are actually functions of soil-water retention parameters, though not specified explicitly. While drain spacing can be solved directly via a numerical model of the Richards equation, the analytical Hooghoudt expression still has attraction in its ease of application. In this regard, the modified Hooghoudt equation presented here has the advantage of giving more accurate results than the original expression and should find application to practical drainage design.

Section 3.3 classifies drain spacing equations into those using the DF assumption and those using the Laplace equation. The steady state Richards equation is then revisited. The system and boundary conditions are described in Section 3.4. The enhanced Hooghoudt equation is presented in Section 3.5.

3.3 Common drain spacing formulae

The standard drain spacing equations and the governing subsurface flow equation are given below. Drain spacing equations have been widely discussed in the literature and only a brief summary is provided here.

3.3.1 Formulae based on DF assumptions

The steady state analytical Hooghoudt equation is widely used to determine drain-spacing (Van der Molen & Wesseling, 1991) and can be written as

$$\frac{q}{K_s} = 4\left(\frac{m}{L}\right)^2 + \frac{8d}{L}\left(\frac{m}{L}\right) \quad \frac{q}{Ks} = 4\left(\frac{m}{L}\right)^2 + \frac{8d}{L}\left(\frac{m}{L}\right) \tag{3.1}$$

$$d = \frac{L}{\frac{(L-D\sqrt{2})^2}{DL} + \frac{8}{\pi}\ln\frac{D}{r_0\sqrt{2}} + f(D,L)} \quad d = \frac{L}{\frac{\left(L-D\sqrt{2}\right)^2}{DL} + \frac{8}{\pi}\ln\frac{D}{r_0\sqrt{2}} + f(D,L)} \tag{3.2}$$

where q is recharge rate per unit surface area [LT^{-1}], K_s is saturated hydraulic conductivity of the medium [LT^{-1}], m is the maximum water table height above the drain level midway between two parallel drains [L], and r_0 is effective drain radius [L]. The function $f(D,L)$ is smaller than the other terms and is generally ignored (Wesseling & Kessler, 1994). Moody approximations of Eq 3.2 can be written as (Moody, 1966):

$$d = \frac{D}{\frac{8D}{\pi L}\ln\left(\frac{D}{\pi r_0}\right) + 1} \text{ for } 0 < \frac{D}{L} \le \frac{1}{4}; \quad d = \frac{\pi L}{8\ln\left(\frac{L}{\pi r_0}\right)} \text{ for } \frac{D}{L} > \frac{1}{4}; \tag{3.3}$$

3.3.2 Formulae based on the Laplace equation

An analytical solution was obtained by Kirkham (1958) for water table height midway between two drains, utilising the 2D steady state Laplace equation. This gives the Kirkham relation:

$$m = \frac{qL}{Ks}\frac{1}{\pi}\left(\ln\frac{L}{\pi r_0} + \sum_{n=1}^{\infty}\frac{1}{n}\left(\cos\frac{2n\pi r_0}{L} - \cos n\pi\right)\coth\frac{2n\pi D}{L} - 1\right) \quad \mathrm{m} = \frac{\mathrm{qL}}{\mathrm{K_s}}\frac{1}{\pi}\left(\ln\frac{\mathrm{L}}{\pi \mathrm{r0}} + \sum_{\mathrm{n=1}}^{\infty}\frac{1}{\mathrm{n}}\left(\cos\frac{2\mathrm{n}\pi \mathrm{r0}}{\mathrm{L}} - \cos \mathrm{n}\pi\right)\coth\frac{2\mathrm{n}\pi \mathrm{D}}{\mathrm{L}} - 1\right) \tag{3.4}$$

In the derivation of Eq 3.4 the simplification is made that water flow above drain level can be ignored (Kirkham, 1958). Dagan (1964) gives a simplified version of Eq 3.4 as:

$$\mathrm{m} = \frac{\mathrm{qL}}{\mathrm{K_s}}\left(\frac{\mathrm{L}}{8\mathrm{D}} - \frac{1}{2\pi}\ln\left(2\cosh\frac{\pi \mathrm{r0}}{\mathrm{D}} - 2\right)\right) \quad m = \frac{qL}{Ks}\left(\frac{L}{8D} - \frac{1}{2\pi}\ln\left(2\cosh\frac{\pi r_0}{D} - 2\right)\right) \qquad (3.5)$$

Van der Molen et al. (1991) show Eq 3.5 gives a good approximation to Eq 3.4 when *D/L* is small.

3.3.3 Steady state Richards equation

For saturated/unsaturated flow in porous media, the steady state Richards equation is utlised:

$$\nabla.(\mathrm{K_w}(\mathrm{h})\nabla(\mathrm{h}+\mathrm{z})) = -\mathrm{qs}\ \nabla(K_w(h)\nabla(h+z)) = -qs \qquad (3.6)$$

where *h* is the pressure head [L], *z* is the elevation [L], *qs* is a general sink/source term [LT^{-1}], and $K_w(h)$ is the hydraulic conductivity. Eq 3.6 is defined in the whole pressure domain as:

$$K_w(h) = \begin{cases} KsKr(h) & for\ h < 0 \\ Ks & for\ h \geq 0 \end{cases} \quad \mathrm{K_w(h)} = \begin{cases} \mathrm{K_s K_r(h)\ for h < 0} \\ \mathrm{K_s\ for h \geq 0} \end{cases} \qquad (3.7)$$

where $K_r(h)$ is the relative permeability [-]. In this study the relative permeability function is used as in the Van Genuchten (1980) model:

$$Kr = Se^{l}\left(1-\left(1-Se^{\frac{1}{M}}\right)^{M}\right)^{2};\ Se = \frac{1}{\left(1+|\alpha h|^{n}\right)^{M}} \qquad (3.8)$$

where *Se* is effective saturation [-], *l* is a pore connectivity parameter usually assumed to be 0.5 [-], α [L^{-1}] and $n > 1$ [-] are the two Van Genuchten curve fitting parameters and $M=1-1/n$. It is evident that for the

special case of *Kr=1* the Richards equation is equivalent to the Laplace equation.

Table 3.1 shows the result of a study by Carsel and Parrish (1988), which provide estimates of *α* and *n* for a range of soil texture groups from their analysis of a large amount of recorded soil water retention data. Malaya and Sreedeep (2011) give a comprehensive review of factors that may influence the soil-water retention curve. Fig 3.1 shows calculated relative permeability from Eq 3.8, plotted on log scales against pressure head for a range of Van Genuchten soil water retention parameters.

Table 3.1 Descriptive statistics of Van Genuchten water retention model parameters (α and n), from Carsel and Parrish (1988)

		α (1/m)			n		
#	Texture	SZ*	Mean	Std dev	SZ*	Mean	Std dev
1	Sand	246	14.5	0.029	246	2.68	0.29
2	Loamy sand	315	12.4	0.043	315	2.28	0.27
3	Sandy loam	1183	7.5	0.037	1183	1.89	0.17
4	Loam	735	3.6	0.021	735	1.56	0.11
6	Clay	400	0.8	0.012	400	1.09	0.09

***** Sample size

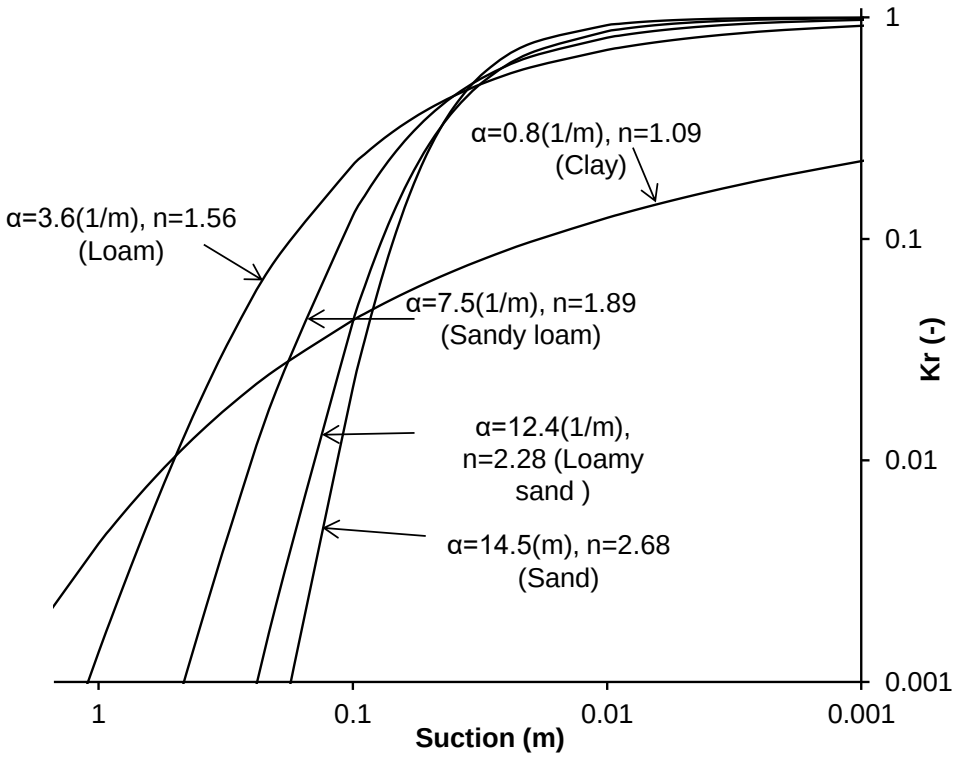

Fig. 3.1 Relative permeability (*Kr*) versus pressure head for a range of van Genuchten soil water retention parameters *α* and *n* (Table 3.1)

3.3.4 System definition

A dimensionless domain is used to compare maximum water table height as calculated from some analytical drainage equations and also from selected numerical simulations. Fig 3.2 shows a set of horizontal parallel drains of radius r_0/L located at elevation *D/L* above datum and depth *H/L* under the ground surface. The soil is assumed homogenous, isotropic, having saturated hydraulic conductivity *Ks* and located above a horizontal impermeable surface.

A Neumann boundary condition (constant discharge boundary CDB) $\partial h/\partial y = -q/Ks\ \partial \mathrm{h}/\ \partial \mathrm{y} = \mathrm{q}/\mathrm{Ks}$ is applied at the top boundary. Due to

simplification assumes drain to remain half full and the condition in the drain is hydrostatic, therefore as an internal boundary condition a Dirichlet boundary condition (constant head boundary CHB) $h=D/L$ is applied to lower half part of drain tube. For upper half part of the drain a Cauchy boundary condition (seepage face boundary SF) is applied, once the surface pressure is get larger than 0, SF boundary condition is let the model to transfer from a CDB to CHB condition. For the rest of the boundaries a no-flow boundary (NFB) condition $\partial \mathrm{h} / \partial \mathrm{y} = 0$ is implemented from symmetry or for representing the lower impervious layer.

To create the "true" reference for comparison, Richards equation is implemented numerically using the finite element SEEP/W code (GEO-SLOPE International Ltd, 2012). A layout of the finite element mesh used in the numerical model and the area surrounded by the drain are illustrated in Fig 3.3 for D/L=0.083, H/L=0.033 and r_0/L=0.00167. The results of Carsel and Parrish (1988) are used for the two Van Genuchten soil water retention parameters α and n (Table 3.1).

To check magnitude of discretizing error, total input flux of the upper boundary condition (Fig 3.2) is compared with the calculated discharge of the drain by developed numerical model. The comparison shows the differences between input flux and calculated discharge are always remain under $10^{-5}q/K$.

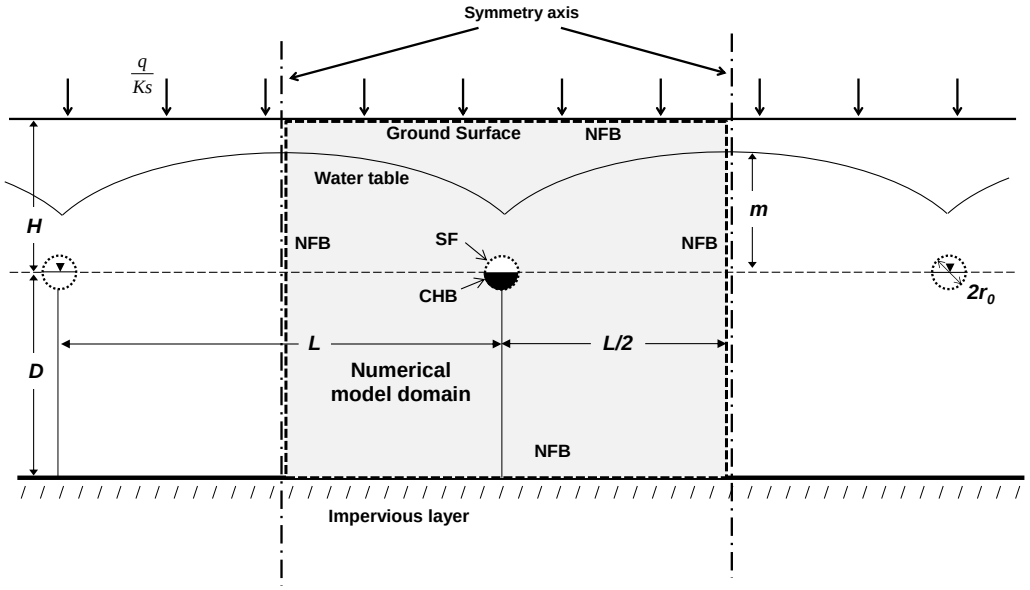

Fig. 3.2 The parallel drainage system and numerical model domain with no-flow boundary NFB, constant head boundary CHB, and a constant discharge boundary CDB

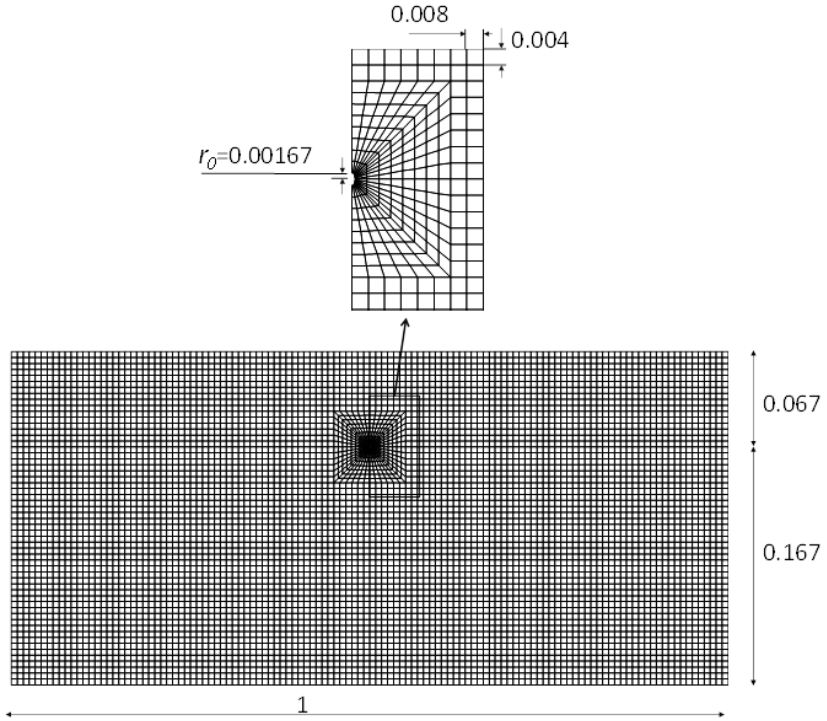

Fig. 3.3 Finite element mesh that has been applied to the model for D/L=0.167, H/L=0.067 and r_0/L=0.00167

3.4 Results and Discussion

Fig 3.4 shows two situations of equipotential lines and water table heights calculated by the numerical solution of Richards equation for $\alpha=0.8$ and $n=1.09$ (clay soils) and for $\alpha=14.5\ m^{-1}$ and $n=2.68$ (sandy soils), with $q/Ks=0.02$, $D/L= 0.083$, $H/L=0.033$, $r0/L=0.00167$. Despite the fact that the two models use the same boundary conditions and sub-domain geometry, the maximum water table height calculated is different for the two cases. That is, m/L is obtained as 0.0195 for $\alpha=0.8$ and $n=1.09$ (clay soils) and as 0.0164 for $\alpha=14.5\ m^{-1}$ and $n=2.68$ (sandy soils).

The maximum water table height midway between two drains m/L is computed for various dimensionless parameter q/Ks, D/L, r_0/L, H/L and van Genuchten soil-water retention parameters α and n. Fig 3.5 shows the relation between q/Ks and m/L for $D/L= 0.083, 0.017, 0.033$ and 0.067 when $r_0/L=0.00167$ and $H/L=0.033$. It is evident that the Hooghoudt equation with the Moody approximation of equivalent depth (Eq 3.3) gives the closest result to the numerical Richards model among the other analytical methods. This similarity is clearly visible for small D/L with clay soils ($\alpha = 0.8\ m^{-1}$, $n = 1.09$). However, the differences between the Richards numerical model and the Hooghoudt-Moody equation become greater as D/L increases. The difference is particularly evident for $\alpha=14.5\ m^{-1}$ and $n=2.68$, which represent sandy soils (Table 3.1). The Kirkham and Dagan equations (Eqs. 3.4 and 3.5 respectively), always overestimate m/L compared to other methods.

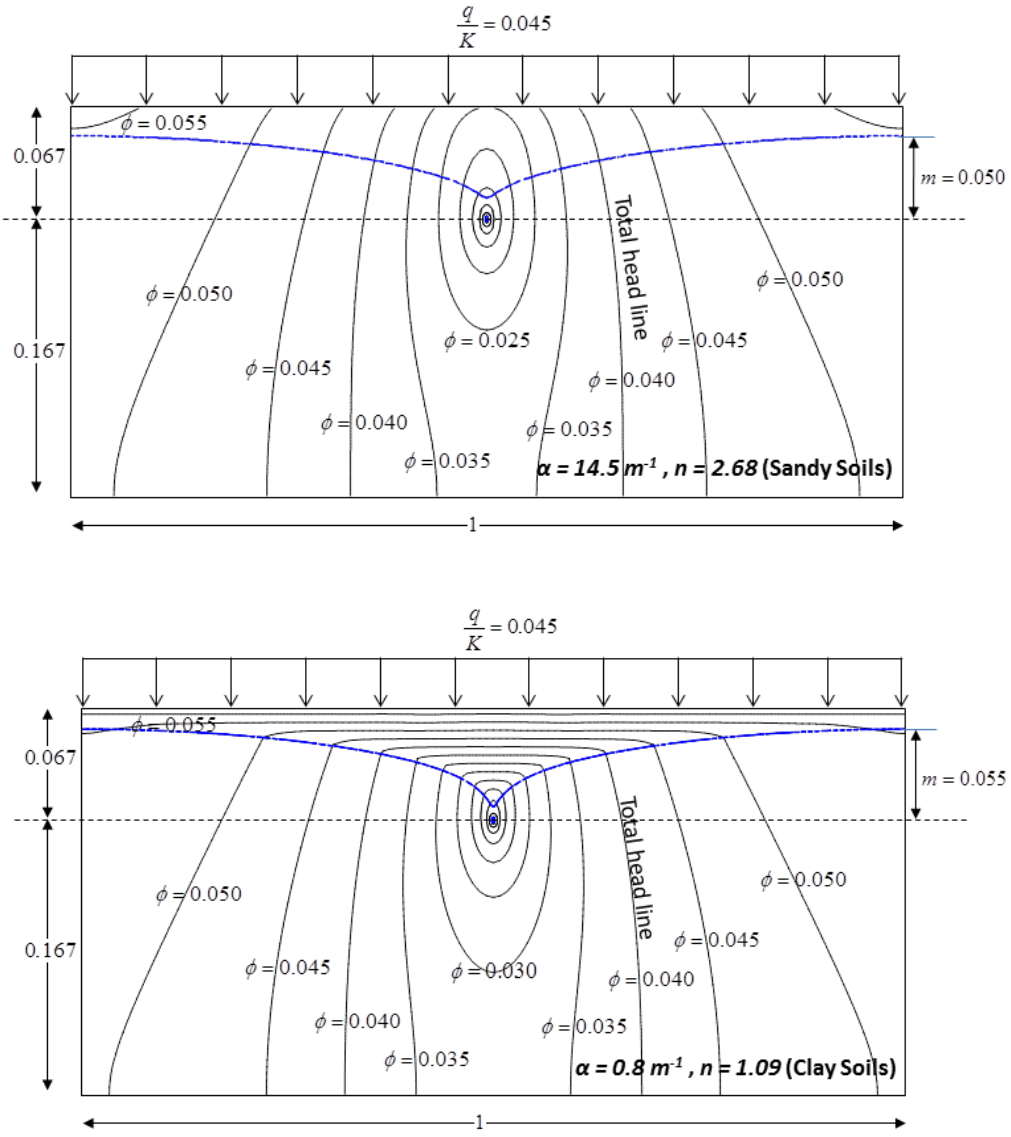

Fig. 3.4 (a,b) Equipotential lines and water table height computed by the numerical solution of Richards equation for clay soils ($\alpha = 0.8\ m^{-1}$, $n = 1.09$) and for sandy soils ($\alpha = 14.5\ m^{-1}$, $n = 2.68$). when $q/Ks=0.01$, $D/L= 0.083$, $H/L=0.033$ and $r0/L=0.00167$, ($\phi = h + z$)

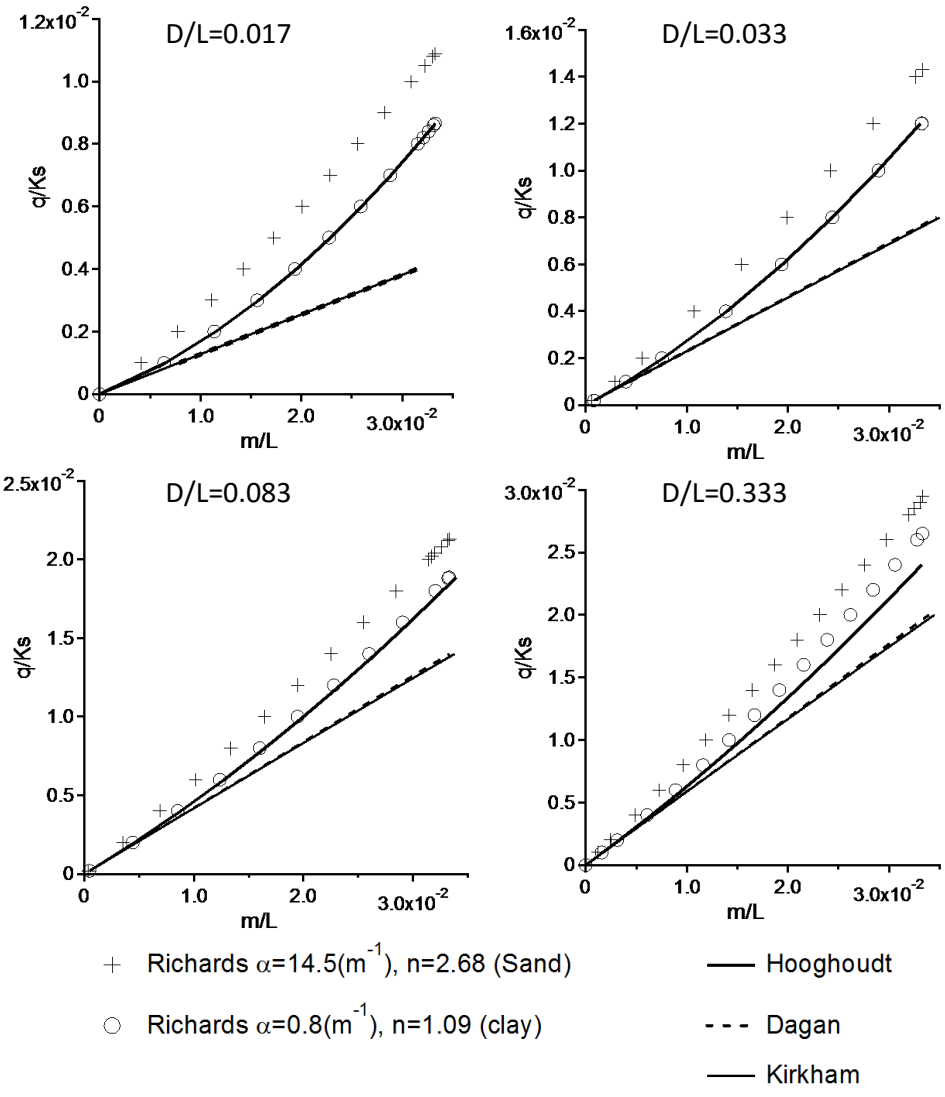

Fig. 3.5 The relation between *q/Ks* versus *m/L* for analytical and numerical results for D/L=0.017, 0.033, 0.083 and 0.333 when $r_0/L=0.00167$ and $H/L=0.033$

3.5 Modification of the Hooghoudt-Moody equation

Eq 3.1 can be expressed as a zero-intercept quadratic expression:

$$y = ax^2 + bx \qquad (3.9)$$

where $y = q/k_s$, x = m/L, a = 4, and $b = 8d/L$. Eq 3.9 was applied as an empirical regression expression $y=a'x^2+b'x$ (where apostrophise denote parameter estimates), to the output of the numerical Richards model as data and obtained the anticipated good fits (Fig 3.6).

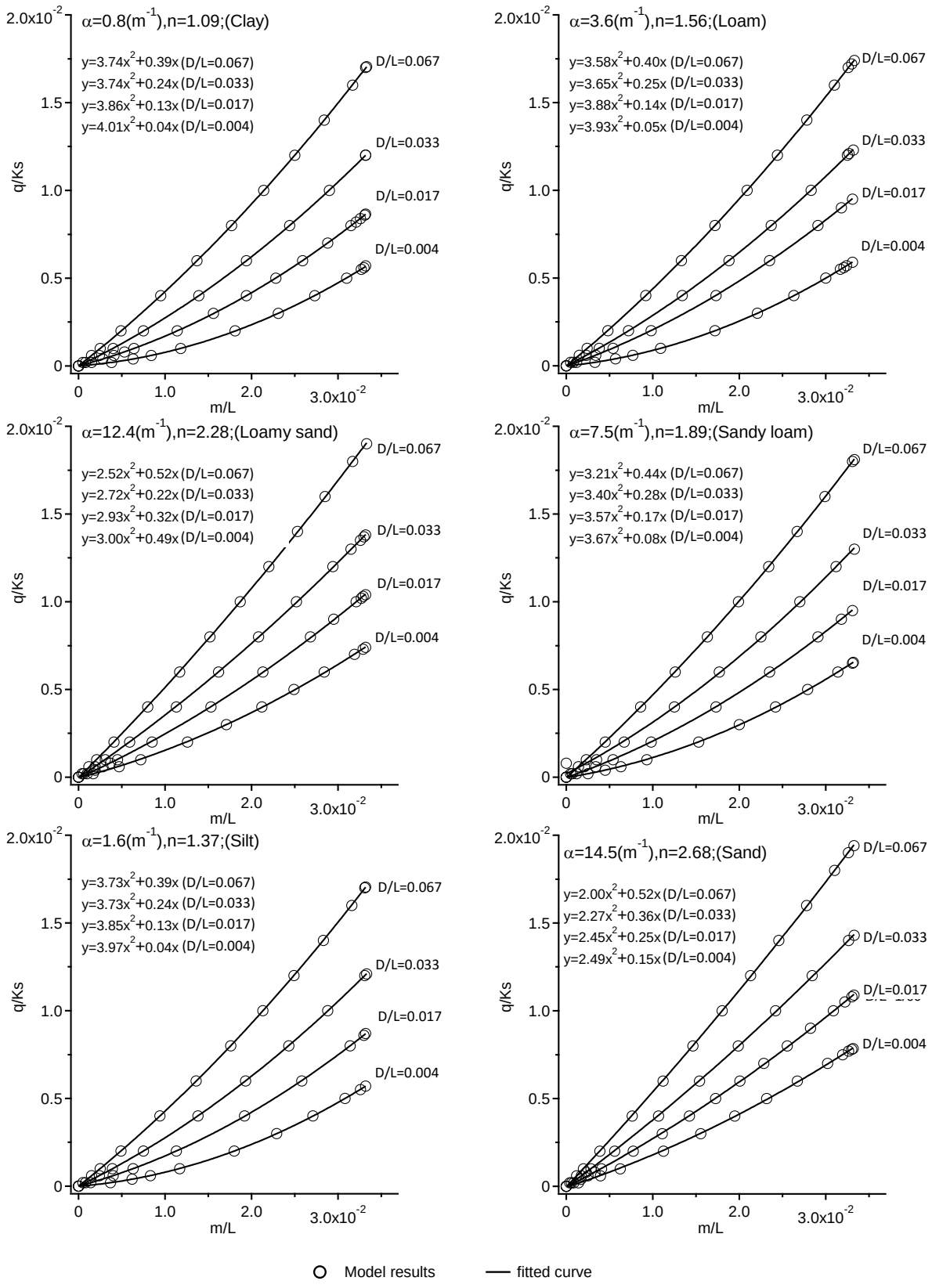

Fig. 3.6 Fitted curves to numerical values (open circles) as obtained from the numerical model of Richards equation for a range of *α, n* and *D/L* when $r_0/L=0.00167$ and $H/L=0.033$

From Eq 3.9 it might be expected that the fit-derived coefficients *a'* and *b'* would be similar to *a* and *b.* However, there are some evident differences. In particular, the difference is considerable for sandy soils and larger *D/L* ratios. To illustrate this difference, for a range of α and *n* from Table 3.1, the ratios of *a'⁄a* and *b'⁄b* (referenced henceforth as β_{d1} and β_{d2} respectively) are plotted against *d/L* (Fig 3.7).

If Eq 3.9 is used as a fitting curve to the results of numerical models it would be expected that a' = a = 4 and b'=b=8d/L (within estimation error) or in other words βd1 =βd2=1 However, Fig 3.7 shows βd1 and βd2 are functions of both d/L and the Van Genuchten soil water retention parameters α and n. Fig 3.7 also shows cubic and exponential curves give go od empirical fits to the numerical model output.

Similar numerical models are set up for r_0/L *=0.0003, 0.0008, 0.00167, 0.0025* and 0.0033 when *D/L=0.083* and *H/L=0.033* and *H/L= 0.017, 0.033, 0.05, 0.067* and *0.083* when r_0/L *=0.00167, D/L=0.083* for a range of Van Genuchten soil water retention values. Then with the same methodology used for defining β_{d1} and β_{d2} , four new parameters (β_{r1} , β_{r2} and β_{H1} , β_{H2}) are obtained. These two parameter pairs are plotted versus r_0/L and *H/L* in Figs. 3.8 and 3.9 respectively.

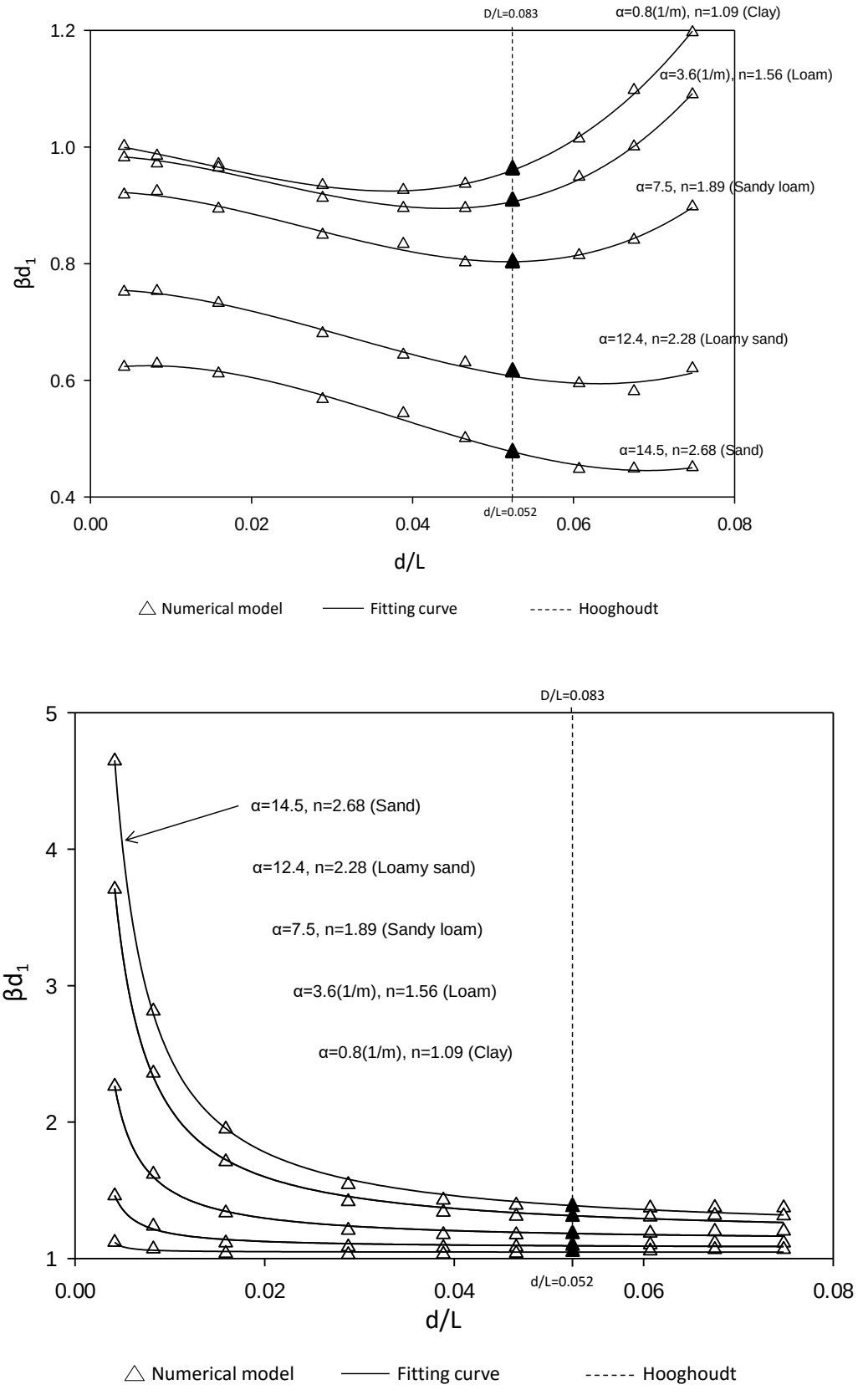

Fig. 3.7 Relation between βd1 and βd2 and d/L for a range of α and n when r0/L=0.00167 and H/L=0.033

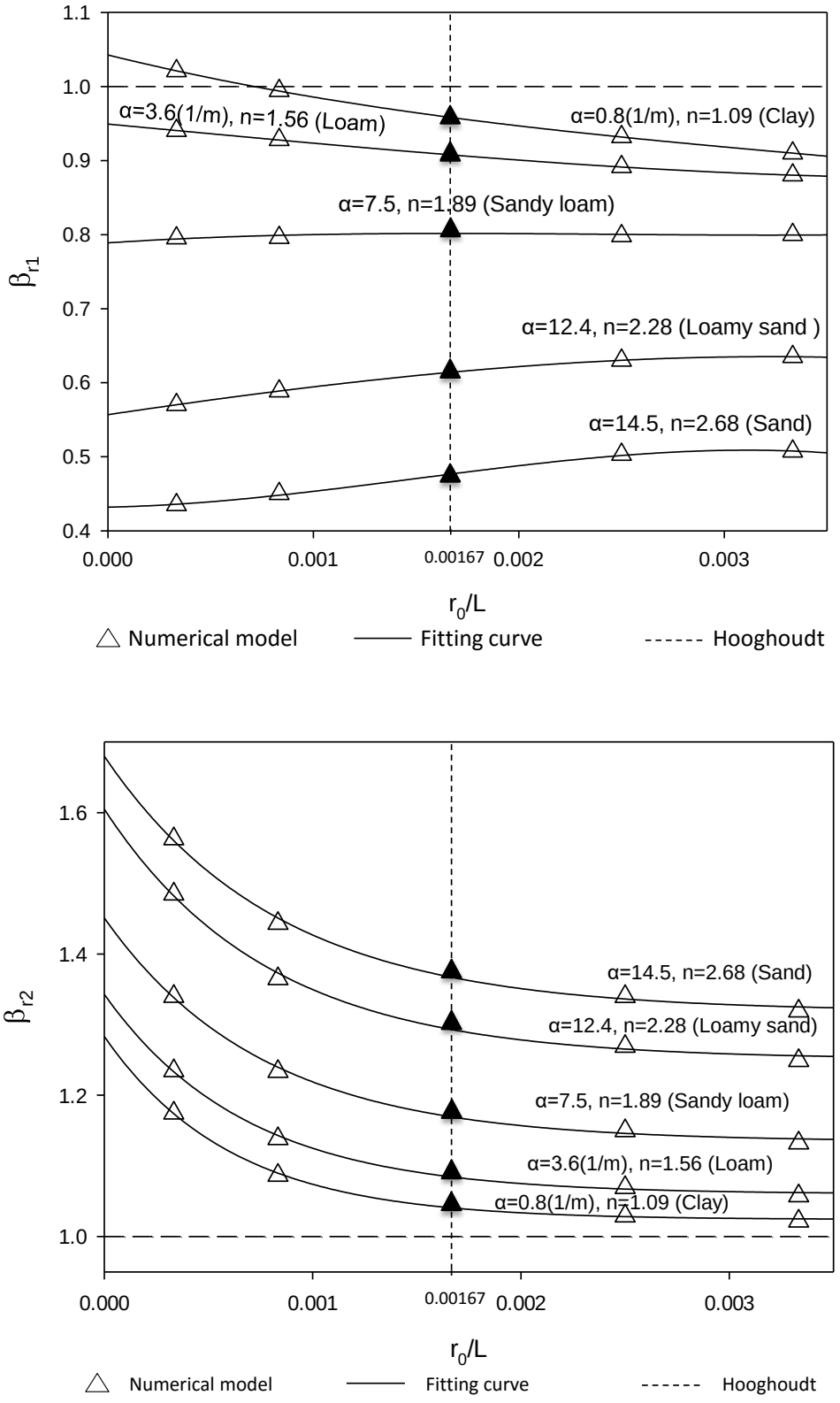

Fig. 3.8 Relation between β_{r1} and β_{r2} and r_0/L for a range of α and n and r_0/L for $D/L=0.083$ and $H/L=0.033$

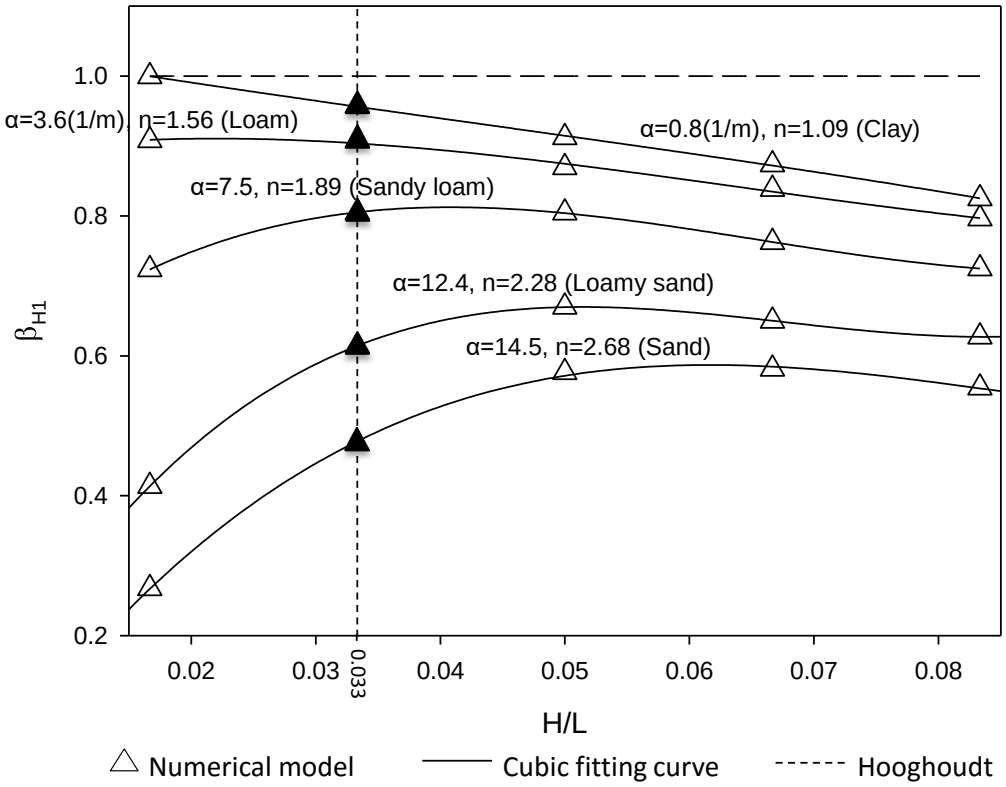

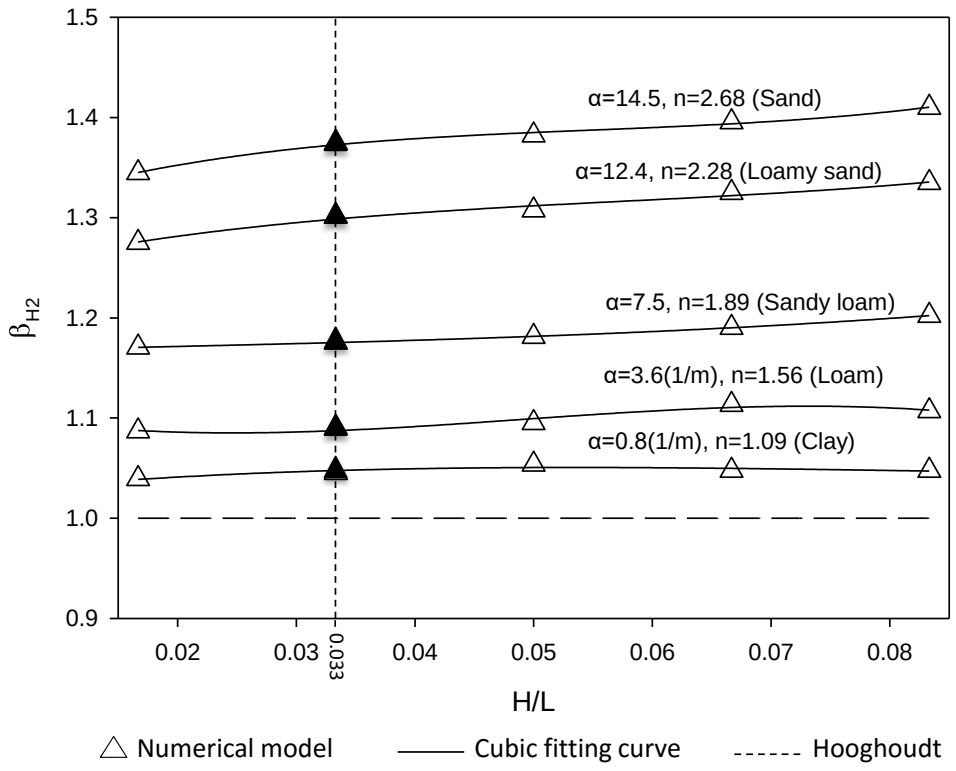

Fig. 3.9 Relation between β_{H1} and β_{H2} and H/L for a range of α and n and H/L for $r_0/L = 0.00167$, $D/L = 0.083$

Each triangle in Figs. 3.7 to 3.9 represents a coefficient of parabolic fitting curves for different model geometries (*D/L*, *H/L* and r_0/L). In Fig 3.7 the numerical model has been set up for $r_0/L=0.00167$, $H/L=0.033$ and a range of *D/L*, in Fig 3.8 for $D/L=0.083$ and $H/L=0.033$ and different r_0/L and in Fig3.9 for $r_0/L=0.00167$, $D/L=0.083$ and a range of *H/L.*

By inspection of Figs. 3.7-3.9 it is evident that a unique and joint model has been repeated in all graphs when $D/L=0.083$, $r_0/L=0.00167$ and $H/L = 0.033$. These unique points (referenced hereafter as "Base Betas") are shown as the black triangles of Figs. 3.7-3.9 and symbolised $\beta 0_1$ and $\beta 0_2$. Calculated values of $\beta 0_1$ and $\beta 0_2$ for a range of soils are listed in Table 3.2.

Table 3.2 Calculated value of base betas (β01 and β02) when D/L=0.083, r0/L=0.00167 and H/L = 0.033 for a range of Van Genuchten soil water retention model parameters (α and n)

#	Texture (Van Genuchten soil water retention model parameters)	$\beta 0_1$	$\beta 0_2$
1	Sand ($\alpha=14.5m^{-1}$, n=2.68)	0.47	1.37
2	Loamy sand ($\alpha=12m^{-1}.4$, n=2.28)	0.61	1.30
3	Sandy loam ($\alpha=7.5m^{-1}$, n=1.89)	0.80	1.18
4	Loam ($\alpha=3.6^{m-1}$, n=1.56)	0.91	1.09
5	Clay ($\alpha=0.8^{m-1}$, n=1.09)	0.96	1.04

The values of the β_d, β_r and β_H shows in the Figs. 7 to 9 are normalized by dividing over the base betas (Eq 3.10).

$$\beta n_{ij} = \frac{\beta_{ij}}{\beta 0_j} \beta n_{ij} = \frac{\beta_{ij}}{\beta_{0j}} \tag{3.10}$$

where βn_{ij} referenced after this as normalized betas and i in the index of β stands for d, r and H and j stands for 1 and 2. Fig 3.10 illustrates calculated normalized betas for a range of d/L, r_0/L, H/L and soil types mentioned in Table 3.1.

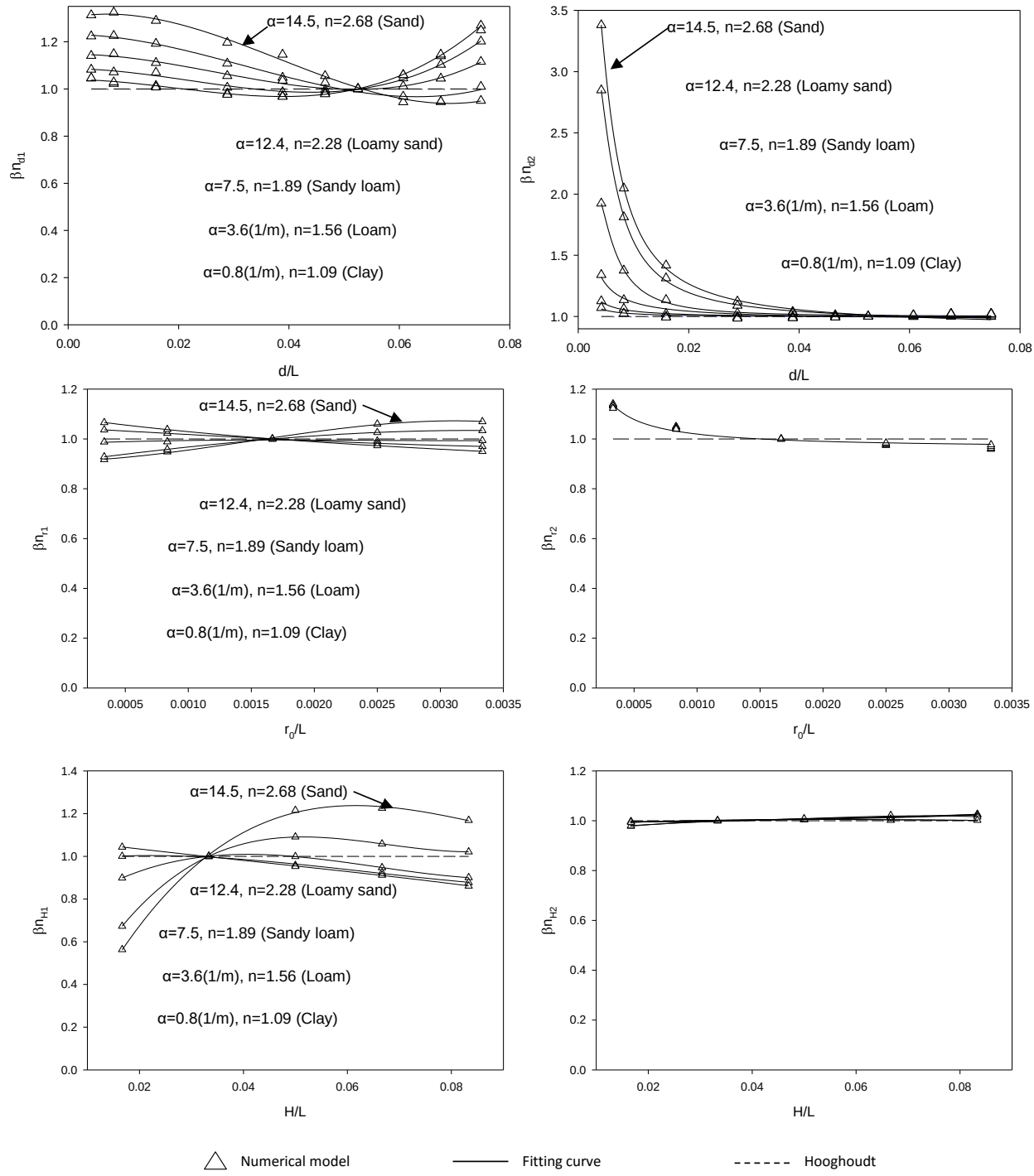

Fig. 3.10 Calculated βn_{d1}, βn_{d2}, βn_{r1}, βn_{r2} βn_{H1}, and βn_{H2} for a range of Van Genuchten soil water retention model parameters (α and n) versus d/l, H/L and r_0/L respectively

The above results indicate that replacing the Hooghoudt a and b parameters with $4\beta 0_1 \beta n_{i1} \beta 0_1 \beta n_{i1}$ and $(8d/L)$ $\beta 0_2 \beta n_{i2} \beta 0_1 \beta n_{i1}$ respectively

will give predictions of the water table height midway between the drains (*m*) which are as accurate as the numerical Richards equation model. These substitutions give the enhanced Hooghoudt equation as:

$$\frac{q}{Ks} = 4\beta_1\left(\frac{m}{L}\right)^2 + \frac{8d}{L}\beta_2\left(\frac{m}{L}\right) \qquad (3.11)$$

where $\beta_1 = \beta 0_1 \beta n_{i1} \beta 1 = \beta 0_1 \beta n_{i1}$ and $\beta_2 = \beta 0_2 \beta n_{i2} \beta 1 = \beta 0_1 \beta n_{i1}$. This expression enables drain spacing to be estimated more accurately than the original Hooghoudt equation (Eq3.1). In particular, the use of Eq 3.11 avoids the overestimation of maximum water table height associated with the Hooghoudt equation in its traditional form.

3.6 Conclusion

A dimensionless finite-element Richards equation model is developed to incorporate the effect of soil-water retention parameters on the maximum water table height between two adjacent drains. This model was then used as a comparison reference to show that the well-known analytical Hooghoudt equation overestimates the maximum water table height midway between two drains, particularly for sandy soils. Furthermore, both of the Hooghoudt equation coefficients are shown to be functions of soil-water retention parameters. Two new dimensionless coefficients β_1 and β_2 are incorporated into the Hooghoudt equation, giving a modified expression which yields between-drain water table height estimates close to those from the numerical reference model. These coefficients are shown to be functions of soil physical properties.

4 Chapter 4

Effect of perched and leaky layers on complex and integrated surface-subsurface flow environments

4.1 Abstract

Perched geological layers play an important role in a hydrological system via redirecting land surface recharge to nearby surface water bodies and also reducing the total recharge volume to regional aquifers. Continuity and permeability of a perched layer can be key physical parameters in surface and subsurface flow connection to the regional groundwater system. Also, a semi-impermeable perched layer with discontinuities, heterogeneity, fractures and faults will increase the spatial complexity of local recharge in an otherwise simple system.

Relatively little is known about how leaky and perched layers might control linkages between surface flow, shallow groundwater flow, and the regional groundwater system. This problem is investigated in a specific instance using the Kawerau shallow groundwater aquifer in New Zealand as a case study. A thin semi-impermeable and fractured layer between two relatively permeable volcanic formations (Rotoiti Pyroclastics and Matahina

Ignimbrite) is developing a leaky and perched aquifer in the Rotoiti Pyroclastics.

A finite element groundwater model of the shallow aquifer is developed in this study to simulate groundwater flow in this environment. It is concluded, in addition to the artificial structures, such as tile drains, which explained in the previous chapters, that natural aspects like the perching layers may have a critical role on controlling the volume and pattern of the flow exchange between the surface, subsurface flow and regional groundwater aquifers.

Keywords: Perched/leaky, aquifer, interaction, Kawerau, Rotoiti, Matahina, coupled, surface/subsurface flow, semi-impermeable, groundwater, surface water

4.2 Introduction

Perched water tables have long been classified as aquifers (Fetter & Fetter, 2001; R.A. Freeze & Cherry, 1979). In addition, surface-subsurface flow interaction has been the subject of many recent research projects (Bayani Cardenas, 2008; Cloke, Anderson, McDonnell, & Renaud, 2006; Ebel et al., 2007; Gauthier et al., 2009; Kollet & Maxwell, 2008a; Lemieux et al., 2008; S. Li & Duffy, 2011; Maxwell & Kollet, 2008; Meyerhoff & Maxwell, 2011; Smerdon et al., 2008). However, the importance of perched aquifers on the surface and subsurface flow integration is not addressed adequately in the literature. Perched aquifers can effectively redirect the land surface recharge along a horizontal impermeable layer to springs, streams, wetlands, and lakes (Amit et al., 2002; Driese et al.,

2001; O'Driscoll & Parizek, 2003; Rabbo, 2000; Von der Heyden & New, 2003), consequently decreasing the volume of vertical recharge to deeper aquifers (Bagtzoglou et al., 2000). Furthermore, continuity and permeability of the perched layer play an important role in connections between the surface-subsurface flow and the regional groundwater system. Where perched layers are fully continuous and impermeable, surface and subsurface flow would be completely isolated from the regional groundwater system (Golden et al., 2014; Pirkle & Brooks, 1959). However, a semi-impermeable perched layer with internal discontinuity, fractures, and faults is likely to have unpredictable effects on the hydrologic environment.

Perched aquifers occur in a range of geological units especially in volcanic formations where texture and structures that affect porosity and permeability vary laterally, sometimes over short distances. One example of a perched aquifer in a volcanic succession is the Kawerau shallow groundwater aquifer in the Okataina Volcanic Centre, in North Island, New Zealand. The Rotoiti Pyroclastics and Matahina Ignimbrite were formed, respectively, at around 61,000 and 320,000 years ago as a result of two large-volume caldera forming eruptions (Leonard, 2010; Wilson et al., 2007) .

Previous studies indicate the upper part of the Matahina Ignimbrite has lower primary porosity and groundwater yield compared to the deeper parts (Gordon, 2001; Tschritter & White, 2014). In addition, a thin semi-permeable layer of variable thickness between the two volcanic units is reported in some geological investigation bores (Sky, Harding, & Khan,

2009). Consequently, this thin layer is controlling the water flux exchange between surface flow, perched aquifer flow and regional aquifer flow due to the relatively high hydraulic conductivity in both formations and low hydraulic conductivity of the perched layer.

Despite their common occurrence, relatively little is known about how a leaky and perched aquifer controls flux exchange in the total hydrological system. In fact, as suggested by previous authors, the importance of perched aquifers in regional groundwater models tends to be neglected, sometimes because of lack of data such as location, position and hydraulic properties of the perched aquifer and sometimes because size of perched aquifer are too small compare to the size of the regional groundwater aquifer (Cable Rains et al., 2006).

The present study investigates the leaky and perched aquifer in the Rotoiti Pyroclastics, New Zealand, by way of a high-resolution finite element model developed for the shallow aquifer. This case study at Kawerau builds upon the primary aim of the thesis which is to develop a better understanding of the roles of leaky and perched aquifers on the interaction between surface flow, subsurface flow and the regional groundwater aquifer. There are also two secondary aims specific to this chapter: firstly, obtaining an estimate of the total recharge volume and the spatial pattern of recharge to the Matahina Ignimbrite, which is the regional aquifer; secondly, estimating various groundwater travel times within the case study catchment area.

4.3 Site description

4.3.1 Location and surface flow system

The Kawerau shallow groundwater aquifer in Rotoiti Pyroclastics, which covers approximately 14.3 km^2, is located to the north of Kawerau township and the west of the Tasman Mill wastewater treatment ponds in the Bay of Plenty region, New Zealand (Fig. 4.1). The catchment associated with the study area is mainly covered by exotic and native forest trees. The catchment has a steady and relatively mild slope (max slope < 26 degrees) along toward the east. The ground surface elevation varies from 180 m at the west site of the catchment's hillslopes to 20 m at the catchment's outlet. The catchment is drained by two relatively small streams which pass through some wetlands and discharge to the Tasman Mill wastewater ponds which include the modified Lake Rotoroa. The lake in turn discharges into some wastewater treatment ponds. In addition to this natural flow, around 128.9 ML/day of wastewater and stormwater from pulp, paper and timber industries at the Tasman site enters the ponds, and then the natural and industrial flux around 124.3 ML/day is discharged into the Tarawera River by control valves and diffusers.

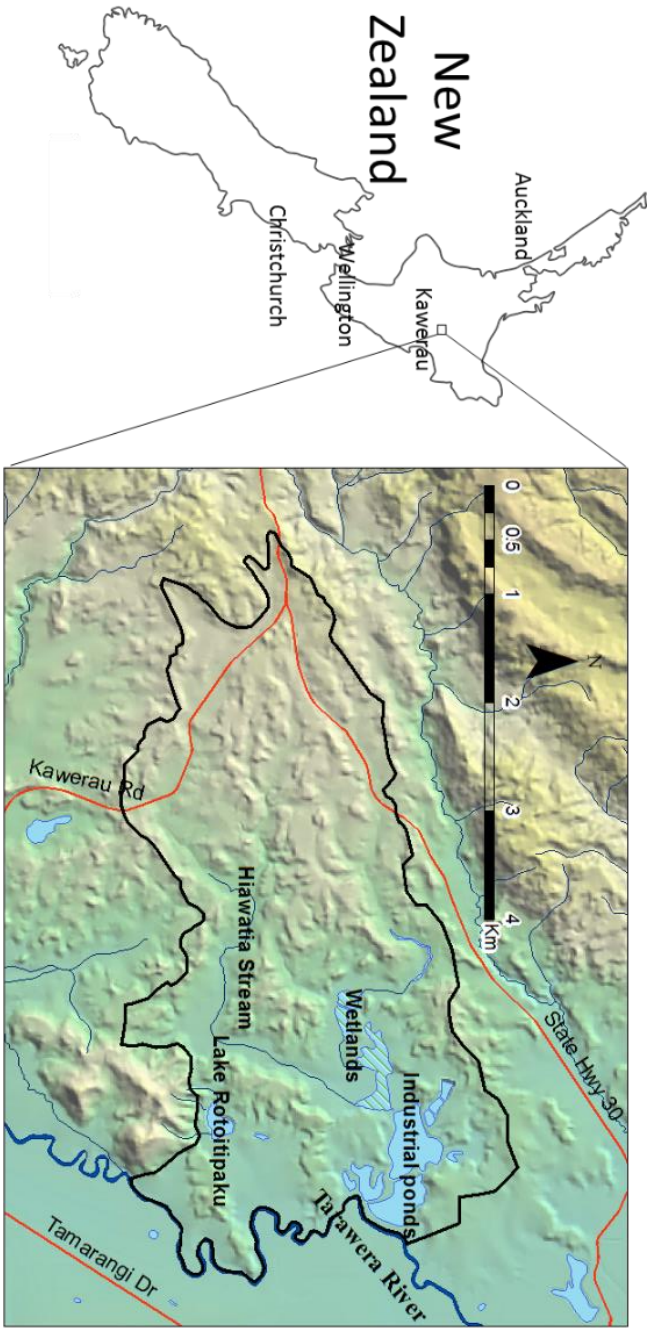

Fig. 4.1 An overview map of the study area

4.3.2 Geological and hydrogeological setting

In the study area the geology comprises a succession of pyroclastic units derived from explosive eruptions of the Taupo Volcanic Zone. Four Holocene shallow volcanic formations in the 20 metres below ground surface, based on geological surveys and available bore-logs are reported

by Sky and et al. (Sky et al., 2009). In order of increasing age and depth, they are respectively the 1886 AD Tarawera Pyroclastics, the 1314 AD Kaharoa Pyroclastics, the c. 232 AD Taupo Pumice Formation and the c.5600 cal yr BP Whakatane Formation (equivalent to Whakatane Pyroclastics) (Sky et al., 2009). All these units are permeable and discontinuous laterally and also vary in thickness.

The main laterally continuous, shallow identified volcanic unit in the study area is the Rotoiti Pyroclastics Formation (equivalent to Rotoiti Breccia). The Rotoiti Pyroclastics were deposited during the eruption of the Rotoiti Caldera at the northern part of Haroharo caldera at 61.0 ± 1.4 ka (Wilson et al., 2007) with magma volume estimates ranging between 80 to 120 km^3 (I. Nairn, 2002; Shane, Nairn, & Smith, 2005; Wilson & Charlier, 2009). The formation consists of airfall deposits and non-welded ignimbrite that has a soft to firm consistency (Charlier & Wilson, 2010), and ranges in thickness from 7.5 to 74 m in the observation bores in the study area. There is little information available in the literature regarding the hydraulic conductivity of the Rotoiti Pyroclastics. However, from results of limited slug tests, the Rotoiti Pyroclastics are fairly porous and permeable (Sky et al., 2009; Thompson, 1974; Tschritter & White, 2014).

Underlying the Rotoiti Pyroclastics is the Matahina Ignimbrite (Bailey & Carr, 1994), covering around 2,000 km^2 with a range in thickness from 5 to 200 m. The Matahina Ignimbrite is a 320 ka (Leonard, 2010) pyroclastic-flow deposit that erupted from the Haroharo Caldera, and has an outflow volume of 120 km^3. The Matahina Ignimbrite has been identified in some investigation bores at the study area (Milicich, Bardsley, Bignall, & Wilson,

2014; Milicich, Wilson, Bignall, Pezaro, & Bardsley, 2013; Sky et al., 2009). In addition an impermeable unit, the 138,000 to 150,000 years old Onepu Formation is observable on the south east of the area (Milicich et al., 2013).

In terms of permeability, previous studies suggest the Matahina Ignimbrite is permeable enough to be able to act as a productive groundwater aquifer (Bailey & Carr, 1994; Tschritter & White, 2014). However, in spite of the permeability of the Rotoiti Pyroclastics and Matahina Ignimbrite, a thin semi-impermeable layer (around 2m thick) between these two formations has been reported in some of the geological surveys (Sky et al., 2009). Similarly, some other studies specify that the upper part of Matahina Ignimbrite has a lower primary porosity and groundwater yields compared to the lower part. Moreover, some faults and fractures are reported to cut across both units (Gordon, 2001; Milicich et al., 2013; I. A. Nairn, 2002; Tschritter & White, 2014).

The existence of the semi-impermeable layer between two relatively permeable formations causes the development of a perched aquifer in the Rotoiti Pyroclastics. On the other hand, the semi-impermeable layer is not fully porous and continuous across the site. Also, fractures and faults may develop some hydraulic connections between the Rotoiti Pyroclastics and Matahina Ignimbrite. The perched layer may thus in fact act as a complex connection between the surface flow shallow aquifer and the regional groundwater system.

4.3.3 Climate

The climate in Kawerau is warm and temperate (oceanic climate) and classified as Cfb by the Köppen-Geiger system (Peel, Finlayson, & McMahon, 2007). For the current study an average annual rainfall and potential evapotranspiration (PET) for a three years period from the beginning of 2008 to the end of 2010, are utilised. The PET data are supported by NIWA virtual climate stations (VCS) (Tait, Henderson, Turner, & Zheng, 2006). Fig 4.2 shows an interpolation map of annual average rainfall and PET. The mean annual rainfall shows a 250 mm difference from around 1750 mm near the industrial ponds to about 1900 mm in the North landfill area.

Catchment actual evaporation (AET) is calculated using the approach of Zhang et al. (2004):

$$\boldsymbol{AET} = \boldsymbol{PET}(\mathbf{1} + \frac{\boldsymbol{P}}{\boldsymbol{PET}} - [\mathbf{1} + (\frac{\boldsymbol{P}}{\boldsymbol{PET}})^{\boldsymbol{w}}]^{\mathbf{1}/\boldsymbol{w}} \qquad (4.1)$$

where *P* is precipitation, and *w* is a dimensionless model parameter. Woods et al. reported that *w=4.35* gives the best fit to New Zealand sites (Woods, Hendrikx, Henderson, & Tait, 2006). A comparison between PET and calculated AET from equation 4.1 shows PET and AET have much less spatial variation than rainfall. The difference between PET and AET is not more than 50 mm over the whole catchment area.

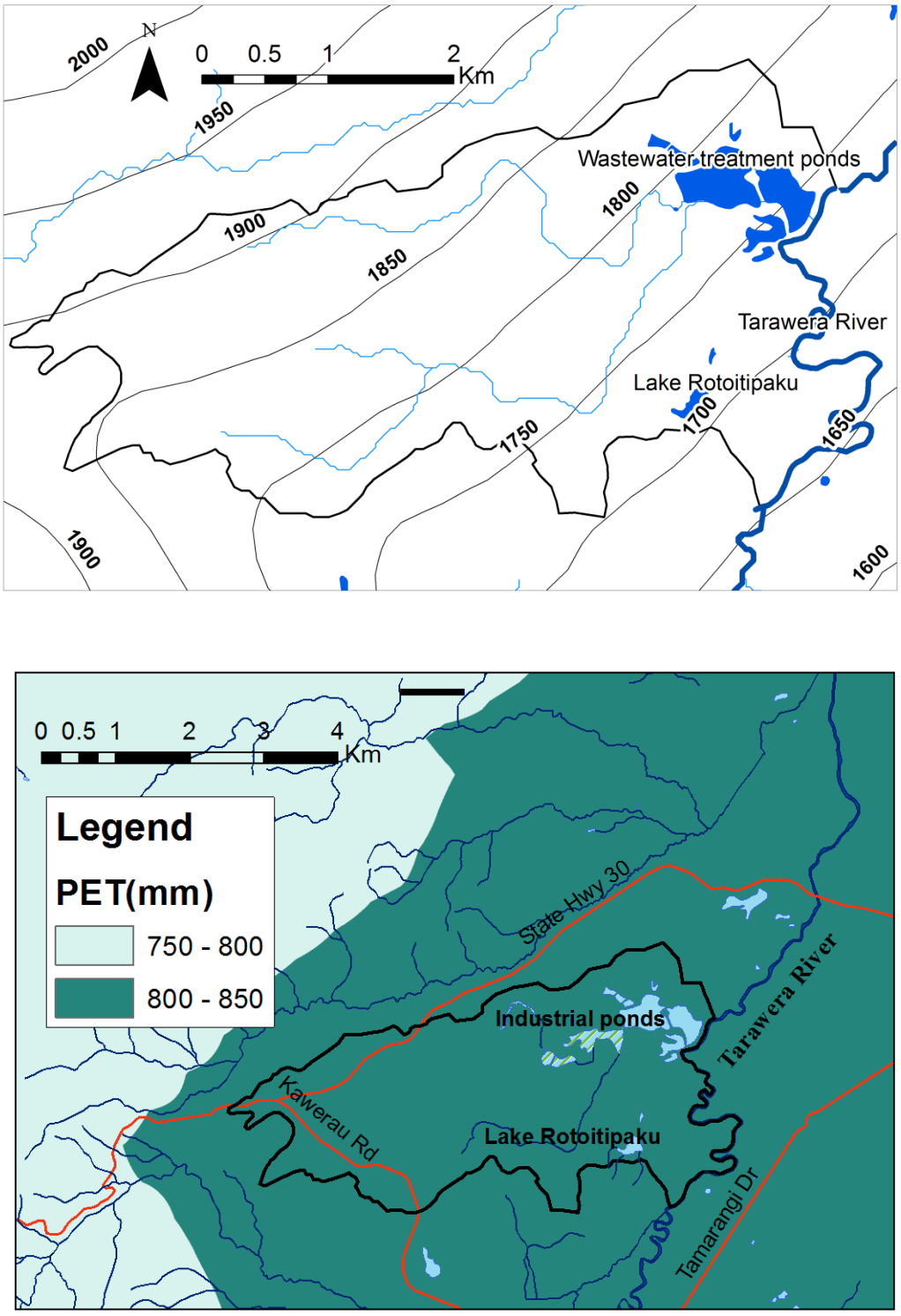

Fig. 4.2 Estimated mean annual rainfall, PET (Tait et al., 2006)

4.4 Industrial Pond Water balance

Sources of pond water include industrial discharge (*QI*), environmental discharge (*QE*), and direct precipitation (*P*). Water sinks are direct

discharged to the Tarawera River (*Qw*), evaporation (*ET*) and seepage (*S*) to the Tarawera River (Fig 4.3).

A pond's water balance equation can be expressed as:

$$(QI + QE + P) - (Qw + ET_0 + S) = \frac{dV}{dt} \quad (4.2)$$

where, $\frac{dV}{dt}$ is the volumetric storage change, assumed to be zero for an annual water budget.

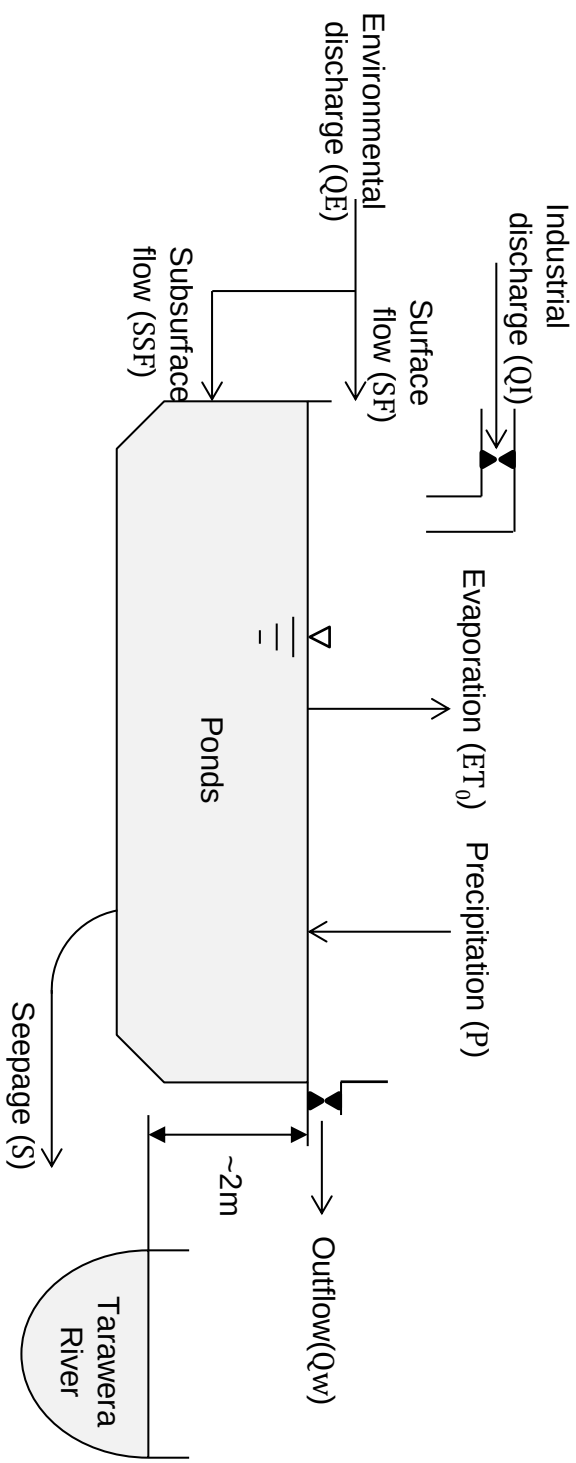

Fig. 4.3 Schematic showing water sources and sinks for the Kawerau industrial ponds.

4.4.1 Qw and QI

Industrial discharge to the ponds and pond outflow to the Tarawera River are monitored by a continuous-flow measurement gauge. The extent to

which direct outfall discharge from the ponds exceeds industrial discharge into the ponds (*Qw- QI*) is obtained as 128.9 - 124.3 = 4.7 ML/day, being the extent to which the mean pond outflow to the Tarawera River exceeds the mean industrial discharge into the ponds (from the beginning of 2008 to the end of 2010).

4.4.2 P and ET

The direct annual volumetric precipitation (*P*) and evaporation (*ET)* for the ponds, are estimated to be equivalent to 1.99 and 0.91 ML/day respectively, as obtained by multiplying the pond area (~0.5 km^2) and daily NIWA VCS data (Tait et al., 2006). For this study the VCS data for a period between 01/01/2008 and 31/12/2010 are utilised.

4.4.3 Seepage to Tarawera River (S)

The seepage rate between the wastewater treatment ponds and Tarawera River is estimated using the steady-state numerical model for solving the Laplace equation. The simplification assumptions that have been made to estimate seepage rate are (i) the seepage flow is steady state and flowing slowly, (ii) the seepage domain is non-fractured, and (iii) the hydraulic conductivity is an isotropic scalar. Regarding the slug test results reported by Sky et al. (Sky et al., 2009), the hydraulic conductivity of the material between the river and ponds are assumed to be 0.38 ± 0.28 m/day respectively. The calculated seepage values are estimated to be 0.20 ± 0.14 ML/day respectively. Comparing the seepage rate with the pond outflow to the Tarawera River, even the upper bound of the calculated seepage rate is less still than 0.3% of the surface outflow discharge.

4.4.4 QE

Using Equation 4.2, the environmental discharge to the ponds (QE) is calculated to be 3.8 ML/day. Considering that the annual rainfall (1801 mm) for the catchment area (12.8 Km^2) is about 63.4 ML/day, an estimated 6% of catchment rainfall volume flows to the ponds yearly.

4.5 Method and materials

A numerical groundwater model for the shallow aquifer is developed in order to increase the level of understanding of groundwater flow as well as the effect of the leaky perched aquifer on surface flow bodies and the regional groundwater system. The numerical model is constructed in FEFLOW (Finite Element subsurface FLOW system) (Trefry & Muffels, 2007), which is a well-known computer program for simulating groundwater flow in porous media.

4.5.1 Monitoring bores and slug test

There are some monitoring bores available in the study area. From the bore casing elevation compared to the Matahina Ignimbrite surface elevation, it is evident that some bores are monitoring the perched aquifer and the others the regional groundwater system of the Matahina Ignimbrite. In terms of data quality, in spite of a large number of monitoring bores, water level records are not continuous and do not cover the study area. Fig 4.4 shows the name and location of available monitoring bores in shallow groundwater system.

Current understanding of hydraulic properties on the site are based on some slug tests (Sky et al., 2009), indicating a “moderate” hydraulic conductivity suggested by Landon (Landon, 2014). Hydraulic conductivity are extrapolated based on six available slug test results (Fig 4.5). This highly speculative contours are used as initial estimation of the numerical model hydraulic conductivity.

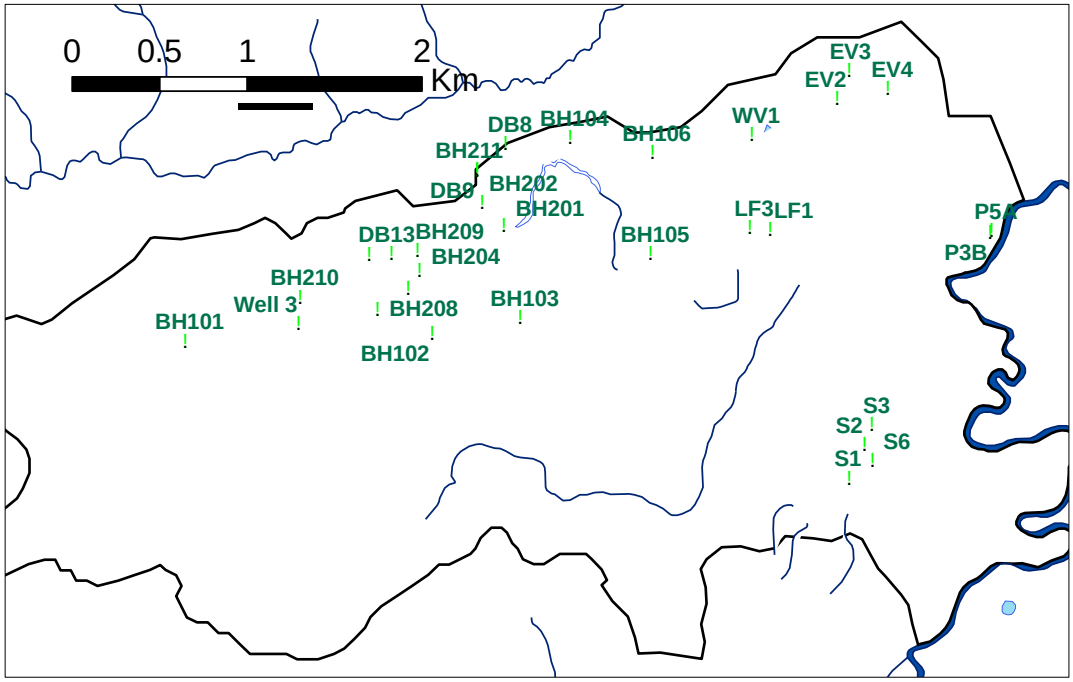

Fig. 4.4 The shallow observation bores that are utilised in the groundwater model calibration.

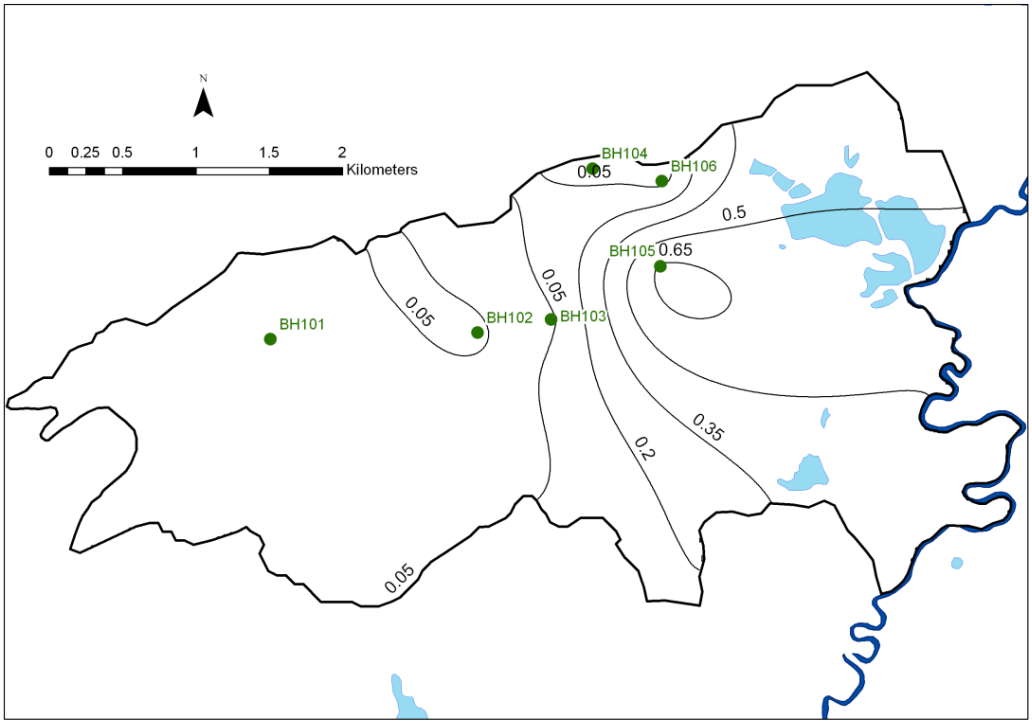

Fig. 4.5 Interpolated hydraulic conductivity of Rotoeiti Pyroclastics m/day from available slug test data

4.5.2 Model structure

The model aquifer boundaries are a combination of the hydrological catchment boundaries from the rivers order 3 and 4, reported by Slender et al. (Snelder, Biggs, & Weatherhead, 2010) and geological units from Nairn (I. A. Nairn, 2002). The shallow and perched groundwater aquifer model includes all permeable units above the Matahina Ignimbrite; including the four upper units namely: Tarawera Pyroclastics, Kaharoa Pyroclastics, Taupo Pumice Formation and Whakatane Formation each of which have a sporadic distribution as well as the Rotoiti Pyroclastics which is a widespread unit. On the other hand, impermeable Onepu Rhyolite within the catchment area is excluded from the conceptual model.

The thin semi-impermeable layer between the Matahina Ignimbrite and Rotoiti Pyroclastics is considered as the leaky basement. The elevation of

this interface surface is interpolated from available information in the geological investigation bore-logs. The top surface boundary is derived from a 5 m resolution topographic map. Fig 4.6 gives an overview of the conceptual model for the Kawerau shallow aquifer. And Fig. 4.7 illustrates the catchment order 3 and 4 reported by Slender et al. (Snelder et al., 2010) and shallow perched groundwater model borders.

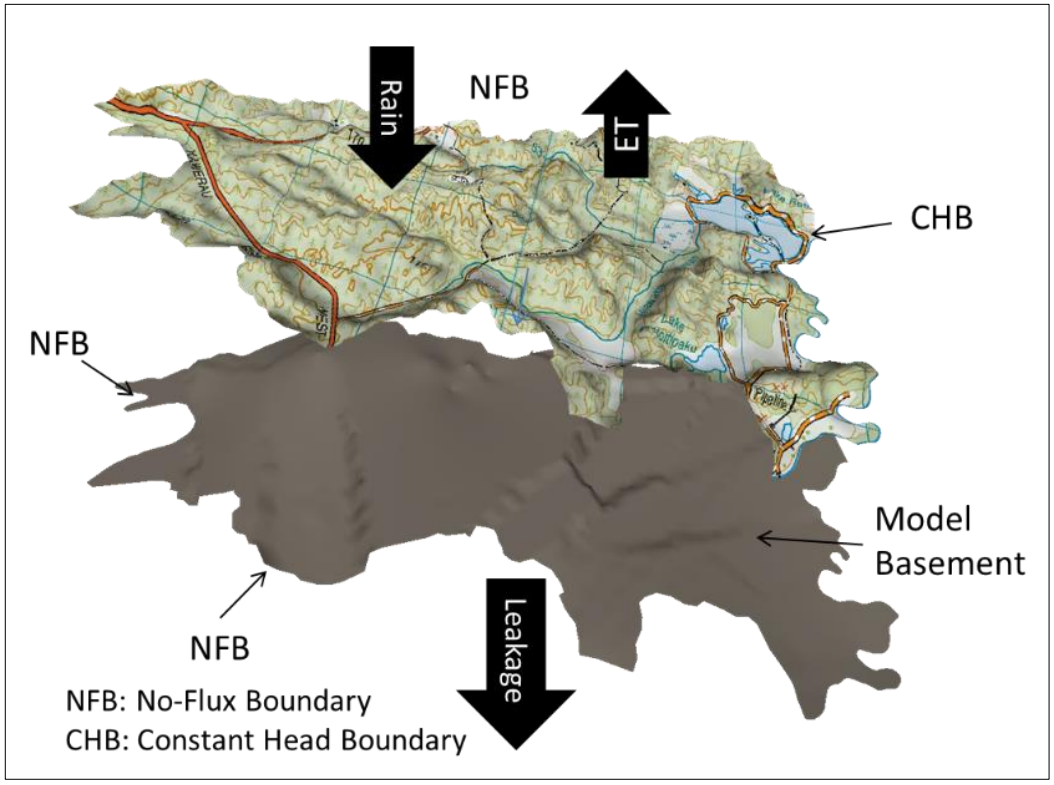

Fig. 4.6 Conceptual model, showing ground surface (topography) and the top of Matahina Ignimbrite surface applied in the model.

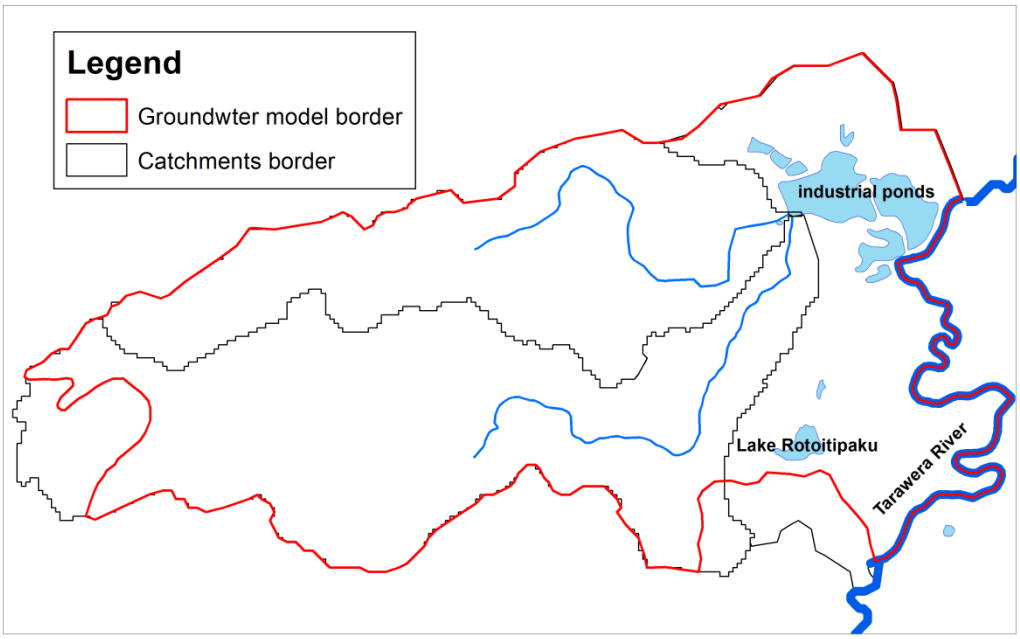

Fig. 4.7 Catchments of order 3 and 4 from New Zealand river environment classification (REC) (Snelder et al., 2010), and shallow perched groundwater border.

4.5.3 Recharge zone

Field observations indicate that sheet-flow would not be likely to occur, even during heavy rainfall, because of vegetation and high soil infiltration. Also, there is no major irrigation, industrial, or domestic water supply wells found inside the model boundaries in the Bay of Plenty Regional Council database (White, 2005). Therefore, recharge from the ground surface either drains to streams or ponds, or recharges the Matahina Ignimbrite.

On the basis of the rainfall and PET values and patterns (Fig 4.2), and the annual rate of environmental discharge to the pond, six recharge zones are defined for the model as 885, 935, 985, 1035, 1085 and 1135 mm/year for zone 1 to 6, respectively (Fig 4.8). On the other hand, the basement is discontinuous and semi-impermeable therefore it is assumed that a

continuous local vertical flux is leaking through the basement to the Matahina Ignimbrite aquifer.

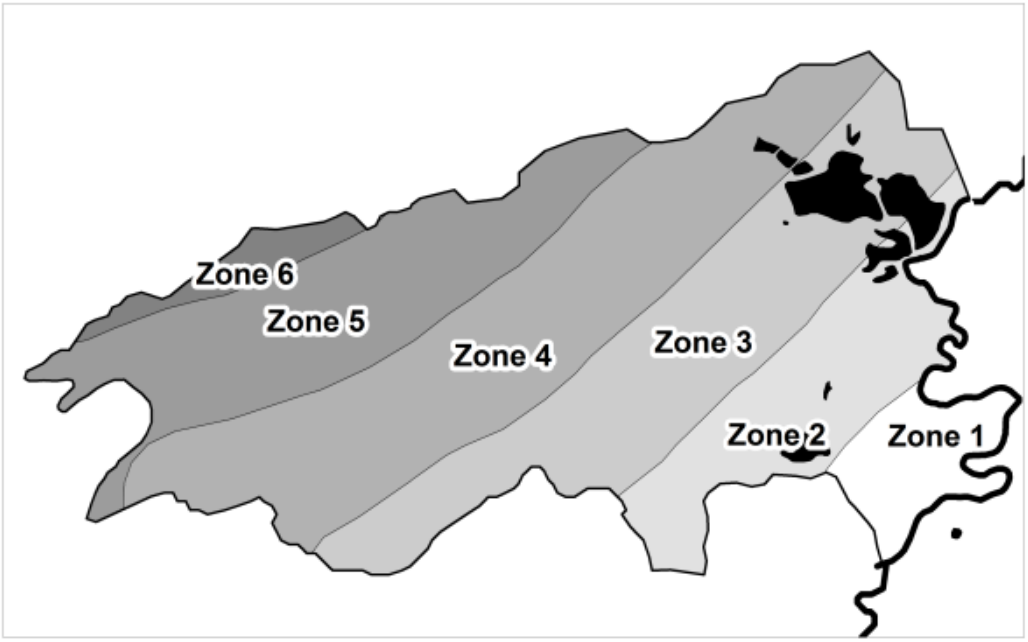

Fig. 4.8 Recharge zones as specified for the model; 885, 935,985 ,1035, 1085 and 1135 mm/year for zone 1 to 6 respectively.

4.6 Numerical model

A steady state finite element groundwater model (FEFLOW) is implemented for this study. The most attractive characteristics of finite element models are the ability to handle complicated boundaries, different mesh types, and varieties of density across the model compared to finite difference models. Mesh density has been increased in the critical zones such as near the wastewater treatment ponds and observation bores to improve the numerical model accuracy. Fig 4.9 shows the generated finite element mesh for the study area.

Water level rise and fall in the ponds and the river have been ignored and an average 14, 20, and 24 m constant head boundary condition is applied

respectively to: the Tarawera River, pond 1 to pond 5, and Lake Rotoitipaku. These constant head boundary conditions may become either a sink or a source, depending on hydraulic gradient conditions generated from the model. For the rest of the boundaries, a no-flow boundary condition is utilised.

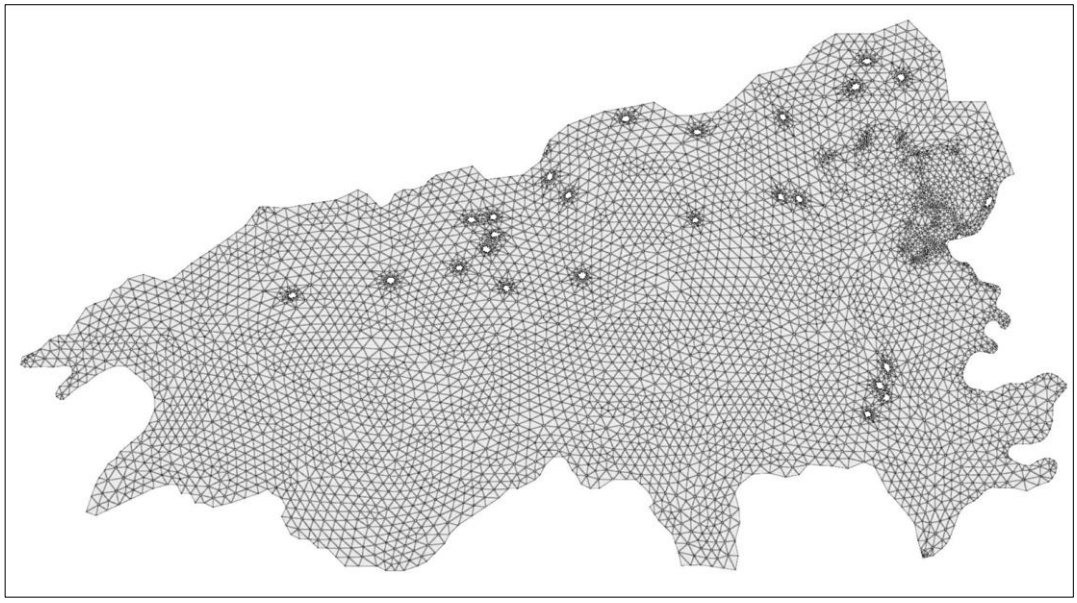

Fig. 4.9 Finite element mesh of the study area, used in the model

4.6.1 Model calibration

The model was calibrated with reference to the time-averaged water tables of each of 26 observation bores, and with reference to pond water balance. An automated calibration procedure was implemented using PEST (parameter estimation software) (Dahlstrom, 2015). In this process 100 pilot points are introduced to the PEST model. Through trial and error, PEST generates a distribution pattern for the basement leakage and a hydraulic conductivity map seeking to have the minimum difference between computed and observed water table. The hydraulic conductivity however is forced to remain within 20% of the values of the slug tests

results at the points of hydraulic conductivity measurements. Comparison between observed and computed total head and pressure head at the monitoring bore locations are shown in Fig 4.10.

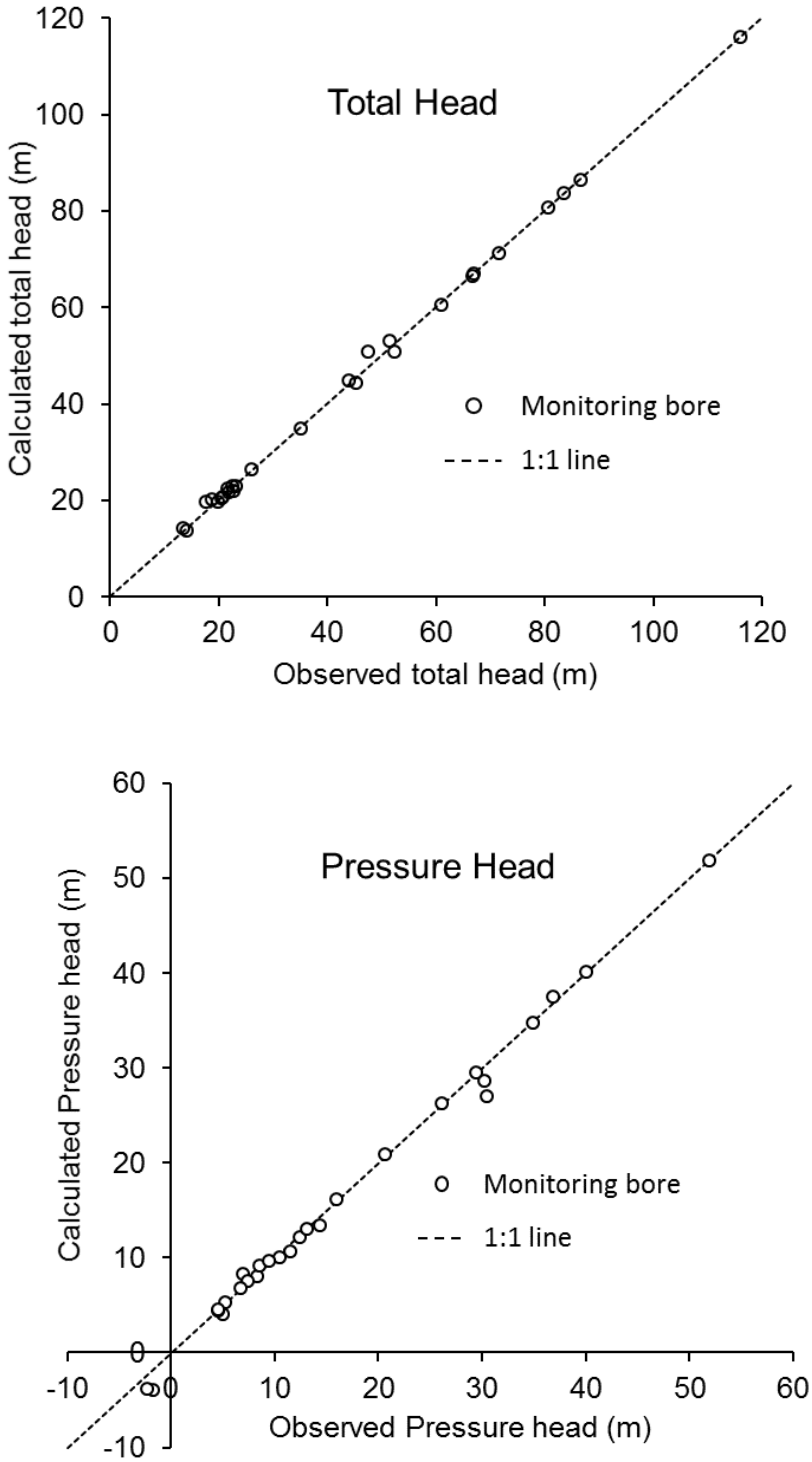

Fig. 4.10 Calibration scatter plot between the calculated (fitted) and observed total head and pressure head at the monitoring bore locations.

4.7 Results and discussion

4.7.1 Perched and regional groundwater interaction

The static water table of the study area as derived by the calibrated model is shown in Fig 4.11. As a general trend, groundwater follows the topographic gradient and therefore the water table becomes shallower closer to the ponds. However, in the north centre of the domain the static water table lines show a different pattern compared to the rest of the domain. This area is highlighted in Fig 4.11 and is known hereafter as the basement leakage zone.

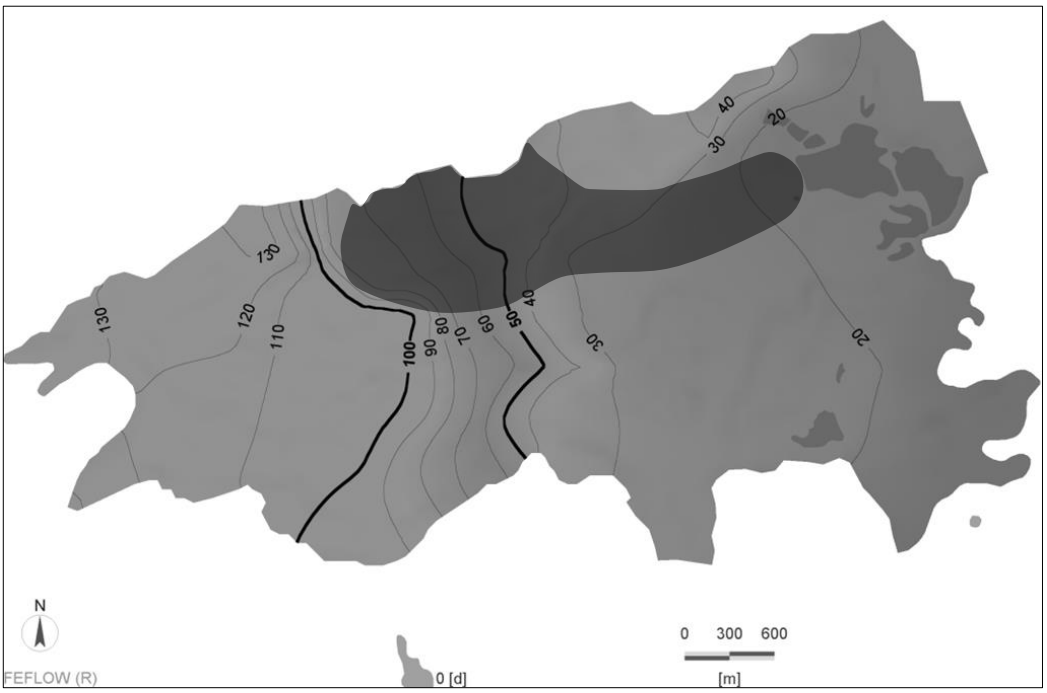

Fig. 4.11 Steady state water table from the calibrated numerical model, and the basement leakage zone. pizometric level units are in metres.

It is a noticeable that the model-generated static water slopes somewhat toward the leakage zone, even sometimes against the general eastward trend in some locations. This strong connection between the perched and regional groundwater table can occur because of the existence of a fault

which is also reported by Sky and et al. (Sky et al., 2009). Because of increasing the recharge rate to the Matahina aquifer on the leakage zone, the water table on the Matahina aquifer rises and almost connects to the perched aquifer in the leakage zone.

Water balance of the calibrated model calculates the total annual recharge from the ground surface, of the model extent, into the perched aquifer is estimated as 1011 mm, of which 904 mm leaks to the Matahina Ignimbrite and around 107 mm is passing to Tarawera River yearly via Rotoiti aquifer. Therefore on average around 11% of the total land surface recharge is redirected by the semi-impermeable layer to the Tarawera River either directly or through the ponds. Consequently 89% of the land-surface recharge leaks to the regional groundwater aquifer.

The leakage volume to the Matahina Ignimbrite, however, varies by location. About 78% of the leakage to the regional groundwater system passes through the leakage zone. This means that the perched layer efficiently changes the regional groundwater recharge pattern from land-surface recharge, which was dictated by rainfall to a new pattern, which comes as a result of a geological feature of the perched layer.

4.7.2 Particle tracing and surface water bodies

The calibrated model estimates the flow paths from different points in the domain. Results of particle tracking for some selected hypothetical points are shown in Fig 4.12a. The particle tracing shows that some flow paths may go directly to the Tarawera River but most go to Tarawera River through the streams and ponds. The semi-impermeable layer causes a

separation between the shallow and the regional groundwater in the study area. Consequently the shallow groundwater system is the source of the surface water bodies including two streams, wetlands and the natural pounds on the catchment. The groundwater model water balance shows 4.2 ML/day of the land surface recharge redirects by the semi-impermeable layer to shallow groundwater system and surface water bodies.

A particle travel time model runs by the calibrated model and the travel time map is shown in Fig 4.12b. Any particles in the groundwater by 1 km distance along north, east and the southwest of the industrial ponds may take up to 10 years to appear in the ponds via the shallow groundwater. For other areas contribution to the ponds, however, it might take more than 50 years for a particle to reach the ponds.

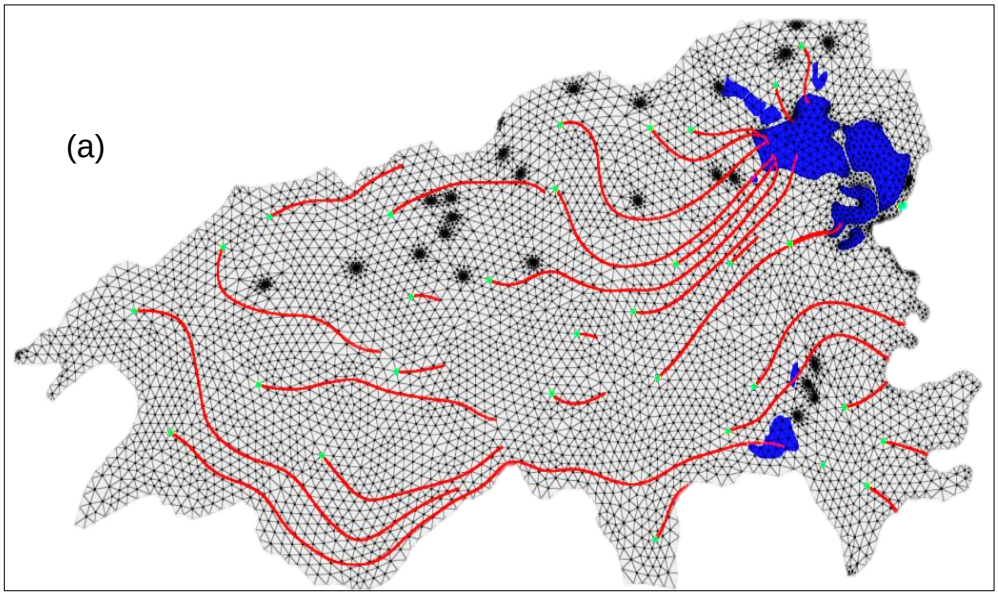

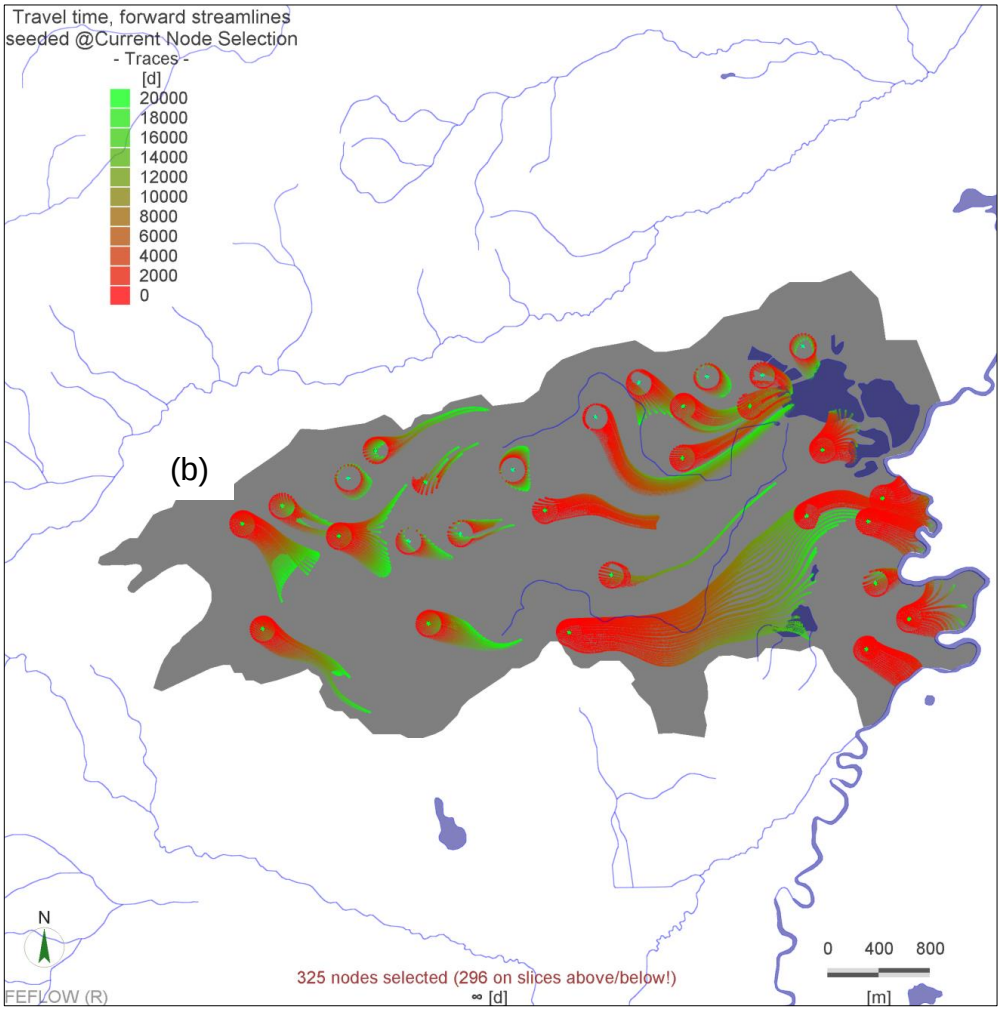

Fig. 4.12.(a) Particle tracking and (b) travel time with the calibrated numerical model in FEFLOW.

4.8 Conclusion

In the previous chapters it is concluded that artificial structures such as tile drains may play an important role in the linkage between surface and subsurface flow. This chapter further concludes that sometimes natural aspects such as perched and leaky aquifers also may have an important role in the connection between surface, subsurface flow and regional groundwater.

Case study of groundwater system in the Kawerau area shows that a thin semi-impermeable layer between two volcanic units, Rotoiti Pyroclastics and Matahina Ignimbrite, results in the development of a shallow water table within Rotoiti Pyroclastics. Modelling indicates there is complex water flux interaction between the surface flow, subsurface flow, and the regional groundwater system of the Matahina Ignimbrite. The perched layer plays an important role in the connection and control of the flux exchange between the surface-subsurface flow and the regional groundwater system. Around 11% of the land surface recharge is redirected by the semi-impermeable layer along horizontal pathways to the surface flow network.

The perched and regional groundwater systems across the study area have both strong and weak connection zones in the vertical sense. The strongest linkage, according to the available data, occurs in an area close to the northern border that could be due to of the existence a fault connecting the Rotoiti Pyroclastics and Matahina Ignimbrite. The calibrated model shows around 78% of the total land surface recharge passes through this leakage zone to the underlying layer. However, there

could be further connections between the perched and regional aquifers within the study area, but to detect additional potential leakage zones, more investigation and monitoring bores are required. Ignoring perched aquifers in regional groundwater models may result in considerable error in recharge spatial variation, thus increasing regional groundwater model inaccuracies.

4.9 Acknowledgements

This material is based upon work funded by Norske Skog Tasman and Carter Holt Harvey Pulp and Paper.

5 Chapter 5

Conclusions

5.1 Overall summary

A review of previous studies on coupled surface and subsurface flow research identified some knowledge gaps regarding the effect of artificial and natural elements on the linkage between surface and subsurface water components. Therefore, the main aims of this doctoral study were:

1. to improve classical tile drain spacing design methods;
2. via a case study, to assess the role of semi-impermeable layers influencing the interaction between surface water and a regional groundwater system.

This doctoral project has made some degree of advancement in numerical models of integrated and complex environmental systems that often occurs as a result of either human activities, such as drainage and irrigation practices, or geological features, such as leaky and perched aquifers.

To address objective 1 the development, tests and applications of *DrainFlow* are presented in chapter 2. *DrainFlow* is a new, fully distributed, physically based and integrated surface - subsurface flow code that is designed for water movement and connections in artificial drainage

projects. Compared to traditional drainage models, *DrainFlow* has the advantage of estimating the land surface recharge directly from the partial differential form of Richards equation rather than through analytical or empirical infiltration approaches, such as the Green and Ampt equation.

To develop the model, a range of surface and subsurface flow modules are first formulated separately. Then, each module is connected to the related modules in the code. Consequently, in each time step, all modules simultaneously work together and use the outcomes of the other modules to yield a unique answer for all domains.

Switching between dry and wet boundary conditions often occurs in these types of models and causes nonlinearity problems. To avoid this issue, a new mechanism is included in the code to provide smooth switching between dry and wet boundary conditions.

To test the *DrainFlow* code, some comparisons are made between *DrainFlow* and a range of surface-subsurface flow codes for five well-known integrated surface and subsurface benchmarks. These benchmarks have been designed to challenge codes for integrated surface and subsurface flow conditions. In general, it is concluded that the *DrainFlow* code shows good agreement with the other coupled surface and subsurface flow codes to predict the flow in the studied benchmarks.

In addition, two new hypothetical examples for tile drain studies are introduced and solved by the *DrainFlow* code. The first example is designed to challenge the *DrainFlow* code in high-resolution and small-scale tile drainage studies. It was shown how the *DrainFlow* code can

compute the impacts of the ground surface Manning roughness coefficients and slopes on the tile drain hydrographs that the traditional tile drainage equation was not able to predict.

In the second hypothetical example *DrainFlow* was up-scaled for 10, 20, 40 and 80 tile drains and the groundwater model domain area was enlarged ten times compared to the first example. It had taken more than ten days for a normal desktop computer to solve such a large example. However, *DrainFlow* overcame the problem by adopting some simplification assumptions both dimensionally and theoretically. The simplified model converged in less than ten minutes using the same computer. Consequently, it was concluded that besides the model comprehensiveness and complexity, *DrainFlow* is fairly flexible. *DrainFlow* could be simplified dimensionally or methodologically into a less or more comprehensive and complex model, based on the conceptual model scale and data availability.

To further develop objective 1, in Chapter 3 of this doctoral thesis, a dimensionless finite-element model of the Richards equation was developed to incorporate the effect of soil-water retention parameters on the maximum water table height between two adjacent tile drains. This model was then used as a comparison reference to show that the well-known analytical Hooghoudt equation in fact overestimates the maximum water table height midway between two tile drains, particularly for sandy soils. Furthermore, both of the well-known Hooghoudt equation coefficients are shown to be functions of soil-water retention parameters.

Consequently, two new dimensionless coefficients, β_1 and β_2, are incorporated into the Hooghoudt equation, giving a modified expression which yields between-drain water table height estimates close to those obtained from the numerical reference model. These coefficients are shown to be functions of soil-water retention curves.

To address objective 2, in Chapter 4 of this doctoral thesis, it was concluded that perched layers play an important role in the connection and control of the flux exchange between the surface-subsurface flow and the regional groundwater system. Around 10% of the land surface recharge is redirected by a semi-impermeable layer along horizontal pathways to the surface flow network. It is concluded that ignoring perched aquifers in regional groundwater models may result in considerable error in recharge spatial variation, consequently increasing regional groundwater model inaccuracies. Furthermore, it is evident that the perched and regional groundwater systems in Rotoiti Pyroclastics and Matahina Ignimbrite in the study area have both strong and weak hydraulic connections because of geologic features. Consequently, one of the strong connection zones between the Rotoiti Pyroclastics and Matahina Ignimbrite was detected. According to the available data and the numerical model, around 80% of the total land surface recharge passes through the detected leakage zone to the regional groundwater system.

5.2 Wider implications

This study emphasises a more integrated approach to the science of hydrology and highlights that artificial and geological elements in the nature play an important role in connecting surface and subsurface

groundwater flow. Isolated surface water and groundwater studies without appropriately considering the connection between groundwater and surface water may result in increasing inaccuracy in numerical models. This doctoral thesis contributes by determining the weaknesses of classical and separate surface and subsurface flow studies and develops practical approaches to enhance the previous methods.

5.3 Future research

Artificial drainage either by tile or ditch drains and influenced by perched and impermeable layers are observed frequently in agricultural catchments. With around two million hectares of poorly or imperfectly drained soils in New Zealand, artificial subsurface drainage networks play a very important role in improving productivity of New Zealand agricultural lands (Bowler, 1980).

Artificial drains and shallow impermeable layers may also act as a shortcut nutrient transfer pathway for nitrate, phosphorus, and sediment by changing the water flow direction from a deeper groundwater aquifer to surface water components. Estimating the effect of artificial drainage networks on the water budget, and the impact this has on nutrient leaching is essential for managing a tile drained agricultural watershed and is an area of research which is overlooked.

5.3.1 Impact on surface water hydrology

In spite of the considerable potential effects of artificial drainage and shallow impermeable layers on freshwater and coastal resources, there are few systematic measurement, modelling or management programs at

a catchment scale reported in previous studies. Most of the tile drainage studies in New Zealand are limited to the lysimeter or farm scale. Even worldwide, the environmental effects of tile drains on freshwater and coastal resources at the catchment and regional scale are only lightly researched.

5.4 Impact on regional groundwater hydrology

Little is known about the impacts of tile drainage and perched aquifer on regional groundwater. Water budget models suggest infiltration to the deeper groundwater system could be decreased by tile drainage or even by the creating change the direction of flow. Therefore, the question of how much water and contaminant is partitioned between surface waterways and groundwater in a tile drainage field is not addressed clearly in previous studies.

To improve our understanding of water (and nutrient) flow processes in surface water and groundwater in a tile drained catchment, a combination of measurements and modelling is required. In terms of modelling, *DrainFlow*, which successfully passed many challenging tests in an interaction surface and subsurface flow study, can be applied to model vertical and horizontal water movement in the vicinity of tile drains and estimate the volume of water that moves to the next layer after passing through a semi-impermeable layer. Then a combination of *DrainFlow* with optimization approaches can give tile drainage management recommendations. This has implications for both land productivity and for water quality management at the catchment scale.

6 References

Aley, T. J., & Fletcher, M. W. (1976). *The Water Tracer's Cookbook: A Guide to the Art and Science of Water Tracing Materials with Particular Emphasis on the Use of Fluorescent Dyes, Lycopodium Spores, and Bacteriophage in Groundwater Investigations* (Vol. 16/2): Lohman, Mo. : Missouri Speleological Survey,.

Amit, H., Lyakhovsky, V., Katz, A., Starinsky, A., & Burg, A. (2002). Interpretation of Spring Recession Curves. *Ground Water, 40*(5), 543-551. doi:10.1111/j.1745-6584.2002.tb02539.x Retrieved from http://dx.doi.org/10.1111/j.1745-6584.2002.tb02539.x

Andrews, C. B., & Anderson, M. P. (1978). Impact of a Power Plant on the Ground-Water System of a Wetland. *Ground Water, 16*(2), 105-111. doi:10.1111/j.1745-6584.1978.tb03209.x Retrieved from http://dx.doi.org/10.1111/j.1745-6584.1978.tb03209.x

Aquanty Inc. (2013). *HydroGeoSphere User Manual*. Waterloo, Ontario, Canada: HGS

Arnold, J. G., & Allen, P. M. (1999). Automated methods for estimating baseflow and ground water recharge from streamflow records. *Journal of the American Water Resources Association, 35*(2), 411-424. Retrieved from http://www.scopus.com/inward/record.url?eid=2-s2.0-0032910167&partnerID=40&md5=878bfdbc5411072e835f7355e98f0609

Bagtzoglou, A. C., Timothy L. Tolley, Stothoff, S. A., & Turner, D. R. (2000). *Perched aquifers in arid environments and inferences for recharge rates* Paper presented at the Tracers and modelling in hydrogeology. Proceedings of TraM'2000, the International Conference on Tracers and Modelling in Hydrogeology, IAHS Publication (No. 262), Liège, Belgium.

Bailey, R. A., & Carr, R. G. (1994). Physical geology and eruptive history of the Matahina Ignimbrite, Taupo Volcanic Zone, North Island, New Zealand. *New Zealand Journal of Geology and Geophysics, 37*(3), 319-344. doi:10.1080/00288306.1994.9514624 Retrieved from http://dx.doi.org/10.1080/00288306.1994.9514624

Baird, A. J., & Wilby, R. L. (2005). *Eco-Hydrology*: Taylor & Francis.

Banks, W. S. L., Paylor, R. L., & Hughes, W. B. (1996). Using thermal-infrared imagery to delineate groundwater discharge. *Ground Water, 34*(3), 434-443. doi:10.1111/j.1745-6584.1996.tb02024.x Retrieved from http://dx.doi.org/10.1111/j.1745-6584.1996.tb02024.x

Banti, M., Zissis, T., & Anastasiadou-Partheniou, E. (2011). Furrow irrigation advance simulation using a surface-subsurface interaction model. *Journal of Irrigation and Drainage Engineering, 137*, 304-314. Retrieved from http://dx.doi.org/10.1061/(ASCE)IR.1943-4774.0000293

Barlow, P. M., Wild, E. C., & Survey, G. (2002). *Bibliography on the Occurrence and Intrusion of Saltwater in Aquifers Along the Atlantic Coast of the United States*: U.S. Department of the Interior, U.S. Geological Survey. Retrieved from pubs.water.usgs.gov/ofr02235/pdfs/text03.pdf

Barua, G., & Tiwari, K. (1996a). Ditch drainage theories for homogeneous anisotropic soil. *Journal of Irrigation and Drainage Engineering, 122*(5), 276-285. doi:doi:10.1061/(ASCE)0733-9437(1996)122:5(276) Retrieved from http://ascelibrary.org/doi/abs/10.1061/%28ASCE%290733-9437%281996%29122%3A5%28276%29

Barua, G., & Tiwari, K. (1996b). Theories of ditch drainage in layered anisotropic soil. *Journal of Irrigation and Drainage Engineering, 122*(6), 321-330. doi:doi:10.1061/(ASCE)0733-9437(1996)122:6(321) Retrieved from

http://ascelibrary.org/doi/abs/10.1061/%28ASCE%290733-9437%281996%29122%3A6%28321%29

Baskin, R. L. (1998). Locating shoreline and submarine springs in two Utah lakes using thermal imagery.

Bayani Cardenas, M. (2008). The effect of river bend morphology on flow and timescales of surface water–groundwater exchange across pointbars. *Journal of Hydrology, 362*(1–2), 134-141. doi:http://dx.doi.org/10.1016/j.jhydrol.2008.08.018 Retrieved from http://www.sciencedirect.com/science/article/pii/S002216940800454X

Belaval, M., Lane Jr, J., Lesmes, D. P., & Kineke, G. C. (2003). Continuous-resistivity profiling for coastal groundwater investigations: three case studies. *SAGEEP Proceedings, Texas, 14*, 1-14. Retrieved from https://water.usgs.gov/ogw/bgas/publications/SAGEEP03_Belaval/SAGEEP03_Belaval.pdf

Bixio, A. C., Gambolati, G., Paniconi, C., Putti, M., Shestopalov, V. M., Bublias, V. N., . . . Rudenko, Y. F. (2002). Modeling groundwater-surface water interactions including effects of morphogenetic depressions in the Chernobyl exclusion zone. *Environmental Geology, 42*(2-3), 162-177. doi:10.1007/s00254-001-0486-7 Retrieved from <Go to ISI>://WOS:000176824000007

Bokuniewicz, H. (1980). Groundwater seepage into Great South Bay, New York. *Estuarine and Coastal Marine Science, 10*(4), 437-444. doi:http://dx.doi.org/10.1016/S0302-3524(80)80122-8 Retrieved from http://www.sciencedirect.com/science/article/pii/S0302352480801228

Bowler, D. G. (1980). *The Drainage of Wet Soils: Hodder and Stoughton*. Auckland, New Zealand.

Brunner, P., & Simmons, C. T. (2012). HydroGeoSphere: A Fully Integrated, Physically Based Hydrological Model. *Ground Water, 50*(2), 170-176. doi:10.1111/j.1745-6584.2011.00882.x Retrieved from http://dx.doi.org/10.1111/j.1745-6584.2011.00882.x

Burnett, W. C., & Dulaiova, H. (2003). Estimating the dynamics of groundwater input into the coastal zone via continuous radon-222 measurements. *Journal of environmental radioactivity, 69*(1), 21-35. doi:http://dx.doi.org/10.1016/S0265-931X(03)00084-5

Cable, J. E., Burnett, W. C., Chanton, J. P., Corbett, D. R., & Cable, P. H. (1997). Field Evaluation of Seepage Meters in the Coastal Marine Environment. *Estuarine, Coastal and Shelf Science, 45*(3), 367-375. doi:http://dx.doi.org/10.1006/ecss.1996.0191 Retrieved from http://www.sciencedirect.com/science/article/pii/S0272771496901912

Cable Rains, M., Fogg, G. E., Harter, T., Dahlgren, R. A., & Williamson, R. J. (2006). The role of perched aquifers in hydrological connectivity and biogeochemical processes in vernal pool landscapes, Central Valley, California. *Hydrological Processes, 20*(5), 1157-1175. doi:10.1002/hyp.5937 Retrieved from http://dx.doi.org/10.1002/hyp.5937

Cambareri, T. C., & Eichner, E. M. (1998). Watershed Delineation and Ground Water Discharge to a Coastal Embayment. *Ground Water, 36*(4), 626-634. doi:10.1111/j.1745-6584.1998.tb02837.x Retrieved from http://dx.doi.org/10.1111/j.1745-6584.1998.tb02837.x

Campbell, C. W., & Keith, A. (2000). Karst groundwater hydrologic analyses based on aerial thermography.

Camporese, M., Paniconi, C., Putti, M., & Orlandini, S. (2010). Surface-subsurface flow modeling with path-based runoff routing, boundary condition-based coupling, and assimilation of multisource observation data. *Water Resources Research, 46*(2), W02512. doi:10.1029/2008WR007536

Camporese, M., Paniconi, C., Putti, M., & Salandin, P. (2009). Ensemble Kalman filter data assimilation for a process-based catchment scale model of surface and subsurface flow. *Water Resources Research, 45*(10). doi:10.1029/2008wr007031 Retrieved from http://dx.doi.org/10.1029/2008WR007031

Carr, M. R., & Winter, T. C. (1980). *An annotated bibliography of devices developed for direct measurement of seepage* (80-344). Retrieved from http://pubs.er.usgs.gov/publication/ofr80344

Carsel, R. F., & Parrish, R. S. (1988). Developing joint probability distributions of soil water retention characteristics. *Water Resources Research, 24*(5), 755-769. doi:10.1029/WR024i005p00755 Retrieved from http://dx.doi.org/10.1029/WR024i005p00755

Castanheira, P., & Santos, F. (2009). A simple numerical analyses software for predicting water table height in subsurface drainage. *Irrigation and Drainage Systems, 23*(4), 153-162. doi:10.1007/s10795-009-9079-5 Retrieved from http://dx.doi.org/10.1007/s10795-009-9079-5

Chapman, T. (1999). A comparison of algorithms for stream flow recession and baseflow separation. *Hydrological Processes, 13*(5), 701-714. doi:10.1002/(sici)1099-1085(19990415)13:5<701::aid-hyp774>3.0.co;2-2 Retrieved from http://dx.doi.org/10.1002/(SICI)1099-1085(19990415)13:5<701::AID-HYP774>3.0.CO;2-2

Charlier, B. L. A., & Wilson, C. J. N. (2010). Chronology and Evolution of Caldera-forming and Post-caldera Magma Systems at Okataina Volcano, New Zealand from Zircon U–Th Model-age Spectra. *Journal of Petrology, 51*(5), 1121-1141. doi:10.1093/petrology/egq015 Retrieved from http://petrology.oxfordjournals.org/content/51/5/1121.abstract

Chavez, C., Fuentes, C., Zavala, M., & Brambila, F. (2011a). Numerical solution of the Boussinesq equation: Application to the agricultural drainage. *African Journal of Agricultural Research, 6*(18), 4210-4222. Retrieved from <Go to ISI>://WOS:000298502900004

Chavez, C., Fuentes, C., Zavala, M., & Zatarain, F. (2011b). Finite difference solution of the Boussinesq equation with variable drainable porosity and fractal radiation boundary condition. *Agrociencia, 45*(8), 911-927. Retrieved from <Go to ISI>://WOS:000298075100005

Childress, C. J. (1991). Hydrology and water quality near the South Well Field, southern Franklin County, Ohio, with emphasis on the simulation of ground-water flow and transport of Scioto River. In R. A. Sheets & E. S. Bair (Eds.). Columbus, Ohio :: U.S. Dept. of the Interior, U.S. Geological Survey ;.

Childs, E. C. (1969). *An introduction to the physical basis of soil water phenomena*: J. Wiley.

Chui, T. F. M., & Freyberg, D. L. (2007). *The Use of COMSOL for Integrated Hydrological Modeling*. Paper presented at the COMSOL Conference 2007, Boston.

Çimen, M. (2008). Discussion of "A new drain spacing formula". *Hydrological Sciences Journal, 53*(4), 933-934. Retrieved from http://www.informaworld.com/10.1623/hysj.53.4.933

Clark, M. P., Rupp, D. E., Woods, R. A., Zheng, X., Ibbitt, R. P., Slater, A. G., . . . Uddstrom, M. J. (2008). Hydrological data assimilation with the ensemble Kalman filter: Use of streamflow observations to update states in a distributed hydrological model. *Advances in Water Resources, 31*(10), 1309-1324. doi:http://dx.doi.org/10.1016/j.advwatres.2008.06.005 Retrieved from http://www.sciencedirect.com/science/article/pii/S0309170808001012

Cloke, H. L., Anderson, M. G., McDonnell, J. J., & Renaud, J. P. (2006). Using numerical modelling to evaluate the capillary fringe groundwater ridging hypothesis of streamflow generation. *Journal of Hydrology, 316*(1–4), 141-162.

doi:http://dx.doi.org/10.1016/j.jhydrol.2005.04.017 Retrieved from http://www.sciencedirect.com/science/article/pii/S0022169405002064
Collis-George, N., & Youngs, E. G. (1958). Some factors determining water-table heights in drained homogeneous soils. *Journal of Soil Science, 9*(2), 332-338. doi:10.1111/j.1365-2389.1958.tb01924.x Retrieved from http://dx.doi.org/10.1111/j.1365-2389.1958.tb01924.x
COMSOL. (May 2012). *COMSOL Multiphysics User's Guide*.
Corbett, D. R., Burnett, W. C., Cable, P. H., & Clark, S. B. (1998). A multiple approach to the determination of radon fluxes from sediments. *Journal of Radioanalytical and Nuclear Chemistry, 236*(1-2), 247-253. doi:10.1007/bf02386351 Retrieved from http://dx.doi.org/10.1007/BF02386351
Dagan, G. (1964). Spacings of drains by an approximate method. *Journal of Irrigation and Drainage Engineering, 91*, 41-46.
Dahlstrom, D. J. (2015). Calibration and Uncertainty Analysis for Complex Environmental Models. *Groundwater, 53*(5), 673-674. doi:10.1111/gwat.12360 Retrieved from http://dx.doi.org/10.1111/gwat.12360
Danielopol, D. L., et al., & Danielopol, D. L. (1997). *Ecotonal animal assemblages; their interest for groundwater studies Groundwater/Surface Water Ecotones: Biological and Hydrological Interactions and Management Options*: Cambridge University Press.
David, P. K., Carl, J. B., Carol, K., & Joel, R. G. (1994). Use of Oxygen-18 and Deuterium To Assess the Hydrology of Groundwater-Lake Systems *Environmental Chemistry of Lakes and Reservoirs* (Vol. 237, pp. 67-90): American Chemical Society.
Day-Lewis, F., White, E., Johnson, C., Lane, J., & Belaval, M. (2006). Continuous resistivity profiling to delineate submarine groundwater discharge—examples and limitations. *The Leading Edge, 25*(6), 724-728. doi:10.1190/1.2210056 Retrieved from http://dx.doi.org/10.1190/1.2210056
Delfs, J.-O., Blumensaat, F., Wang, W., Krebs, P., & Kolditz, O. (2012). Coupling hydrogeological with surface runoff model in a Poltva case study in Western Ukraine. *Environmental Earth Sciences, 65*(5), 1439-1457. doi:10.1007/s12665-011-1285-4 Retrieved from http://dx.doi.org/10.1007/s12665-011-1285-4
Delfs, J.-O., Wang, W., Kalbacher, T., Singh, A., & Kolditz, O. (2013). A coupled surface/subsurface flow model accounting for air entrapment and air pressure counterflow. *Environmental Earth Sciences, 69*(2), 395-414. doi:10.1007/s12665-013-2420-1 Retrieved from http://dx.doi.org/10.1007/s12665-013-2420-1
Delfs, J. O., Kalbus, E., Park, C. H., & Kolditz, O. (2009). A physically based model concept for transport modelling in coupled hydrosystems. *Grundwasser, 14*(3), 219-235. doi:10.1007/s00767-009-0114-0 Retrieved from <Go to ISI>://WOS:000269912300006
Delfs, J. O., Park, C. H., & Kolditz, O. (2009). A sensitivity analysis of Hortonian flow. *Advances in Water Resources, 32*(9), 1386-1395. doi:http://dx.doi.org/10.1016/j.advwatres.2009.06.005 Retrieved from http://www.sciencedirect.com/science/article/pii/S0309170809000955
Donato, M. M. (1998). *Surface-water/ground-water relations in the Lemhi River Basin, east-central Idaho* (98-4185). Retrieved from Reston, VA: http://pubs.er.usgs.gov/publication/wri984185
Dong, Q., Xu, D., Zhang, S., Bai, M., & Li, Y. (2013). A hybrid coupled model of surface and subsurface flow for surface irrigation. *Journal of Hydrology, 500*, 62-74. doi:http://dx.doi.org/10.1016/j.jhydrol.2013.07.018 Retrieved from http://www.sciencedirect.com/science/article/pii/S0022169413005350
Driese, S. G., McKay, L. D., & Penfield, C. P. (2001). Lithologic and Pedogenic Influences on Porosity Distribution and Groundwater Flow in Fractured Sedimentary Saprolite: A New Application of Environmental Sedimentology. *Journal of*

Sedimentary Research, 71(5), 843-857. doi:10.1306/2dc4096d-0e47-11d7-8643000102c1865d Retrieved from http://jsedres.sepmonline.org/content/71/5/843.abstract

Ebel, B. A., Loague, K., Vanderkwaak, J. E., Dietrich, W. E., Montgomery, D. R., Torres, R., & Anderson, S. P. (2007). Near-surface hydrologic response for a steep, unchanneled catchment near Coos Bay, Oregon: 2. Physics-based simulations. *American Journal of Science, 307*(4), 709-748. doi:10.2475/04.2007.03 Retrieved from http://www.ajsonline.org/content/307/4/709.abstract

Eckhardt, K. (2005). How to construct recursive digital filters for baseflow separation. *Hydrological Processes, 19*(2), 507-515. doi:10.1002/hyp.5675 Retrieved from http://www.scopus.com/inward/record.url?eid=2-s2.0-13244299362&partnerID=40&md5=75011681ca99dca4ce4f545a399e24ef

Eckhardt, K. (2008). A comparison of baseflow indices, which were calculated with seven different baseflow separation methods. *Journal of Hydrology, 352*(1–2), 168-173. doi:http://dx.doi.org/10.1016/j.jhydrol.2008.01.005 Retrieved from http://www.sciencedirect.com/science/article/pii/S0022169408000310

Ernst, L. F. (1962). *Grondwaterstromingen in de verzadigde zone en hun berekening bij aanwezigheid van horizontale evenwijdige open leidingen*: Centrum voor Landbouwpublikaties en Landbouwdocumetatie.

Fellows, C. R., & Brezonik, P. L. (1980). Seepage Flow Into Florida Lakes. *JAWRA Journal of the American Water Resources Association, 16*(4), 635-641. doi:10.1111/j.1752-1688.1980.tb02442.x Retrieved from http://dx.doi.org/10.1111/j.1752-1688.1980.tb02442.x

Fetter, C. W., & Fetter, C. (2001). *Applied hydrogeology* (Vol. 3): Prentice Hall Upper Saddle River.

Freeze, R. A., & Cherry, J. A. (1979). *Groundwater*: Prentice-Hall.

Freeze, R. A., & Harlan, R. L. (1969). Blueprint for a physically-based, digitally-simulated hydrologic response model. *Journal of Hydrology, 9*(3), 237-258. doi:http://dx.doi.org/10.1016/0022-1694(69)90020-1 Retrieved from http://www.sciencedirect.com/science/article/pii/0022169469900201

Fuentes, C., Haverkamp, R., & Parlange, J.-Y. (1992). Parameter constraints on closed-form soilwater relationships. *Journal of Hydrology, 134*(1–4), 117-142. doi:http://dx.doi.org/10.1016/0022-1694(92)90032-Q Retrieved from http://www.sciencedirect.com/science/article/pii/002216949290032Q

Fuentes, C., Zavala, M., & Saucedo, H. (2009). Relationship between the storage coefficient and the soil-water retention curve in subsurface agricultural drainage systems: water table drawdown. *Journal of Irrigation and Drainage Engineering, 135*(3), 279-285.

Galloway, D. L., Alley, W. M., Barlow, P. M., Reilly, T. E., & Tucci, P. (2003). *Evolving issues and practices in managing ground-water resources : case studies on the role of science* (1247). Retrieved from http://pubs.er.usgs.gov/publication/cir1247

Garrett, J. W., Bennett, D. H., Frost, F. O., & Thurow, R. F. (1998). Enhanced Incubation Success for Kokanee Spawning in Groundwater Upwelling Sites in a Small Idaho Stream. *North American Journal of Fisheries Management, 18*(4), 925-930. doi:10.1577/1548-8675(1998)018<0925:eisfks>2.0.co;2 Retrieved from http://dx.doi.org/10.1577/1548-8675(1998)018<0925:EISFKS>2.0.CO;2

Gassman, P. W., Reyes, M. R., Green, C. H., & Arnold, J. G. (2007). The soil and water assessment tool: historical development, applications, and future research directions. *Transactions of the American Society of Agricultural and Biological Engineers, 50*, 1211–1250.

Gauthier, M. J., Camporese, M., Rivard, C., Paniconi, C., & Larocque, M. (2009). A modeling study of heterogeneity and surface water-groundwater interactions in

the Thomas Brook catchment, Annapolis Valley (Nova Scotia, Canada). *Hydrology and Earth System Sciences, 13*(9), 1583-1596. doi:10.5194/hess-13-1583-2009 Retrieved from http://www.hydrol-earth-syst-sci.net/13/1583/2009/hess-13-1583-2009.pdf

GEO-SLOPE International Ltd. (2012). Seepage modeling with SEEP/W. Retrieved from http://www.geo-slope.com/ website:

Glennon, R. J. (2004). *Water Follies: Groundwater Pumping and the Fate of America's Fresh Waters*: Island Press.

Golden, H. E., Lane, C. R., Amatya, D. M., Bandilla, K. W., Raanan Kiperwas, H., Knightes, C. D., & Ssegane, H. (2014). Hydrologic connectivity between geographically isolated wetlands and surface water systems: A review of select modeling methods. *Environmental Modelling & Software, 53*, 190-206. doi:http://dx.doi.org/10.1016/j.envsoft.2013.12.004 Retrieved from http://www.sciencedirect.com/science/article/pii/S1364815213003071

Gordon, D. (2001). Bay of Plenty. In M. R. Rosen & P. A. White (Eds.), *Groundwaters of New Zealand* (pp. 327–354). Wellington, New Zealand: New Zealand Hydrological Society.

Green, W. H., & Ampt, G. A. (1911). Studies on soil physics, 1, The flow of air and water through soils. *Journal of Agricultural Science, 4*(1), 1-24. doi:http://dx.doi.org/10.1017/S0021859600001441

Guay, C., Nastev, M., Paniconi, C., & Sulis, M. (2013). Comparison of two modeling approaches for groundwater–surface water interactions. *Hydrological Processes, 27*(16), 2258-2270. doi:10.1002/hyp.9323 Retrieved from http://dx.doi.org/10.1002/hyp.9323

Gureghian, A. B., & Youngs, E. G. (1975). The calculation of steady-state water-table heights in drained soils by means of the finite-element method. *Journal of Hydrology, 27*(1–2), 15-32. doi:http://dx.doi.org/10.1016/0022-1694(75)90096-7 Retrieved from http://www.sciencedirect.com/science/article/pii/0022169475900967

Hammad, H. Y. (1962). Depth and spacing of tile drain systems. *Proceedings of ASCE, Journal of the Irrigation and Drain. div., 83*, 15-33.

Hare, D. K., Briggs, M. A., Rosenberry, D. O., Boutt, D. F., & Lane, J. W. (2015). A comparison of thermal infrared to fiber-optic distributed temperature sensing for evaluation of groundwater discharge to surface water. *Journal of Hydrology*, 153–166. doi:http://dx.doi.org/10.1016/j.jhydrol.2015.09.059

Harte, P. T., Division, U. S. E. P. A. R. I. W. M., & Survey, G. (1997). *Information on Hydrologic and Physical Properties of Water to Assess Transient Hydrology of the Milford-Souhegan Glacial-drift Aquifer, Milford, New Hampshire*: U.S. Geological Survey.

Harvey, F. E., Lee, D. R., Rudolph, D. L., & Frape, S. K. (1997). Locating groundwater discharge in large lakes using bottom sediment electrical conductivity mapping. *Water Resources Research, 33*(11), 2609-2615. doi:10.1029/97wr01702 Retrieved from http://dx.doi.org/10.1029/97WR01702

Harvey, J. W., Wagner, B. J., & Bencala, K. E. (1996). Evaluating the reliability of the stream tracer approach to characterize stream-subsurface water exchange. *Water Resources Research, 32*(8), 2441-2451.

Hatch, C. E., Fisher, A. T., Revenaugh, J. S., Constantz, J., & Ruehl, C. (2006). Quantifying surface water–groundwater interactions using time series analysis of streambed thermal records: Method development. *Water Resources Research, 42*(10), W10410. doi:10.1029/2005WR004787

Heppner, C. S., Loague, K., & VanderKwaak, J. E. (2007). Long-term InHM simulations of hydrologic response and sediment transport for the R-5 catchment. *Earth*

Surface Processes and Landforms, 32(9), 1273-1292. doi:10.1002/esp.1474 Retrieved from http://dx.doi.org/10.1002/esp.1474

Herbert, L. R., Thomas, B. K., Survey, G., Rights, U. D. o. W., & Resources, U. D. o. N. (1992). *Seepage Study of the Bear River Including Cutler Reservoir in Cache Valley, Utah and Idaho*: Utah Department of Natural Resources, Division of Water Rights.

Hill, M. C., Protection, N. J. D. o. E., Energy, & Survey, G. (1992). *Geohydrology Of, and Simulation of Ground-water Flow In, the Valley-fill Deposits in the Ramapo River Valley, New Jersey*: U.S. Department of the Interior, U.S. Geological Survey. Retrieved from pubs.usgs.gov/wri/1990/4151/report.pdf

Hooghoudt, S. B. (1940). Bijdragen tot de kennis van eenige natuurkundige grootheden van den grond. No. 7. Algemeene beschouwing van het probleem van de detailontwatering en de infiltratie door middel van parallel loopende drains, greppels, slooten en kanalen. *Verslagen van Landbouwkundige Onderzoekingen, 46* (14), 515-707.

Hutson, S. S. (2004). *Estimated Use of Water in the United States in 2000* (9780607978186). Retrieved from pubs.water.usgs.gov/circ1268

Ivanov, V. Y., Bras, R. L., & Vivoni, E. R. (2008). Vegetation-hydrology dynamics in complex terrain of semiarid areas: 1. A mechanistic approach to modeling dynamic feedbacks. *Water Resources Research, 44*(3). doi:10.1029/2006wr005588 Retrieved from http://dx.doi.org/10.1029/2006WR005588

Ivanov, V. Y., Fatichi, S., Jenerette, G. D., Espeleta, J. F., Troch, P. A., & Huxman, T. E. (2010). Hysteresis of soil moisture spatial heterogeneity and the "homogenizing" effect of vegetation. *Water Resources Research, 46*(9). doi:10.1029/2009wr008611 Retrieved from http://dx.doi.org/10.1029/2009WR008611

Jiang, X.-W., Wan, L., Yeh, T.-C. J., Wang, X.-S., & Xu, L. (2010). Steady-state discharge into tunnels in formations with random variability and depth–decaying trend of hydraulic conductivity. *Journal of Hydrology, 387*(3–4), 320-327. doi:http://dx.doi.org/10.1016/j.jhydrol.2010.04.024 Retrieved from http://www.sciencedirect.com/science/article/pii/S0022169410002118

Johannes, R. E. (1980). The Ecological Significance of the Submarine Discharge of Groundwater. *Marine Ecology-progress Series, 3*, 365-373. doi:10.3354/meps003365

Johannes, R. E., & Hearn, C. J. (1985). The effect of submarine groundwater discharge on nutrient and salinity regimes in a coastal lagoon off Perth, Western Australia. *Estuarine, Coastal and Shelf Science, 21*(6), 789-800. doi:http://dx.doi.org/10.1016/0272-7714(85)90073-3 Retrieved from http://www.sciencedirect.com/science/article/pii/0272771485900733

Jones, J. P., Sudicky, E. A., Brookfield, A. E., & Park, Y. J. (2006). An assessment of the tracer-based approach to quantifying groundwater contributions to streamflow. *Water Resources Research, 42*(2), W02407. doi:10.1029/2005wr004130 Retrieved from http://dx.doi.org/10.1029/2005WR004130

Jones, J. P., Sudicky, E. A., & McLaren, R. G. (2008). Application of a fully-integrated surface-subsurface flow model at the watershed-scale: A case study. *Water Resources Research, 44*(3), W03407. doi:10.1029/2006wr005603 Retrieved from http://dx.doi.org/10.1029/2006WR005603

Jones, W. K. (1984). *Water Tracing Special Issue*: National Speleological Society.

Kalbus, E., Reinstorf, F., & Schirmer, M. (2006). Measuring methods for groundwater? surface water interactions: a review. *Hydrology and Earth System Sciences, 10*(6), 873-887.

Kalcic, M. M., Frankenberger, J., & Chaubey, I. (2015). Spatial Optimization of Six Conservation Practices Using Swat in Tile-Drained Agricultural Watersheds. *JAWRA Journal of the American Water Resources Association*, 1-17. doi:10.1111/1752-1688.12338 Retrieved from http://dx.doi.org/10.1111/1752-1688.12338

Kaleris, V. (1998). Quantifying the exchange rate between groundwater and small streams. *Journal of Hydraulic Research, 36*(6), 913-932. doi:10.1080/00221689809498593 Retrieved from http://dx.doi.org/10.1080/00221689809498593

Kendall, C., & McDonnell, J. J. (2012). *Isotope tracers in catchment hydrology*: Elsevier.

Khan, S., & Rushton, K. R. (1996a). Reappraisal of flow to tile drains III. Drains with limited flow capacity. *Journal of Hydrology, 183*(3–4), 383-395. doi:http://dx.doi.org/10.1016/0022-1694(95)02949-4 Retrieved from http://www.sciencedirect.com/science/article/pii/0022169495029494

Khan, S., & Rushton, K. R. (1996b). Reappraisal of flow to tile drains II. Time-variant response. *Journal of Hydrology, 183*(3–4), 367-382. doi:http://dx.doi.org/10.1016/0022-1694(95)02948-6 Retrieved from http://www.sciencedirect.com/science/article/pii/0022169495029486

Khan, S., & Rushton, K. R. (1996c). Reappraisal of flow to tile drains I. Steady state response. *Journal of Hydrology, 183*(3–4), 351-366. doi:http://dx.doi.org/10.1016/0022-1694(95)02947-8 Retrieved from http://www.sciencedirect.com/science/article/pii/0022169495029478

Kilpatrick, F. A., & Cobb, E. D. (1985). *Measurement of discharge using tracers*: Department of the Interior, US Geological Survey.

Kim, J., Ivanov, V. Y., & Katopodes, N. D. (2013). Modeling erosion and sedimentation coupled with hydrological and overland flow processes at the watershed scale. *Water Resources Research, 49*(9), 5134-5154. doi:10.1002/wrcr.20373 Retrieved from http://dx.doi.org/10.1002/wrcr.20373

Kirkham, D. (1958). Seepage of steady rainfall through soil into drains. *Transactions - American Geophysical Union, 36*(5), 892–908.

Kirkham, D. (1966). Steady-state theories for land drainage. *Journal of Irrigation and Drainage Engineering, 92*, 19–39.

Koch, S., Bauwe, A., & Lennartz, B. (2013). Application of the SWAT Model for a Tile-Drained Lowland Catchment in North-Eastern Germany on Subbasin Scale. *Water Resources Management, 27*(3), 791-805. doi:10.1007/s11269-012-0215-x Retrieved from http://dx.doi.org/10.1007/s11269-012-0215-x

Kollet, S. J., & Maxwell, R. M. (2006). Integrated surface-groundwater flow modeling: A free-surface overland flow boundary condition in a parallel groundwater flow model. *Advances in Water Resources, 29*, 945-958. Retrieved from http://dx.doi.org/10.1016/j.advwatres.2005.08.006

Kollet, S. J., & Maxwell, R. M. (2008a). Capturing the influence of groundwater dynamics on land surface processes using an integrated, distributed watershed model. *Water Resources Research, 44*. Retrieved from http://dx.doi.org/10.1029/2007WR006004

Kollet, S. J., & Maxwell, R. M. (2008b). Demonstrating fractal scaling of baseflow residence time distributions using a fully-coupled groundwater and land surface model. *Geophysical Research Letters, 35*(7). doi:10.1029/2008gl033215 Retrieved from http://dx.doi.org/10.1029/2008GL033215

Kumar, M., Duffy, C. J., & Salvage, K. M. (2009). A Second-Order Accurate, Finite Volume–Based, Integrated Hydrologic Modeling (FIHM) Framework for Simulation of Surface and Subsurface Flow. *Vadose Zone Journal, 8*(4), 873-890. doi:10.2136/vzj2009.0014 Retrieved from http://dx.doi.org/10.2136/vzj2009.0014

LaBaugh, J. W., Rosenberry, D. O., & Winter, T. C. (1995). Groundwater contribution to the water and chemical budgets of Williams Lake, Minnesota, 1980–1991. *Canadian Journal of Fisheries and Aquatic Sciences, 52*(4), 754-767. doi:10.1139/f95-075 Retrieved from http://dx.doi.org/10.1139/f95-075

LaBaugh, J. W., Winter, T. C., Rosenberry, D. O., Schuster, P. F., Reddy, M. M., & Aiken, G. R. (1997). Hydrological and chemical estimates of the water balance of a closed-basin lake in north central Minnesota. *Water Resources Research, 33*(12), 2799-2812. doi:10.1029/97wr02427 Retrieved from http://dx.doi.org/10.1029/97WR02427

Lambert K. Smedema, W. F. V., David W. Rycroft. (2004). *Modern Land Drainage: Planning, Design and Management of Agricultural Drainage Systems*: Taylor & Francis.

Landon, J. R. (2014). *Booker Tropical Soil Manual: A Handbook for Soil Survey and Agricultural Land Evaluation in the Tropics and Subtropics*: Taylor & Francis.

Lee, D. R. (1977). A device for measuring seepage flux in lakes and estuaries1. *Limnology and Oceanography, 22*(1), 140-147. doi:10.4319/lo.1977.22.1.0140 Retrieved from http://dx.doi.org/10.4319/lo.1977.22.1.0140

Lee, D. R., & Cherry, J. A. (1979). A field exercise on groundwater flow using seepage meters and mini-piezometers. *Journal of Geological Education, 27*(1), 6-10.

Lee, T. M., & Swancar, A. (1997). *Influence of evaporation, ground water, and uncertainty in the hydrologic budget of Lake Lucerne, a seepage lake in Polk County, Florida* (2439). Retrieved from http://pubs.er.usgs.gov/publication/wsp2439

Lemieux, J. M., Sudicky, E. A., Peltier, W. R., & Tarasov, L. (2008). Dynamics of groundwater recharge and seepage over the Canadian landscape during the Wisconsinian glaciation. *Journal of Geophysical Research: Earth Surface, 113*(F1). doi:10.1029/2007jf000838 Retrieved from http://dx.doi.org/10.1029/2007JF000838

Leonard, G. S. B., J.G.; Wilson, C.J.J. . (2010). *Geology of the Rotorua area: scale 1:250,000* (Vol. 5): Institute of Geological & Nuclear Sciences 1:250,000 geological map.

Li, Q., Unger, A. J. A., Sudicky, E. A., Kassenaar, D., Wexler, E. J., & Shikaze, S. (2008). Simulating the multi-seasonal response of a large-scale watershed with a 3D physically-based hydrologic model. *Journal of Hydrology, 357*(3–4), 317-336. doi:http://dx.doi.org/10.1016/j.jhydrol.2008.05.024 Retrieved from http://www.sciencedirect.com/science/article/pii/S0022169408002382

Li, S., & Duffy, C. J. (2011). Fully coupled approach to modeling shallow water flow, sediment transport, and bed evolution in rivers. *Water Resources Research, 47*(3). doi:10.1029/2010wr009751 Retrieved from http://dx.doi.org/10.1029/2010WR009751

Liang, D., Falconer, R. A., & Lin, B. (2007). Coupling surface and subsurface flows in a depth averaged flood wave model. *Journal of Hydrology, 337*, 147-158. Retrieved from http://dx.doi.org/10.1016/j.jhydrol.2007.01.045

Liggett, J. E., Werner, A. D., Smerdon, B. D., Partington, D., & Simmons, C. T. (2014). Fully integrated modeling of surface-subsurface solute transport and the effect of dispersion in tracer hydrograph separation. *Water Resources Research, 50*(10), 7750-7765. doi:10.1002/2013wr015040 Retrieved from http://dx.doi.org/10.1002/2013WR015040

Linderfelt, W. R., & Turner, J. V. (2001). Interaction between shallow groundwater, saline surface water and nutrient discharge in a seasonal estuary: the Swan–Canning system. *Hydrological Processes, 15*(13), 2631-2653. doi:10.1002/hyp.302 Retrieved from http://dx.doi.org/10.1002/hyp.302

Lindgren, R. J., & Landon, M. K. (2000). *Effects of ground-water withdrawals on the Rock River and associated valley aquifer, eastern Rock County, Minnesota* (99-4157). Retrieved from http://pubs.er.usgs.gov/publication/wri994157

List, E. J. (1964). The steady flow of precipitation to an infinite series of tile drains above an impervious layer. *Journal of Geophysical Research, 69*(16), 3371-3381. doi:10.1029/JZ069i016p03371 Retrieved from http://dx.doi.org/10.1029/JZ069i016p03371

Liu, M., Chen, X., Yao, H., & Chen, Y. (2015). A coupled modeling approach to evaluate nitrogen retention within the Shanmei Reservoir watershed, China. *Estuarine, Coastal and Shelf Science, 166*(B), 189-198. doi:http://dx.doi.org/10.1016/j.ecss.2015.06.008 Retrieved from http://www.sciencedirect.com/science/article/pii/S0272771415002176

Lodge, D. M., Krabbenhoft, D. P., & Striegl, R. G. (1989). A positive relationship between groundwater velocity and submersed macrophyte biomass in Sparkling Lake Wisconsin. *Limnology and Oceanography, 34*(1), 235-239. doi:10.4319/lo.1989.34.1.0235 Retrieved from http://dx.doi.org/10.4319/lo.1989.34.1.0235

Loke, M., & Lane Jr, J. W. (2004). Inversion of data from electrical resistivity imaging surveys in water-covered areas. *Exploration Geophysics, 35*(4), 266-271.

Lovell, C. J., & Youngs, E. G. (1984). A comparison of steady-state land-drainage equations. *Agricultural Water Management, 9*(1), 1-21. doi:http://dx.doi.org/10.1016/0378-3774(84)90015-5 Retrieved from http://www.sciencedirect.com/science/article/pii/0378377484900155

Malaya, C., & Sreedeep, S. (2011). Critical Review on the Parameters Influencing Soil-Water Characteristic Curve. *Journal of Irrigation and Drainage Engineering, 138*(1), 55-62.

Malcolm, I. A., Soulsby, C., Youngson, A. F., & Petry, J. (2003). Heterogeneity in ground water–surface water interactions in the hyporheic zone of a salmonid spawning stream. *Hydrological Processes, 17*(3), 601-617. doi:10.1002/hyp.1156 Retrieved from http://dx.doi.org/10.1002/hyp.1156

Malcolm, I. A., Youngson, A. F., & Soulsby, C. (2003). Survival of salmonid eggs in a degraded gravel-bed stream: effects of groundwater–surface water interactions. *River Research and Applications, 19*(4), 303-316. doi:10.1002/rra.706 Retrieved from http://dx.doi.org/10.1002/rra.706

Manheim, F. T., Krantz, D. E., & Bratton, J. F. (2004). Studying Ground Water Under Delmarva Coastal Bays Using Electrical Resistivity. *Ground Water, 42*(7), 1052-1068. doi:10.1111/j.1745-6584.2004.tb02643.x Retrieved from http://dx.doi.org/10.1111/j.1745-6584.2004.tb02643.x

Maxwell, R. M., & Kollet, S. J. (2008). Quantifying the effects of three-dimensional subsurface heterogeneity on Hortonian runoff processes using a coupled numerical, stochastic approach. *Advances in Water Resources, 31*(5), 807-817. doi:http://dx.doi.org/10.1016/j.advwatres.2008.01.020 Retrieved from http://www.sciencedirect.com/science/article/pii/S0309170808000201

Maxwell, R. M., & Miller, N. L. (2005). Development of a Coupled Land Surface and Groundwater Model. *Journal of Hydrometeorology, 6*(3), 233-247. doi:doi:10.1175/JHM422.1 Retrieved from http://journals.ametsoc.org/doi/abs/10.1175/JHM422.1

Maxwell, R. M., Putti, M., Meyerhoff, S., Delfs, J.-O., Ferguson, I. M., Ivanov, V., . . . Sulis, M. (2014). Surface-subsurface model intercomparison: A first set of benchmark results to diagnose integrated hydrology and feedbacks. *Water Resources Research, 50*(2), 1531-1549. doi:10.1002/2013wr013725 Retrieved from http://dx.doi.org/10.1002/2013WR013725

McCarthy, K. A., McFarland, W. D., Wilkinson, J. M., & White, L. D. (1992). The dynamic relationship between ground water and the Columbia River: using deuterium and oxygen-18 as tracers. *Journal of Hydrology, 135*(1-4), 1-12. Retrieved from http://pubs.er.usgs.gov/publication/70017093

Meyerhoff, S., & Maxwell, R. (2011). Quantifying the effects of subsurface heterogeneity on hillslope runoff using a stochastic approach. *Hydrogeology Journal, 19*(8), 1515-1530. doi:10.1007/s10040-011-0753-y Retrieved from http://dx.doi.org/10.1007/s10040-011-0753-y

Miles, J. C., & Kitmitto, K. (1989). New drain flow formula. *Journal of Irrigation and Drainage Engineering, 115*, 215-230.

Milicich, S. D., Bardsley, C., Bignall, G., & Wilson, C. J. N. (2014). 3-D interpretative modelling applied to the geology of the Kawerau geothermal system, Taupo Volcanic Zone, New Zealand. *Geothermics, 51*, 344-350. doi:http://dx.doi.org/10.1016/j.geothermics.2014.03.002 Retrieved from http://www.sciencedirect.com/science/article/pii/S0375650514000261

Milicich, S. D., Wilson, C. J. N., Bignall, G., Pezaro, B., & Bardsley, C. (2013). Reconstructing the geological and structural history of an active geothermal field: A case study from New Zealand. *Journal of Volcanology and Geothermal Research, 262*, 7-24. doi:http://dx.doi.org/10.1016/j.jvolgeores.2013.06.004 Retrieved from http://www.sciencedirect.com/science/article/pii/S0377027313001789

Mirus, B. B., Loague, K., VanderKwaak, J. E., Kampf, S. K., & Burges, S. J. (2009). A hypothetical reality of Tarrawarra-like hydrologic response. *Hydrological Processes, 23*(7), 1093-1103. doi:10.1002/hyp.7241 Retrieved from http://dx.doi.org/10.1002/hyp.7241

Mishra, G. C., & Singh, V. (2007). A new drain spacing formula. *Hydrological Sciences Journal, 52*(2), 338 - 351. Retrieved from http://www.informaworld.com/10.1623/hysj.52.2.338

Mishra, G. C., & Singh, V. (2008). Reply to discussion of “A new drain spacing formula”. *Hydrological Sciences Journal, 53*(4), 935-937. Retrieved from http://www.informaworld.com/10.1623/hysj.53.4.935

Moody, W. (1966). Nonlinear differential equation of drain spacing. *Journal of Irrigation and Drainage Engineering, 92*, 1–10.

Moore, W. S. (1996). Large groundwater inputs to coastal waters revealed by 226Ra enrichments. *Nature, 380*(6575), 612-614. Retrieved from http://dx.doi.org/10.1038/380612a0

Moore, W. S. (1999). The subterranean estuary: a reaction zone of ground water and sea water. *Marine Chemistry, 65*(1–2), 111-125. doi:http://dx.doi.org/10.1016/S0304-4203(99)00014-6 Retrieved from http://www.sciencedirect.com/science/article/pii/S0304420399000146

Moore, W. S. (2000). Determining coastal mixing rates using radium isotopes. *Continental Shelf Research, 20*(15), 1993-2007. doi:http://dx.doi.org/10.1016/S0278-4343(00)00054-6 Retrieved from http://www.sciencedirect.com/science/article/pii/S0278434300000546

Moriasi, D. N., Gowda, P. H., Arnold, J. G., Mulla, D. J., Ale, S., & Steiner, J. L. (2013). Modeling the impact of nitrogen fertilizer application and tile drain configuration on nitrate leaching using SWAT. *Agricultural Water Management, 130*, 36-43. doi:http://dx.doi.org/10.1016/j.agwat.2013.08.003 Retrieved from http://www.sciencedirect.com/science/article/pii/S0378377413002060

Morrison, A. K. (2014). *Limitations on the study of tile drainage using a distributed parameter hydrologic model and stable isotopes.* (M.Sc.), Iowa State University.

Mull, D. S., Liebermann, T., Smoot, J., & Woosley, L. (1988). *Application of dye-tracing techniques for determining solute-transport characteristics of ground water in*

karst terranes. Retrieved from http://karstwaters.org/wp-content/uploads/2015/04/dye-tracing.pdf

Nairn, I. (2002). Rotoehu Ash and the Rotoiti Breccia Formation, Taupo volcanic zone, New Zealand. *New Zealand Journal of Science, 15*(2), 251-261.

Nairn, I. A. (2002). *Geology of the Okataina Volcanic Centre mapping*. Lower Hutt, N.Z. : Institute of Geological and Nuclear Sciences.

O'Driscoll, M., & Parizek, R. (2003). The hydrologic catchment area of a chain of karst wetlands in central Pennsylvania, USA. *Wetlands, 23*(1), 171-179. doi:10.1672/0277-5212(2003)023[0171:thcaoa]2.0.co;2 Retrieved from http://dx.doi.org/10.1672/0277-5212%282003%29023%5B0171%3ATHCAOA%5D2.0.CO%3B2

Oxtobee, J. P., & Novakowski, K. (2002). A field investigation of groundwater/surface water interaction in a fractured bedrock environment. *Journal of Hydrology, 269*(3), 169-193.

Panday, S., & Huyakorn, P. S. (2004). A fully coupled physically-based spatially-distributed model for evaluating surface/subsurface flow. *Advances in Water Resources, 27*, 361–382.

Pandey, R., Bhattacharya, A., Singh, O., & Gupta, S. (1992). Drawdown Solutions with Variable Drainable Porosity. *Journal of Irrigation and Drainage Engineering, 118*(3), 382-396. doi:doi:10.1061/(ASCE)0733-9437(1992)118:3(382) Retrieved from http://ascelibrary.org/doi/abs/10.1061/%28ASCE%290733-9437%281992%29118%3A3%28382%29

Partington, D., Brunner, P., Frei, S., Simmons, C. T., Werner, A. D., Therrien, R., . . . Fleckenstein, J. H. (2013). Interpreting streamflow generation mechanisms from integrated surface-subsurface flow models of a riparian wetland and catchment. *Water Resources Research, 49*(9), 5501-5519. doi:10.1002/wrcr.20405 Retrieved from http://dx.doi.org/10.1002/wrcr.20405

Partington, D., Brunner, P., Simmons, C. T., Therrien, R., Werner, A. D., Dandy, G. C., & Maier, H. R. (2011). A hydraulic mixing-cell method to quantify the groundwater component of streamflow within spatially distributed fully integrated surface water-groundwater flow models. *Environmental Modelling & Software, 26*(7), 886-898. Retrieved from http://www.sciencedirect.com/science/article/pii/S136481521100034X

Peel, M. C., Finlayson, B. L., & McMahon, T. A. (2007). Updated world map of the Köppen-Geiger climate classification. *Hydrology and Earth System Sciences, 11*(5), 1633-1644. doi:10.5194/hess-11-1633-2007 Retrieved from http://www.hydrol-earth-syst-sci.net/11/1633/2007/hess-11-1633-2007.pdf

Pirkle, E. C., & Brooks, H. K. (1959). Origin and Hydrology of Orange Lake, Santa Fe Lake, and Levys Prairie Lakes of North-Central Peninsular Florida. *The Journal of Geology, 67*(3), 302-317. doi:10.2307/30057083 Retrieved from http://www.jstor.org/stable/30057083

Ponce, V., & Hawkins, R. (1996). Runoff Curve Number: Has It Reached Maturity? *Journal of Hydrologic Engineering, 1*(1), 11-19. doi:10.1061/(asce)1084-0699(1996)1:1(11) Retrieved from http://dx.doi.org/10.1061/(ASCE)1084-0699(1996)1:1(11)

Power, G., Brown, R. S., & Imhof, J. G. (1999). Groundwater and fish—insights from northern North America. *Hydrological Processes, 13*(3), 401-422. doi:10.1002/(sici)1099-1085(19990228)13:3<401::aid-hyp746>3.0.co;2-a Retrieved from http://dx.doi.org/10.1002/(SICI)1099-1085(19990228)13:3<401::AID-HYP746>3.0.CO;2-A

Puckett, L. J., Cowdery, T. K., McMahon, P. B., Tornes, L. H., & Stoner, J. D. (2002). Using chemical, hydrologic, and age dating analysis to delineate redox processes and flow paths in the riparian zone of a glacial outwash aquifer-stream system.

Water Resources Research, 38(8). doi:10.1029/2001wr000396 Retrieved from http://dx.doi.org/10.1029/2001WR000396

Qu, Y., & Duffy, C. J. (2007). A semidiscrete finite volume formulation for multiprocess watershed simulation. *Water Resources Research, 43*(8). doi:10.1029/2006wr005752 Retrieved from http://dx.doi.org/10.1029/2006WR005752

Rabbo, A. A. (2000). The geohydrology and water quality of the springs and wells of the western catchment to the Dead Sea, West Bank, Palestine. *Water Science & Technology, 42*(1), 7-12.

Rallison, R. E. (1980). *Origin and evolution of the SCS runoff equation.* Paper presented at the Symposium on Watershed Management 1980.

Ran, Q., Heppner, C. S., VanderKwaak, J. E., & Loague, K. (2007). Further testing of the integrated hydrology model (InHM): multiple-species sediment transport. *Hydrological Processes, 21*(11), 1522-1531. doi:10.1002/hyp.6642 Retrieved from http://dx.doi.org/10.1002/hyp.6642

Richards, L. A. (1931). Capillary conduction of liquids through porous mediums. *PHYSICS, 1*, 318 333.

Robinove, C. J. (1965). Infrared photography and imagery in water resources research. *Journal - American Water Works Association, 57*(7), 834-840. Retrieved from http://pubs.er.usgs.gov/publication/70112254

Rocha, J., Roebeling, P., & Rial-Rivas, M. E. (2015). Assessing the impacts of sustainable agricultural practices for water quality improvements in the Vouga catchment (Portugal) using the SWAT model. *Science of The Total Environment, 536*, 48-58. doi:http://dx.doi.org/10.1016/j.scitotenv.2015.07.038 Retrieved from http://www.sciencedirect.com/science/article/pii/S0048969715303818

Rosenberry, D. O., & Lebaugh, J. W. (2014). *Field Techniques for Estimating Water Fluxes Between Surface Water and Ground Water*: Createspace Independent Pub. Retrieved from http://pubs.usgs.gov/tm/04d02/

Rosenberry, D. O., Striegl, R. G., & Hudson, D. C. (2000). Plants as indicators of focused ground water discharge to a northern Minnesota lake. *Groundwater, 38*(2), 296-303.

Rozemeijer, J. C., van der Velde, Y., McLaren, R. G., van Geer, F. C., Broers, H. P., & Bierkens, M. F. P. (2010). Integrated modeling of groundwater–surface water interactions in a tile-drained agricultural field: The importance of directly measured flow route contributions. *Water Resources Research, 46*(11). doi:10.1029/2010wr009155 Retrieved from http://dx.doi.org/10.1029/2010WR009155

Rutledge, A. (1998). *Computer programs for describing the recession of ground-water discharge and for estimating mean ground-water recharge and discharge from streamflow records-update*. Retrieved from https://pubs.er.usgs.gov/publication/wri984148

Sacks, L. A., District, S. F. W. M., & Survey, G. (2002). *Estimating Ground-water Inflow to Lakes in Central Florida Using the Isotope Mass-balance Approach*: U.S. Department of the Interior, U.S. Geological Survey. Retrieved from fl.water.usgs.gov/PDF_files/wri02_4192_sacks.pdf

Sakkas, J. G., & Antonopoulos, V. Z. (1981). Simple equations for hooghoudt equivalent depth. *Journal of Irrigation and Drainage Engineering, 107*, 411-414.

Schoups, G., Hopmans, J. W., Young, C. A., Vrugt, J. A., Wallender, W. W., Tanji, K. K., & Panday, S. (2005). Sustainability of irrigated agriculture in the San Joaquin Valley, California. *Proceedings of the National Academy of Sciences, 102*(43), 15352-15356. doi:10.1073/pnas.0507723102 Retrieved from http://www.pnas.org/content/102/43/15352.abstract

Shane, P., Nairn, I. A., & Smith, V. C. (2005). Magma mingling in the ~50 ka Rotoiti eruption from Okataina Volcanic Centre: implications for geochemical diversity and chronology of large volume rhyolites. *Journal of Volcanology and Geothermal Research, 139*(3–4), 295-313. doi:http://dx.doi.org/10.1016/j.jvolgeores.2004.08.012 Retrieved from http://www.sciencedirect.com/science/article/pii/S0377027304003087

Sheets, R. A., Darner, R. A., & Whitteberry, B. L. (2002). Lag times of bank filtration at a well field, Cincinnati, Ohio, USA. *Journal of Hydrology, 266*(3-4), 162-174. doi:10.1016/s0022-1694(02)00164-6 Retrieved from http://pubs.er.usgs.gov/publication/70024282

Shen, C., & Phanikumar, M. S. (2010). A process-based, distributed hydrologic model based on a large-scale method for surface–subsurface coupling. *Advances in Water Resources, 33* 1524–1541.

Shokri, A. (2011). *Developing a new numerical surface/subsurface model for irrigation and drainage system design.* Paper presented at the Symposium H01 on Conceptual and Modelling Studies of Integrated Groundwater, Surface Water, and Ecological Systems, Held During the 25th General Assembly of the International Union of Geodesy and Geophysics, IUGG 2011, June 28, 2011 - July 7, 2011, Melbourne, VIC, Australia.

Shokri, A. (April 2015). *Development, test and application of a coupled surface-subsurface flow model*. Paper presented at the Integrated Hydrosystem Modelling Tübingen, Germany.

Shokri, A. (December 2012). *An improvement of the Hooghoudt drain-spacing equation*. Paper presented at the The New Zealand Hydrological Society Annual Conference, Nelson, New Zealand.

Shokri, A. (December 2011). *A numerical methodology for designing drainage systems*. Paper presented at the The New Zealand Hydrological Society Annual Conference, Wellington, New Zealand.

Shokri, A. (Nov 2014). *Developing a fully distributed interaction surface/subsurface flows model*. Paper presented at the New Zealand Hydrological Society Annual Conference, Blenheim, New Zealand

Shokri, A. (November 2013). *An application of Richards equation for water table height midway between two drains*. Paper presented at the The New Zealand Hydrological Society and the Meteorological Society of New Zealand, Palmerston North, New Zealand.

Shokri, A. (Sep 2015). *Fully distributed integrated Surface/subsurface flow models: perspectives, applications and future*. Paper presented at the GW-SW Interaction Workshop, Wellington, New Zealand.

Shokri, A., & Bardsley, E. (2015). *Drainflow: a fully distributed integrated surface/subsurface flow model for drainage studies*. Paper presented at the EGU General Assembly Vienna, Austria.

Shokri, A., & Bardsley, W. (2014). Enhancement of the Hooghoudt Drain-Spacing Equation. *Journal of Irrigation and Drainage Engineering, 141*(6), 04014070. doi:10.1061/(asce)ir.1943-4774.0000835 Retrieved from http://dx.doi.org/10.1061/(ASCE)IR.1943-4774.0000835

Simmons, G. (1992). Importance of Submarine Groundwater Discharge (SGWD) and Seawater Cycling to Material Flux across Sediment/Water Interfaces in Marine Environments. *Marine Ecology Progress Series MESEDT, 84*(2), 173-184. Retrieved from http://www.int-res.com/articles/meps/84/m084p173.pdf

Simonds, F. W., & Sinclair, K. A. (2002). *Surface water-ground water interactions along the lower Dungeness River and vertical hydraulic conductivity of streambed sediments, Clallam County, Washington, September 1999-July 2001* (2002-4161). Retrieved from http://pubs.er.usgs.gov/publication/wri024161

Skaggs, R. W. (1980). *DRAINMOD: Reference Report - Methods for Design and Evaluation of Drainage-Water Management Systems for Soils with High Water Tables*: USDA-SCS. Fort Worth, TX.

Skaggs, R. W. (1980). *A water management model for artificially drained soils*: North Carolina Agricultural Research Service.

Sky, K., Harding, B., & Khan, A. (2009). *North Valley Landfill Technical Assessment of Environmental Effects*. Retrieved from Pattle Delamore Partners ltd (PDP)

Smart, P. L., & Laidlaw, I. M. S. (1977). An evaluation of some fluorescent dyes for water tracing. *Water Resources Research, 13*(1), 15-33. doi:10.1029/WR013i001p00015 Retrieved from http://dx.doi.org/10.1029/WR013i001p00015

Smedema, L. K., Poelman, A., & De Haan, W. (1985). Use of the Hooghoudt formula for drain spacing calculation

s in homogeneous-anisotropic soils. *Agricultural Water Management, 10*(4), 283-291. doi:http://dx.doi.org/10.1016/0378-3774(85)90017-4 Retrieved from http://www.sciencedirect.com/science/article/pii/0378377485900174

Smerdon, B. D., Mendoza, C. A., & Devito, K. J. (2008). Influence of subhumid climate and water table depth on groundwater recharge in shallow outwash aquifers. *Water Resources Research, 44*(8). doi:10.1029/2007wr005950 Retrieved from http://dx.doi.org/10.1029/2007WR005950

Snelder, T., Biggs, B., & Weatherhead, M. (2010). *New Zealand river environment classification user guide*: Ministry for the Environment.

Steele, G. V., & Verstraeten, I. M. (1999). *Effects of pumping collector wells on river-aquifer interaction at Platte River Island near Ashland, Nebraska, 1998* (99-4161). Retrieved from Reston, VA: http://pubs.er.usgs.gov/publication/wri994161

Stonestrom, D. A., Constantz, J., & Survey, G. (2003). *Heat as a tool for studying the movement of ground water near streams*: U.S. Dept. of the Interior, U.S. Geological Survey. Retrieved from pubs.usgs.gov/circ/2003/circ1260/pdf/Circ1260.pdf

Stromberg, J. C., Tiller, R., & Richter, B. (1996). Effects of Groundwater Decline on Riparian Vegetation of Semiarid Regions: The San Pedro, Arizona. *Ecological Applications, 6*(1), 113-131. doi:10.2307/2269558 Retrieved from http://www.jstor.org/stable/2269558

Sudicky, E., Jones, J., Park, Y.-J., Brookfield, A., & Colautti, D. (2008). Simulating complex flow and transport dynamics in an integrated surface-subsurface modeling framework. *Geosciences Journal, 12*(2), 107-122. doi:10.1007/s12303-008-0013-x Retrieved from http://dx.doi.org/10.1007/s12303-008-0013-x

Sulis, M., Paniconi, C., & Camporese, M. (2011). Impact of grid resolution on the integrated and distributed response of a coupled surface–subsurface hydrological model for the des Anglais catchment, Quebec. *Hydrological Processes, 25*(12), 1853-1865. doi:10.1002/hyp.7941 Retrieved from http://dx.doi.org/10.1002/hyp.7941

Tait, A., Henderson, R., Turner, R., & Zheng, X. (2006). Thin plate smoothing spline interpolation of daily rainfall for New Zealand using a climatological rainfall surface. *International Journal of Climatology, 26*(14), 2097-2115. doi:10.1002/joc.1350 Retrieved from http://dx.doi.org/10.1002/joc.1350

Taniguchi, M., Burnett, W. C., Cable, J. E., & Turner, J. V. (2002). Investigation of submarine groundwater discharge. *Hydrological Processes, 16*(11), 2115-2129. doi:10.1002/hyp.1145 Retrieved from http://dx.doi.org/10.1002/hyp.1145

Thompson, B. N. (1974). *Geology of the Rotorua geothermal district*. Retrieved from Department of Scientific and Industrial Research, Wellington:

Tiemeyer, B., Moussa, R., Lennartz, B., & Voltz, M. (2007). MHYDAS-DRAIN: A spatially distributed model for small, artificially drained lowland catchments. *Ecological Modelling, 209*(1), 2-20. doi:http://dx.doi.org/10.1016/j.ecolmodel.2007.07.003 Retrieved from http://www.sciencedirect.com/science/article/pii/S0304380007003559

Trefry, M. G., & Muffels, C. (2007). FEFLOW: A Finite-Element Ground Water Flow and Transport Modeling Tool. *Ground Water, 45*(5), 525-528. doi:10.1111/j.1745-6584.2007.00358.x Retrieved from http://dx.doi.org/10.1111/j.1745-6584.2007.00358.x

Tschritter, C., & White, P. (2014). *Three-dimensional geological model of the greater. Lake Tarawera catchment* (2013/1552014). Retrieved from https://www.boprc.govt.nz/media/417987/three-dimensional-geological-model-of-the-greater-lake-tarawera-catchment.pdf

Valiela, I., Costa, J., Foreman, K., Teal, J., Howes, B., & Aubrey, D. (1990). Transport of groundwater-borne nutrients from watersheds and their effects on coastal waters. *Biogeochemistry, 10*(3), 177-197. doi:10.1007/bf00003143 Retrieved from http://dx.doi.org/10.1007/BF00003143

Van Beers, W. F. J. (1979). *Some nomographs for the calculation of drain spacings* (Third ed. Vol. Bulletin 8). Wageningen: ILRI.

Van der Molen, W. H., & Wesseling, J. (1991). A solution in closed form and a series solution to replace the tables for the thickness of the equivalent layer in Hooghoudt's drain spacing formula. *Agricultural Water Management, 19*(1), 1-16. Retrieved from http://www.sciencedirect.com/science/article/B6T3X-487HP69-1C/2/1d921b85bc85b222211f2276bbf8cd2c

Van Genuchten, M. T. (1980). Closed-form equation for predicting the hydraulic conductivity of unsaturated soils. *Soil Sci Soc Am J., 44*(5), 892-898. Retrieved from http://www.scopus.com/inward/record.url?eid=2-s2.0-0019057216&partnerID=40&md5=9caf8cbebcd55775324a8ec4bd536e4a

Van Schilfgaarde, J. (1963). Design of tile drainage for falling water tables. *Proc Am Soc Civil Engrs, 89*, 1-11.

VanderKwaak, J. E., & Loague, K. (2001). Hydrologic-Response simulations for the R-5 catchment with a comprehensive physics-based model. *Water Resources Research, 37*(4), 999-1013. doi:10.1029/2000wr900272 Retrieved from http://dx.doi.org/10.1029/2000WR900272

Von der Heyden, C. J., & New, M. G. (2003). The role of a dambo in the hydrology of a catchment and the river network downstream. *Hydrology and Earth System Sciences, 7*(3), 339-357. doi:10.5194/hess-7-339-2003 Retrieved from http://www.hydrol-earth-syst-sci.net/7/339/2003/hess-7-339-2003.pdf

Weill, S., Mazzia, A., Putti, M., & Paniconi, C. (2011). Coupling water flow and solute transport into a physically-based surface-subsurface hydrological model. *Advances in Water Resources, 34*(1), 128-136. Retrieved from http://www.sciencedirect.com/science/article/B6VCF-516M7F8-1/2/baf37c1ef1e2cce5a53caac9cf0f0d8d

Weiyan, T. (1992). *Shallow Water Hydrodynamics Mathematical Theory and Numerical Solution for a Two - dimensional System of Shallow Water Equations*. China: Water and Power Press, Beijing.

Wentz, D. A., Rose, W. J., & Webster, K. E. (1995). Long-Term Hydrologic and Biogeoehemieal Responses of a Soft Water Seepage Lake in North Central Wisconsin. *Water Resources Research, 31*(1), 199-212. doi:10.1029/94wr02230 Retrieved from http://dx.doi.org/10.1029/94WR02230

Wesseling, J., & Kessler, J. (1994). *Drainage Principles and Applications: Theories of field drainage and watershed runoff*: International Institute for Land Reclamation and Improvement, Wageningen (ILRI), The Netherlands.

White, P. A. (2005). *Future use of groundwater resources in the Bay of Plenty region*. Retrieved from https://www.boprc.govt.nz/media/32422/GNS-091118-FutureUseofGroundwaterResources.pdf

Williams, J. (1969). Flood routing with variable travel time or variable storage coefficients. *Trans. ASAE, 12*(1), 100-103.

Wilson, C. J. N., & Charlier, B. L. A. (2009). Rapid Rates of Magma Generation at Contemporaneous Magma Systems, Taupo Volcano, New Zealand: Insights from U–Th Model-age Spectra in Zircons. *Journal of Petrology, 50*(5), 875-907. doi:10.1093/petrology/egp023 Retrieved from http://petrology.oxfordjournals.org/content/50/5/875.abstract

Wilson, C. J. N., Rhoades, D. A., Lanphere, M. A., Calvert, A. T., Houghton, B. F., Weaver, S. D., & Cole, J. W. (2007). A multiple-approach radiometric age estimate for the Rotoiti and Earthquake Flat eruptions, New Zealand, with implications for the MIS 4/3 boundary. *Quaternary Science Reviews, 26*(13–14), 1861-1870. doi:http://dx.doi.org/10.1016/j.quascirev.2007.04.017 Retrieved from http://www.sciencedirect.com/science/article/pii/S0277379107001163

Woods, R., Hendrikx, J., Henderson, R., & Tait, A. (2006). Estimating mean flow of New Zealand rivers. *Journal of Hydrology (NZ), 45*(2), 95-110. Retrieved from http://www.hydrologynz.co.nz/downloads/20110419-115957-JoHNZ_2006_v45_2_Woods.pdf

Youngs, E. (2012). Effect of the Capillary Fringe on Steady-State Water Tables in Drained Lands. *Journal of Irrigation and Drainage Engineering, 138*(9), 809-814. doi:doi:10.1061/(ASCE)IR.1943-4774.0000467 Retrieved from http://ascelibrary.org/doi/abs/10.1061/%28ASCE%29IR.1943-4774.0000467

Youngs, E. (2013). Effect of the Capillary Fringe on Steady-State Water Tables in Drained Lands. II: Effect of an Underlying Impermeable Bed. *Journal of Irrigation and Drainage Engineering, 139*(4), 309-312. doi:doi:10.1061/(ASCE)IR.1943-4774.0000531 Retrieved from http://ascelibrary.org/doi/abs/10.1061/%28ASCE%29IR.1943-4774.0000531

Youngs, E. G. (1965). Horizontal seepage through unconfined aquifers with hydraulic conductivity varying with depth. *Journal of Hydrology, 3*(3-4), 283-296. Retrieved from http://www.scopus.com/inward/record.url?eid=2-s2.0-0242715733&partnerID=40&md5=79ec10c78387b6a1fa3df2f36606feb2

Youngs, E. G. (1975). The effect of the depth of an impermeable barrier on water-table heights in drained homogeneous soils. *Journal of Hydrology, 24*(3-4), 283-290. Retrieved from http://www.scopus.com/inward/record.url?eid=2-s2.0-0016470985&partnerID=40&md5=0b4f9ef5c4cd17f2662c4af04599abc4

Zaradny, H. (2001). Application of confined aquifer theory for verification of solutions of water flow towards a drain in saturated–unsaturated soil. *Agricultural Water Management, 47*(2), 155-178. doi:http://dx.doi.org/10.1016/S0378-3774(00)00100-1 Retrieved from http://www.sciencedirect.com/science/article/pii/S0378377400001001

Zaradny, H., & Feddes, R. A. (1979). Calculation of non-steady flow towards a drain in saturated-unsaturated soil by finite elements. *Agricultural Water Management, 2*(1), 37-53. doi:http://dx.doi.org/10.1016/0378-3774(79)90012-X Retrieved from http://www.sciencedirect.com/science/article/pii/037837747990012X

Zarriello, P. J., Ries, K. G., Management, M. D. o. E., Protection, M. D. o. E., & Survey, G. (2000). *A precipitation-runoff model for analysis of the effects of water withdrawals on streamflow, Ipswich River Basin, Massachusetts*: U.S. Dept. of the Interior, U.S. Geological Survey. Retrieved from pubs.usgs.gov/wri/wri004029/

Zavala, M., Fuentes, C., & Saucedo, H. (2007). Non-linear radiation in the Boussinesq equation of the agricultural drainage. *Journal of Hydrology, 332*(3-4), 374-380.

Retrieved from http://www.sciencedirect.com/science/article/B6V6C-4KXVD7F-1/2/6b70403ff4b9dd24481b89bb3eedf408

Zavala, M., Saucedo, H., Bautista, C., & Fuentes, C. (2012). Comparison of two nonlinear radiation models for agricultural subsurface drainage. In M. S. Javaid (Ed.), *Drainage Systems* (pp. 165-180): InTech.

Zekster, I. S. (1995). Groundwater discharge into lakes: A review of recent studies with particular regard to large saline lakes in central Asia. *International Journal of Salt Lake Research, 4*(3), 233-249. doi:10.1007/bf02001493 Retrieved from http://dx.doi.org/10.1007/BF02001493

Zerihun, D., Furman, A., Warrick, A. W., & Sanchez, C. A. (2005a). Coupled surface-subsurface flow model for improved basin irrigation management. *Journal of Irrigation and Drainage Engineering, 131*, 111-128. Retrieved from http://dx.doi.org/10.1061/(ASCE)0733-9437(2005)131:2(111)

Zerihun, D., Furman, A., Warrick, A. W., & Sanchez, C. A. (2005b). Coupled surface-subsurface solute transport model for irrigation borders and basins. I. Model development. *Journal of Irrigation and Drainage Engineering, 131*, 396-406. Retrieved from http://dx.doi.org/10.1061/(ASCE)0733-9437(2005)131:5(396)

Zhang, L., Hickel, K., Dawes, W. R., Chiew, F. H. S., Western, A. W., & Briggs, P. R. (2004). A rational function approach for estimating mean annual evapotranspiration. *Water Resources Research, 40*(2), W02502. doi:10.1029/2003wr002710 Retrieved from http://dx.doi.org/10.1029/2003WR002710